ISSN: 2408-2384 (Online)
ISSN: 1686-5456 (Print)

Environment and Natural Resources Journal

Volume 19, Number 2, March - April 2021

Environment and Natural Resources Journal (EnNRJ)

Volume 19, Number 2, March - April 2021 ISSN: 1686-5456 (Print)
ISSN: 2408-2384 (Online)

AIMS AND SCOPE

The Environment and Natural Resources Journal is a peer-reviewed journal, which provides insight scientific knowledge into the diverse dimensions of integrated environmental and natural resource management. The journal aims to provide a platform for exchange and distribution of the knowledge and cutting-edge research in the fields of environmental science and natural resource management to academicians, scientists and researchers. The journal accepts a varied array of manuscripts on all aspects of environmental science and natural resource management. The journal scope covers the integration of multidisciplinary sciences for prevention, control, treatment, environmental clean-up and restoration. The study of the existing or emerging problems of environment and natural resources in the region of Southeast Asia and the creation of novel knowledge and/or recommendations of mitigation measures for sustainable development policies are emphasized.

The subject areas are diverse, but specific topics of interest include:

- Biodiversity
- Climate change
- Detection and monitoring of polluted sources e.g., industry, mining
- Disaster e.g., forest fire, flooding, earthquake, tsunami, or tidal wave
- Ecological/Environmental modelling
- Emerging contaminants/hazardous wastes investigation and remediation
- Environmental dynamics e.g., coastal erosion, sea level rise
- Environmental assessment tools, policy and management e.g., GIS, remote sensing, Environmental Management System (EMS)
- Environmental pollution and other novel solutions to pollution
- Remediation technology of contaminated environments
- Transboundary pollution
- Waste and wastewater treatments and disposal technology

Schedule

Environment and Natural Resources Journal (EnNRJ) is published 6 issues per year in January-February, March-April, May-June, July-August, September-October, and November-December.

Publication Fees

There is no cost of the article-processing and publication.

Ethics in publishing

EnNRJ follows closely a set of guidelines and recommendations published by Committee on Publication Ethics (COPE).

Environment and Natural Resources Journal (EnNRJ)

Volume 19, Number 2, March - April 2021

ISSN: 1686-5456 (Print)
ISSN: 2408-2384 (Online)

Editorial Office Address
Research Management and Administration Section,
Faculty of Environment and Resource Studies, Mahidol University
999, Phutthamonthon Sai 4 Road, Salaya, Phutthamonthon, Nakhon Pathom, Thailand, 73170
Phone +662 441 5000 ext. 2108 Fax. +662 441 9509-10
Website: https://ph02.tci-thaijo.org/index.php/ennrj/index
E-mail: ennrjournal@gmail.com

Environment and Natural Resources Journal (EnNRJ)

Volume 19, Number 2, March - April 2021 ISSN: 1686-5456 (Print)
ISSN: 2408-2384 (Online)

CONTENT

Association between Noise Exposure and Quality of Life among People Living Near Stone-Mortar Factories, Phayao Province, Northern Thailand

Sakesun Thongtip[1,2*], Sarawut Sangkham[1], Piyavadee Srivichai[1], and Patipat Vongruang[1,2]

[1]Department of Environmental Health, School of Medicine, University of Phayao, Phayao 56000, Thailand
[2]Atmospheric Pollution and Climate Change Research Unit, University of Phayao, Phayao 56000, Thailand

ARTICLE INFO

Received: 22 Mar 2020 Received in revised: 21 Sep 2020
Accepted: 9 Oct 2020
Published online: 2 Dec 2020
DOI: 10.32526/ennrj/19/2020050

Keywords:
Noise exposure/ Residential distance/ Quality of life/ People living near stone-mortar factories

*** Corresponding author:**
E-mail: sake_115@hotmail.com

ABSTRACT

Noise may have adverse effects on health and quality of life (QoL). This study assessed the association between noise exposure and QoL among people living near stone-mortar factories. A cross-sectional descriptive study was conducted using 269 subjects. The data was collected using questionnaires, sound level meter, and a geographic information system technique. The statistical analysis was carried out using independent t-test, ANOVA, Pearson's correlation coefficient test and multiple binary logistic regression analysis. The average noise in factory no. 2, 4, and 5 was found to be higher than the standard level of NIOSH at 85 dB(A) and OSHA at 90 dB(A) for an 8-hour TWA. The multiple binary logistic regression analysis showed that an increasing residential distance was associated with high noise exposure after adjusting for age, education, income, length of stay in community, and overall QoL. The local policy makers should be required to emphasize on the reduction of noise pollution in stone-mortar factories and health surveillance of the residential neighborhood.

1. INTRODUCTION

Noise is one of the major global environmental issues, apart from being an unwanted nuisance (WHO, 2011). Moreover, exposure to high levels of noise may have adverse effects on the health and the quality of life (QoL) of not only the workers at the site but also of the people living around these noise sources (Seidman and Standring, 2010; Padungtod et al., 2011). The sources of noise pollution may be natural or artificial such as agriculture, mining, construction, transportation, and industries (Chepesiuk, 2005; WHO, 2011; Sordello et al., 2019). Approximately 16% of the world population suffers from hearing loss, ranging from 7% to 21% in the various subregions (Nelson et al., 2005). The World Health Organization (WHO) reported that the number of people affected by hearing loss was approximately over 466 million people in 2018 globally (WHO, 2018).

Against the same backdrop, many studies have found links between environmental noise and a multitude of health disorders, including cardiovascular diseases, sleep disturbance, tinnitus, annoyance, hypertension, and hearing loss (WHO, 2011; Basner et al., 2014). The sound pressure level generated depends on factors such as human activities, type of noise source, and distance from the source to the residence (Han et al., 2015; Sordello et al., 2019). The primary cause of occupational noise-induced hearing loss (NIHL) is damage to the hair cells of the cochlea. Exposure to excessive noise can cause temporary or permanent hearing loss. Especially, the case of continuous or repeated long-term exposure to noise is extremely perilous as it can lead to permanent threshold shift (WHO, 2011; Chen et al., 2014; WHO, 2018). According to previous studies, those exposed to high noise level were found to have a significantly poorer QoL (Nitschke et al., 2014; Welch et al., 2018). QoL is a multidimensional concept comprised of physical component summary (PCS) and mental component summary (MCS). It is included in widely-used health surveys, as an end point in medical care (Han et al., 2018).

Citation: Thongtip S, Sangkham S, Srivichai P, Vongruang P. Association between noise exposure and quality of life among people living near stone-mortar factories, Phayao Province, Northern Thailand. Environ. Nat. Resour. J. 2021;19(2):95-102. (https://doi.org/10.32526/ennrj/19/2020050)

NIHL is a major health disorder prevailing in Asia. Lack of healthcare access, lack of preventive management, and lack of awareness are some factors that exacerbate the situation. (Fuente and Hickson, 2011; Alshehri et al., 2019). Stone-mortar industries are one of the major sources of noise pollution, due to the noisy nature of the processes involved. Most stone-mortar factories employ informal labor. The factories then generate loud noise owing to the stone-mortar processes such as stone cutting, and stone grinding (Thongtip et al., 2020a; Thongtip et al., 2020b). These processes have a drastic effect on the health and QoL of the workers and the people living near these factories (Kitcher et al., 2012; Huang et al., 2018). Therefore, we aimed to assess the association between noise exposure and QoL among people living near stone-mortar factories in Phayao Province, Northern Thailand.

2. METHODOLOGY

2.1 Study design, population, and sampling

A cross-sectional descriptive study population was selected from people living near five stone-mortar factories (Figure 1), using a simple random sampling from February to April 2019 in Phayao Province, Northern Thailand. The stone-mortar process in each factory consisted of stone cutting and grinding. The inclusion criteria were subjects who were 18 years old and above, and had lived near the stone-mortar factories for at least one year. The exclusion criteria was subjects who were unable to communicate in Thai language.

The sample size was calculated based on the proportion of quality of life from noise exposure among Thai residents. It was eligible for further

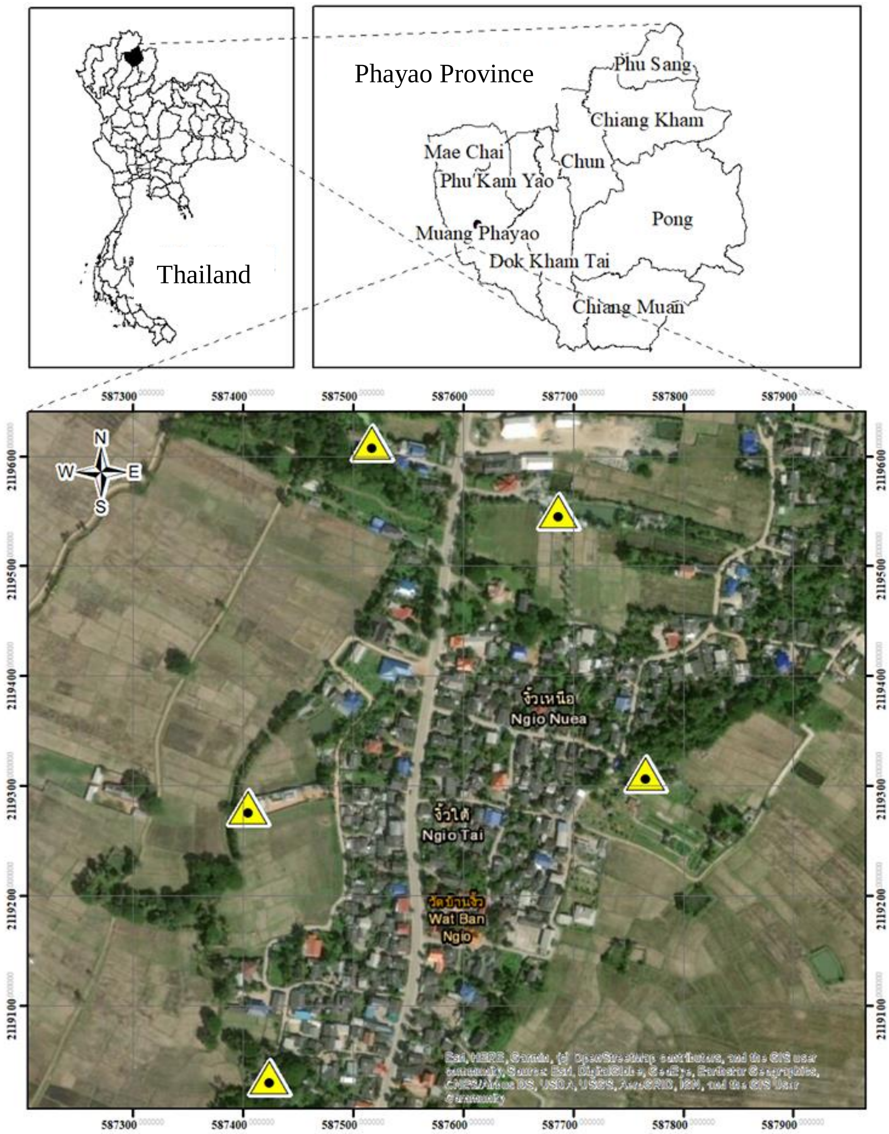

Figure 1. Stone-mortar factories in Phayao Province, Northern of Thailand

analysis at 39.42% (Padungtod et al., 2011). The equation used to obtain the sample size output:

$$n = \frac{N_p(1-p)Z^2 1-\alpha/2}{d^2(N-1)+p(1-p)Z^2 1-\alpha/2}$$

Where; size of population (N) is 642; p=0.3942, Delta (d) is 0.05; Alpha is 0.05, Z (0.975) is 1.960; and sample size (n) is 233.7.

We added at least 15% more to the estimated sample size to allow for losses. Therefore, the sample size was required to be 269 subjects.

2.2 Data collection and measurement

The data was collected utilizing questionnaires that inquired information related to demographic data (sex, age, income, marital status, education, and occupation), lifestyle habits (cigarette and alcohol usage), residential distance, and length of stay in the community.

The noise levels were measured using 21 samplers from five stone-mortar factories. The instrument used for measuring the noise level was the sound level meter: RION, Japan calibrated with the help of a calibrator of 94 dB at 1,000 Hz. Sound level meters set on the A-scale with slow response can be used to assess the noise level effectively. The meter was set up at ear height. Furthermore, the residential distance was measured using Geographic Information System (GIS) technique.

The SF-36 is a generic measure of health status in accordance with which the questionnaire was designed. It was developed by Ware et al. (1994) and Ware et al. (1998) and the Thai version of SF-36 was translated by Jirarattanaphochai et al. (2005). The SF-36 is a questionnaire assessing the QoL with two components: PCS and MCS. It has 36 items and eight scales: physical functioning (PF), physical role limitations (RP), bodily pain (BP), general health (GH), vitality/energy/fatigue (VT), social functioning (SF), emotional role limitations (RE), and mental health (MH). Component analysis showed that there are two distinct concepts measured by the SF-36: a physical dimension, represented by PCS, and a mental dimension, represented by MCS.

2.3 Statistical analysis

Descriptive statistics illustrated frequencies, percentage, means, standard deviations, and maximum-minimum values. Inferential statistics utilized independent t-test, ANOVA, and Pearson's correlation coefficient test. Additionally, the association of residential distance with noise exposure was estimated using the multiple binary logistic regression analysis. Statistically significance was defined at p-value <0.05.

2.4 Ethical consideration

The study was approved by the Research Ethics Committee of University of Phayao, Thailand (No. 2/079/61).

3. RESULTS

Stone-mortar factories entailed informal labor, and most people lived near the five stone-mortar factories as shown in Figure 1. The results revealed that among the participants, 166 were females (61.7%) and 103 were males (38.3%). The average age of the sample was 55.4 years old, with an average income of 4,307 baht per month. The average length of stay in community was found to be 52.2 years. Furthermore, the average distance between the residents and stone-mortar factories was calculated to be 139.3 m. The proportion of noise at ≥85 dB(A) was 71.4% (Table 1).

Table 1. Characteristics of sample populations

Characteristics (n=269)	n (%)
Sex	
Male	103 (38.3)
Female	166 (61.7)
Age (years), mean±SD	55.4±15.1
≤40	38 (14.1)
41-59	134 (49.8)
≥60	97 (36.1)
Income (baht/month), mean±SD	4,748.7±5,758.3
≤1,000	99 (36.8)
1,001-4,000	71 (26.4)
≥4,001	99 (36.8)
Marital status	
Single	33 (12.3)
Married	209 (77.7)
Divorce	27 (10.0)
Education	
≤Primary school	200 (74.3)
>Secondary school	69 (25.7)
Occupation	
Unemployed	68 (25.3)
Daily hired workers	79 (29.4)
Agriculture	57 (21.2)
Others	65 (24.2)

Table 1. Characteristics of sample populations (cont.)

Characteristics (n=269)	n (%)
Length of stay in the community (years), mean±SD	52.2±18.5
≤40	63 (23.4)
41-59	116 (43.1)
≥60	90 (33.5)
Cigarette usage	
No	228 (84.8)
Yes	41 (15.2)
Alcohol usage	
No	207 (77.0)
Yes	62 (23.0)
Residential distance (m), mean±SD	139.3±52.4
≤150 m	163 (60.6)
>150 m	106 (39.4)
Noise exposure (dB(A)), mean±SD	90.1±6.6
<85	77 (28.6)
≥85	192 (71.4)

The average noise in factory no. 4 and 5 was higher than the standard level assigned by the National Institute for Occupational Safety and Health (NIOSH) at 85 dB(A) and the Occupational Safety and Health Administration (OSHA) at 90 dB(A) for an 8-hour time-weighted average (TWA), while the average noise in factories no. 1 and 3 was lower than the standard level of NIOSH at 85 dB(A) and OSHA at 90 dB(A) for an 8-hour TWA (Table 2).

Table 2. Noise exposure in stone mortar factories

Stone mortar factories (n=21)	Noise level (dB(A))	
	Mean±SD	Max-Min
Factory 1 (n=4)	79.9±10.7	106.7-49.5
Factory 2 (n=2)	90.6±6.2*	105.8-47.1
Factory 3 (n=5)	83.0±10.6	102.0-52.5
Factory 4 (n=5)	93.4±8.3*	110.2-68.3
Factory 5 (n=5)	95.5±6.7*	113.4-54.8

n=number of noise samplers for each factory; *Higher than the standard level of NIOSH at 85 dB(A) and OSHA at 90 dB(A) for an 8-hour TWA (NIOSH, 2018)

The average PCS scores obtained from the QoL assessment were found to be higher than those of the healthy Thai national volunteers. The values corresponded to 81.2 and 75.1, respectively. The average MCS and SF scores were lower than those of healthy Thai national volunteers, corresponding to 75.6, 68.8, and 76.7, respectively (Table 3).

Table 3. Mean±SD of QoL score of subjects and Thais' healthy national volunteers

QoL domains	QoL	QoL
	Overall	Thais' volunteer[a]
Physical component summary (PCS)	81.2±15.9	75.1±20.6
- Physical functioning (PF)	88.9±17.4	77.3±17.4
- Physical role limitations (RP)	83.2±33.4	82.2±28.6
- Bodily pain (BP)	85.5±18.6	75.6±18.4
- General health (GH)	67.2±17.6	65.1±18.1
Mental component summary (MCS)	75.6±11.8*	76.7±19.1
- Vitality/energy/fatigue (VT)	70.6±13.6	62.2±13.3
- Social functioning (SF)	68.8±22.0*	78.2±18.2
- Emotional role limitations (RE)	87.8±29.8	80.4±31.9
- Mental health (MH)	75.2±14.5	66.1±12.9

[a]Thais' healthy national volunteers (Lim et al., 2008) *Lower than the QoL Thais' volunteer

Significant differences were observed in the income, marital status, education, and PCS of people living near the stone-mortar factories. However, there were not significant differences found in demographics, health characteristics (cigarette and alcohol consumptions usage), residential distance, noise exposure, and QoL (Table 4).

There was a significant correlation found between residential distance from stone-mortar factories (m) and the noise exposure to the people living near these factories. However, there was no significant difference exhibited in the value of noise exposure and QoL of people living near stone-mortar factories (Table 5).

Table 4. Association between demographics, health characteristics, residential distance, noise exposure, and QoL

Characteristics	PCS	p-value	MCS	p-value	Overall	p-value
Sex[a]						
Male	82.0±16.7	0.487	75.4±12.2	0.827	78.7±13.1	0.734
Female	80.7±15.4		75.7±11.6		78.2±12.1	
Age (years)[b]						
≤40	85.0±13.6	0.09	73.8±10.4	0.477	79.4±10.7	0.706

Table 4. Association between demographics, health characteristics, residential distance, noise exposure, and QoL (cont.)

Characteristics	PCS	p-value	MCS	p-value	Overall	p-value
41-59	81.9±14.3		75.4±11.9		78.7±11.7	
≥60	78.7±18.4		76.5±12.1		77.6±14.0	
Income (baht/month)[b]						
≤1,000	78.8±17.9	0.045*	75.7±12.8	0.729	77.3±13.9	0.192
1,001-4,000	80.2±17.4		74.7±12.1		77.4±13.0	
≥4,001	84.3±11.7		76.1±10.5		80.2±10.2	
Marital status[b]						
Single	87.5±8.5	0.039*	78.7±7.9	0.258	83.1±6.0	0.060
Married	80.0±16.7		75.1±12.5		77.8±13.2	
Divorce	78.3±15.2		75.5±9.6		76.9±10.9	
Education[a]						
≤Primary school	80.1±16.5	0.035*	75.2±11.9	0.312	77.6±12.7	0.087
>Secondary school	84.4±13.6		76.8±11.5		80.6±11.6	
Occupation[b]						
Unemployed	79.5±18.6	0.432	76.1±13.5	0.960	75.2±14.7	0.881
Daily hired workers	81.5±15.5		75.6±10.5		78.2±11.4	
Agriculture	79.9±15.5		75.6±11.8		76.4±12.2	
Others	83.7±13.6		75.0±11.6		79.0±11.4	
Length of stay in community (years)[b]						
≤40	83.2±14.3	0.145	73.2±11.0	0.166	78.5±11.3	0.683
41-59	82.1±14.3		76.1±12.0		77.4±11.9	
≥60	78.6±18.4		76.6±12.0		76.0±13.9	
Cigarette usage[a]						
No	80.9±16.0	0.538	75.3±12.2	0.305	78.1±12.7	0.380
Yes	82.6±15.2		77.3±9.4		80.0±19.7	
Alcohol usage[a]						
No	80.6±16.1	0.242	75.6±11.9	0.955	78.1±12.7	0.440
Yes	83.3±15.0		75.7±11.4		79.5±11.7	
Residential distance (m)[a]						
≤150 m	81.5±15.9	0.650	76.2±11.6	0.314	78.7±12.1	0.444
>150 m	80.6±15.9		74.7±12.0		77.7±12.9	
Noise exposure (dB(A))[a]						
<85	79.6±18.3	0.295	74.6±13.0	0.393	77.1±14.3	0.283
≥85	81.8±14.8		75.9±11.3		78.9±11.6	

[a]Presented as Independent t-test, [b]ANOVA; *p<0.05

Table 5. Association between demographics, residential distance and QoL

Characteristics	Noise exposure[a]		p-value	Noise exposure[b]
	<85 dB(A)	≥85 dB(A)		p-value
Age (years)	55.1±13.5	55.5±15.8	0.855	0.959
Income (baht/month)	5,252.8±7,751.5	3,940.9±4,568.5	0.181	0.067
Length of stay in community (years)	51.2±17.2	52.6±19.0	0.576	0.617
Residential distance (m)	129.6±43.4	123.2±55.2	0.032*	0.299
Quality of life (QoL)				
PCS	79.6±18.3	81.8±14.8	0.295	0.301
MCS	74.6±13.0	76.0±11.3	0.393	0.388
Overall	77.1±14.3	78.9±11.6	0.283	0.285

[a]Presented as Independent t-test, [b]Pearson's correlation coefficient test; *p<0.05

The multiple binary logistic regression analysis showed that an increasing residential distance must be associated with a high noise exposure after adjusting for age (years), education, income (baht/month), length of stay in community (years), and overall QoL (Table 6).

Table 6. Association between residential distance and noise exposure using multiple binary logistic regression analysis

Associated factors	B	SE	p-value
Residential distance (m)	0.006	0.003	0.032*

Adjust with age (years), education, income (baht/month), length of stay in community (years), and overall QoL; *p<0.05

4. DISCUSSION

Noise is an unwanted sound and excessive and prolonged exposure to noise may have adverse effects on the health of workers and people living around those noise sources (Padungtod et al., 2011; WHO, 2011). Our study found that the average distance between residents and stone-mortar factories was 139.3 m. The proportion of noise at ≥85 dB(A) was 71.4%. The average noise in factory no. 2, 4, and 5 was higher than the standard level of the NIOSH Recommended Exposure Limit (REL) for occupational noise exposure standard of 85 dB(A) and OSHA's permissible exposure limit (PEL) is 90 dB(A) for an 8-hour TWA (NIOSH, 2018). Noise levels above the standard level may be caused due to the work processes involved such as stone cutting and grinding, maintenance, etc. (Landen et al., 2004; Huang et al., 2018). Additionally, several studies have suggested that the sources of noise pollution should be provided engineering controls, administrative controls, and work practices to loud noise (WHO, 2001; Fonseca et al., 2016).

The average MCS and SF scores exhibited by our study were lower than those of healthy Thai national volunteers (Lim et al., 2008). Significant differences were found in income, marital status, education, and PCS of people living near stone-mortar factories. Evidence suggests that abnormal MCS and SF may be related to depressive symptoms, comorbid mental health, as well as emotional and behavioral coping. These aspects may eventually lead to lasting social impairment (McKnight and Kashdan, 2009; D'Souza et al., 2013). The findings were hence consistent with our hypothesis, that demographics are significantly associated with the QoL (Wang et al., 2008).

As aforementioned, our study found that there existed significant differences in the income, marital status, education, and PCS of people living near stone-mortar factories. However, no significant differences were revealed in the demographics, health characteristics (cigarette or alcohol usage), residential distance, noise exposure, and QoL. There was no significant association found between noise exposure and QoL of people living near stone-mortar factories. Previous studies have found that factors such as marriage, shorter duration of stay in the community, education, economic status, enduring illness, social, cognitive, emotional and behavioral coping were significantly associated with QoL (D'Souza et al., 2013). QoL may have several possible confounding factors that affect this association such as daily activities, BMI, chronic diseases, and geographical region (Wang et al., 2008). Besides that, noise pollution is also emitted by community activities, traffic, and other industries (Ali et al., 2018; Sordello et al., 2019).

Our study found that there was significant difference between residential distance from stone-mortar factories (m) and noise exposure to people living near these factories. Interestingly, the multiple binary logistic regression analysis showed that an increasing residential distance is associated with a high noise exposure after adjusting for age (years), education, income (baht/month), length of stay in community (years), and overall QoL. The findings were inconsistent with our results that statistically significantly higher levels of environmental noise sources when compared to people living near environmental noise sources (Tenailleau et al., 2015; Boyle et al., 2017). Previous studies have suggested that increased age was the main issue with regards to hearing loss in stone-mortar workers (Thongtip et al., 2020a). This conclusion was found to be consistent with our results that the average age of people living near stone-mortar factories was 55.4 years old with an average length of stay in the community of 52.2 years. In additional to that, all stone-mortar factories were located around communities as shown in figure 1. Therefore, there are other possible determinants including socioeconomic status, air pollution, roadway proximity variables, community activities, traffic, and other industries that might be taken into consideration to reach a conclusive result (Correia et al., 2013; Ali et al., 2018; Sordello et al., 2019).

A limitation of this study was the cross-sectional design to explore the association of residential distance with noise exposure. Therefore, further research is required to focus on a longitudinal study that factors in other aspects such as noise levels in all seasons with respect to the adverse health effects associated with living in close proximity to stone-mortar factories. Moreover, further research should measure noise levels in the receptors or people living near these factories.

To conclude, findings of this study indicate that people living near stone-mortar factories are being exposed to low environmental noise. In order to examine the detrimental effects of the same, other possible confounders might be take into consideration. However, the average noise in some factories was found to be higher than the standard level of NIOSH at 85 dB(A) and OSHA at 90 dB(A) for an 8-hour TWA. Therefore, the local policy makers should be required to emphasize the reduction of noise pollution in stone-mortar factories, and increase the health surveillance of the residential neighborhood.

ACKNOWLEDGEMENTS

The authors sincerely thank the factory and stone-mortar workers for supporting this research.

REFERENCES

Ali A, Hussain RM, Dom NC, Rashid RI. A profile of noise sensitivity on the health-related quality of life among young motorcyclists. Noise and Health 2018;20(93):53-9.

Alshehri KA, Alqulayti WM, Yaghmoor BE, Alem H. Public awareness of ear health and hearing loss in Jeddah, Saudi Arabia. South African Journal of Communication Disorders 2019;66(1):1-6.

Basner M, Babisch W, Davis A, Brink M, Clark C, Janssen S, et al. Auditory and non-auditory effects of noise on health. Lancet 2014;383(9925):1325-32.

Boyle MD, Soneja S, Quirós-Alcalá L, Dalemarre L, Sapkota AR, Sangaramoorthy T, et al. A pilot study to assess residential noise exposure near natural gas compressor stations. PloS One. 2017;12(4):e0174310.

Chen GD, Decker B, Muthaiah VP, Sheppard A, Salvi R. Prolonged noise exposure-induced auditory threshold shifts in rats. Hearing Research 2014;317:1-8.

Chepesiuk R. Decibel hell: The effects of living in a noisy world. Environmental Health Perspectives 2005;113(1):34-41.

Correia AW, Peters JL, Levy JI, Melly S, Dominici F. Residential exposure to aircraft noise and hospital admissions for cardiovascular diseases: Multi-airport retrospective study. British Medical Journal 2013;347:f5561.

D'Souza MS, Karkada SN, Somayaji G. Factors associated with health-related quality of life among Indian women in mining and agriculture. Health Qual Life Outcomes 2013;11:9.

Fonseca VR, Marques J, Panegalli F, Gonçalves CGO, Souza W. Prevention of the evolution of workers' hearing loss from noise-induced hearing loss in noisy environments through a hearing conservation program. International Archives of Otorhinolaryngology 2016;20(1):43-7.

Fuente A, Hickson L. Noise-induced hearing loss in Asia. International Journal of Audiology 2011;50(sup1):3-10.

Han L, Li Y, Yan W, Xie L, Wang S, Wu Q, et al. Quality of life and influencing factors of coal miners in Xuzhou, China. Journal of Thoracic Disease 2018;10(2):835-44.

Han ZX, Lei ZH, Zhang CL, Xiong W, Gan ZL, Hu P, et al. Noise monitoring and adverse health effects in residents in different functional areas of Luzhou, China. Asia Pacific Journal of Public Health 2015;27(sup2):93-9.

Huang FJ, Hsieh CJ, Young CH, Chung SH, Tseng CC, Yiin LM. The assessment of exposure to occupational noise and hearing loss for stoneworkers in Taiwan. Noise and Health 2018;20(95):146-51.

Jirarattanaphochai K, Jung S, Sumananont C, Saengnipanthkul S. Reliability of the medical outcomes study short-form survey version 2.0 (Thai version) for the evaluation of low back pain patients. Journal of the Medical Association of Thailand 2005;88(10):1355-61.

Kitcher ED, Ocansey G, Tumpi DA. Early occupational hearing loss of workers in a stone crushing industry: our experience in a developing country. Noise and Health 2012;14(57):68-71.

Landen D, Wilkins S, Stephenson M, McWilliams L. Noise exposure and hearing loss among sand and gravel miners. Journal of Occupational and Environmental Hygiene 2004;1(8):532-41.

Lim LL, Seubsman SA, Sleigh A. Thai SF-36 health survey: Tests of data quality, scaling assumptions, reliability and validity in healthy men and women. Health and Quality of Life Outcomes 2008;6(1):52.

McKnight PE, Kashdan TB. The importance of functional impairment to mental health outcomes: A case for reassessing our goals in depression treatment research. Clinical Psychology Review 2009;29(3):243-59.

National Institute for Occupational Safety and Health (NIOSH). Noise and hearing loss prevention guidance and regulations [Internet]. 2018 [cited 2020 Feb 20]. Available from: https://www.cdc.gov/niosh/topics/noise/reducenoiseexposure/regsguidance.html.

Nelson DI, Nelson RY, Concha-Barrientos M, Fingerhut M. The global burden of occupational noise-induced hearing loss. American Journal of Industrial Medicine 2005;48(6):446-58.

Nitschke M, Tucker G, Simon DL, Hansen AL, Pisaniello DL. The link between noise perception and quality of life in South Australia. Noise and Health 2014;16(70):137-42.

Padungtod C, Ekpanyaskul C, Nuchpongsai P, Laemun N, Matsui T, Hiramatsu K. Aircraft noise exposure and its effects on quality of life and cognitive function among thai residents. Epidemiology 2011;22(1):259.

Seidman MD, Standring RT. Noise and quality of life. International Journal of Environmental Research and Public Health 2010;7(10):3730-8.

Sordello R, De Lachapelle FF, Livoreil B, Vanpeene S. Evidence of the environmental impact of noise pollution on biodiversity: A systematic map protocol. Environmental Evidence 2019;8(1):8.

Tenailleau QM, Bernard N, Pujol S, Houot H, Joly D, Mauny F. Assessing residential exposure to urban noise using environmental models: Does the size of the local living neighborhood matter?. Journal of Exposure Science and Environmental Epidemiology 2015;25(1):89-96.

Thongtip S, Sangkham S, Sukpromson R. Factors associated with occupational hearing loss among stone-mortar workers in Phayao Province, Northern Thailand. Journal of Health Science and Medical Research 2020a;38(3):213-9.

Thongtip S, Siviroj P, Prapamontol T, Deesomchok A, Wisetborisut A, Nangola S, et al. A suitable biomarker of effect, club cell protein 16, from crystalline silica exposure among Thai stone-carving workers. Toxicology and Industrial Health 2020b;36(4):287-96.

Wang R, Wu C, Zhao Y, Yan X, Ma X, Wu M, et al. Health related quality of life measured by SF-36: A population-based study in Shanghai, China. BMC Public Health 2008;8(1):292.

Ware Jr JE, Gandek B. The SF-36 health survey: Development and use in mental health research and the IQOLA Project. International Journal of Mental Health 1994;23(2):49-73.

Ware Jr JE, Gandek B. Overview of the SF-36 health survey and the International Quality of Life Assessment (IQOLA) Project. Journal of Clinical Epidemiology 1998;51(11):903-12.

Welch D, Dirks KN, Shepherd D, McBride D. Health-related quality of life is impacted by proximity to an airport in noise-sensitive people. Noise and Health 2018;20(96):171-7.

World Health Organization (WHO). Occupational exposure to noise: Evaluation, prevention and control [Internet]. 2001 [cited 2020 Feb 20]. Available from: https://www.who.int/occupational_health/publications/occup noise/en/.

World Health Organization (WHO). Burden of disease from environmental noise [Internet]. 2011 [cited 2020 Feb 20]. Available from: https://www.who.int/quantifying_ehimpacts/publications/e94888/en/.

World Health Organization (WHO). Addressing the rising prevalence of hearing loss [Internet]. 2018 [cited 2020 Feb 20]. Available from: https://apps.who.int/iris/handle/10665/260336.

Estimation of the Recyclable Waste amount Collected by Informal Recycling Shops: Case Study in Nay Pyi Taw, Myanmar

Chit Oo Ko*, Ye Tun, Naing Htet Lwin, Thazin Moe, and Juu Eaindray

Environmental Conservation Department, Ministry of Natural Resources and Environmental Conservation, Nay Pyi Taw 15011, Myanmar

ARTICLE INFO

Received: 4 Aug 2020
Received in revised: 6 Oct 2020
Accepted: 14 Oct 2020
Published online: 2 Dec 2020
DOI: 10.32526/ennrj/19/2020157

Keywords:
Nay Pyi Taw/ Recyclable waste/ Type/ Amount/ Informal recycling shops

*** Corresponding author:**
E-mail: uchitooko.env@gmail.com

ABSTRACT

The study investigates and estimates the type and amount of recyclable waste collected by informal recycling shops in Nay Pyi Taw by using face to face interview for 23 informal recycling shops in Nay Pyi Taw in May 2020. The descriptive statistics (frequency and percentage) and inferential statistics (two-sample paired t-test and Pearson's correlation) were applied. According to the results, the average estimated waste amount collected by each recycling shop per day before and during the novel coronavirus (COVID-19) pandemic was 1,798 kg (Min. 0 to Max. 1,401 kg) and 856 kg (Min. 0 to Max. 892 kg), respectively. As a result of this study, it can be seen that the amount of daily collected waste has a positive relationship with the daily income of recycling shops, and COVID-19 has impacted the income of informal recycling shops. According to the results, getting an official license, financial problems, and limited land for managing buying recyclable waste, unstable market conditions, no factory in Nay Pyi Taw and no definitive legislation or laws, seasonal changes are the main challenges for informal recycling shops. This study indicates the ways to mainstream the informal sectors in waste management schemes. In addition, the results of this study can be useful in developing national and regional waste management plans and programs.

1. INTRODUCTION

Due to the increasing population and waste generation in developing countries, it is challenging for municipalities, to provide basic infrastructure and waste collection as well (Kyessi et al., 2017; Omar, 2019). Myanmar, one of the developing countries, also faces these kinds of challenges due to the increasing population, lack of effective waste management systems, limited basic infrastructure, etc. Such challenges increase the negative impacts on public health and environment which result from the increase of waste generation in the three largest cities (Yangon, Mandalay, and Nay Pyi Taw) in Myanmar (ECD, 2020).

There is no doubt that the rate of waste generation is beyond the ability of responsible authorities to manage it, especially in the developing countries like Myanmar. Moreover, rapid urban growth in developing countries can also be challenging to the authorities who provide basic infrastructure for their residents. More than 50% of the waste cannot be dealt with in developing countries (Omar, 2019). Municipalities and other formal sectors have financial and organizational limitations for recycling all recyclable wastes (Gerold, 2009).

Currently, city and township development committees are the focal departments in charge of collecting and disposing waste in Myanmar (ECD, 2020). It is clear that in Myanmar, the above-mentioned challenges can also definitely be faced. For instance, the waste amount generated by three major cities (Yangon (2,000 mg/day), Mandalay (955 mg/day), and Nay Pyi Taw (200 mg/day)) were only estimated based on the volume of waste reaching city dump sites, but did not include other uncollected, burned, dumped, recycled, or reused waste (ECD, 2020). Not surprisingly, this is a major challenge to get a complete and realistic estimate of waste generation in this country.

Citation: Ko CO, Tun Y, Lwin NH, Moe T, Eaindray J. Estimation of the recyclable waste amount collected by informal recycling shops: Case study in Nay Pyi Taw, Myanmar. Environ. Nat. Resour. J. 2021;19(2):103-111. (https://doi.org/10.32526/ennrj/19/2020157)

In solid waste management, the informal sector plays a significant role in waste collection activity, especially in low-income and middle-income countries. Informal waste pickers, traders, shops, and recyclers are very important players to establish a strong official waste management system although they are still illegal according to the present legislation, rules and regulations (Schneider et al., 2017). They also contribute effectively to waste management and resource efficiency by collecting, sorting, and trading (Wahab and Ola, 2017).

Informal recycling waste enterprises can contribute to many of the Millennium Development Goals (MDGs) (Gerold, 2009). Therefore, they can also contribute to many of the 17 UN Sustainable Development Goals. Among them, for example, goal (1): end poverty; goal (8): decent work and economic growth; goal (10): reduce inequality; goal (12) ensure sustainable consumption and production patterns; goal (13): deal with climate change; goal (14): improve life below water; goal (15): life on land; etc. could be achieved through mainstreaming the role of informal recycling waste sectors in waste management schemes. For instance, creating jobs and increasing income through informal recycling enterprises can reduce poverty among the community so that the well-being of the local community can be achieved. Moreover, natural resources depletion, reducing waste disposal and required land area for waste disposal, and reducing greenhouse gases can be addressed by recycling waste (Gerold, 2009; Hoornweg and Bhada-Tata, 2012). There is no doubt that the essence of recycling is to conserve and protect natural resources, both life on land and in the water, which means that the SDG goal (14) and (15) can also be addressed through mainstreaming of recycling sectors. Ngoc and Schnitzer (2009) also stated that the recovery of waste materials (reuse and recycle) is the way to reach the goal of "using everything, nothing left".

In Myanmar, the amount of greenhouse gases (GHGs) emissions could be saved around 1,100 Gg of CO_2-eq per year by changing the waste management system to landfill 65%, recycling 10%, incineration 1%, anaerobic digestion 1%, composting 10%, and others 13% from business-as-usual, open dumping 83%, recycling 2%, incineration 1%, anaerobic digestion 1%, and others 13%. This saving could be achieved by increasing the percentage of recycling from 2% to 10%. To conclude, a huge amount of GHG emissions could be saved in the recycling sector by saving raw materials and natural resources (Tun and Juchelková, 2018).

Nay Pyi Taw became the new capital city of Myanmar in 2005, and it is also the seat of the Union Government. As the late arrival new city, there are limited data and information in all sectors including waste management related to informal waste sectors. As informal waste sectors are crucial not only for developing strong waste management systems but also for creating a cleaner environment, estimating the amount of recyclable waste collected by informal recycling shops would create more understanding of their role in the waste management sector for the relevant decision makers. Therefore, this study aims to estimate the amount of recyclable waste collected by informal recycling shops in Nay Pyi Taw. The result of this study can not only contribute to a better understanding of the role of informal recycling shops, but it can also be used to support the decision makers, especially in terms of how to mainstream them in the waste management scheme through investigating their difficulties and challenges.

2. METHODOLOGY

2.1 Data collection

This study was conducted in Nay Pyi Taw, Myanmar. This is the new capital city of Myanmar with a total area of 70,571 km^2. It is located at 19.75 latitude and 96.13 longitude and situated at elevation 122 m.a.s.l. A total of 1,160,242 residents are living in Nay Pyi Taw which consists of two districts and eight townships as shown in Figure 1 (Department of Population, 2015).

In this study, both snowball and quota sampling methods were used. The snowball method was used to find where recycling shops are situated because there is no secondary data regarding recycling shops in Nay Pyi Taw. According to the initial investigation using the snowball method, there are around 200 recycling shops in Nay Pyi Taw. Based on this estimation, 23 informal recycling shops in Nay Pyi Taw were selected with ±20 margin of error and 95% confidence level (Israel, 1992; Conroy, 2006). In order to cover all the areas of Nay Pyi Taw, the interviewed shops were selected in all eight townships of Nay Pyi Taw. However, there is no exact data relating to how many recycling shops are in each township. That is why the selection of the shops in each township was based on the population size of the respective township, hoping that the more populated township would dispose more waste, and have more recycling shops. Therefore, the interviewed recycling shops were selected as shown in Table 1. The first interviewed shop in each township was selected by asking people who live in that township, and determining where these shops are located. The next destinations were also selected based on the first interviewed shop. The quota sampling method was applied to meet the target of respondents in each township. The questionnaire was composed of both open-ended and close-ended questions, and it was completed with face to face interviews.

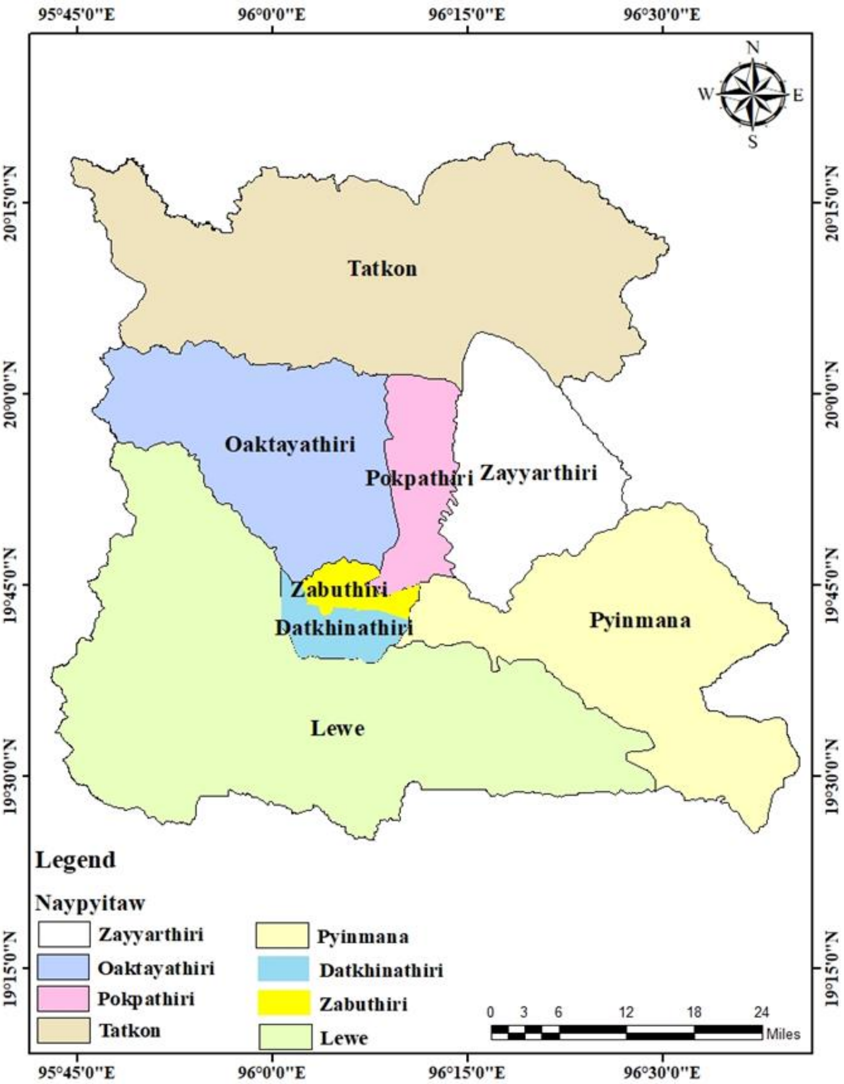

Figure 1. Map of the study area

Table 1. Selected number of recycling shops in each township

No	Township	Population	Selected number of recycling shops
1	Lewe	284,393	5
2	Tatkon	217,093	4
3	Pyinmana	187,565	4
4	Pokpathiri	116,491	2
5	Zayyarthiri	111,293	2
6	Zabuthiri	110,459	2
7	Oaktayathiri	81,620	2
8	Datkhinathiri	51,328	2
Total		1,160,242	23

Source: Department of Population (2015)

2.2 Estimation of the recyclable waste amount collected by informal recycling shops

The data resulting from the field survey was analyzed with the aid of the Statistical Package for Social Sciences (SPSS) software (Version 24), and presented using descriptive statistics in the form of frequency distribution of the types of waste collected by recycling shops in order to estimate how much recyclable waste was collected by informal recycling shops.

To determine the relationship between the daily income of waste recycling shops and the amount of daily collected waste by them, the Pearson's correlation (equation 1) was used. The value of correlation coefficient is between -1 and +1 (Obilor and Amadi, 2018; Ceylan et al., 2018). Interpreting the correlation coefficients are accepted based on the following points: 0 and 0.3 (0 and -0.3) indicate a weak positive (negative) linear relationship; 0.3 and 0.7 (0.3 and -0.7) indicate a moderate positive (negative) linear relationship; 0.7 and 1.0 (-0.7 and -1.0) indicate a strong positive (negative) linear relationship (Ratner, 2009).

$$r = \frac{S_{xy}}{S_x\,S_y} \tag{1}$$

Where; r is the correlation coefficient, S_{xy} is the covariance of variable x (daily collected waste amount-kg) and variable y (daily income in Myanmar kyat-MMK), S_x is the standard deviation of variable x (collected waste amount-kg) and S_y is the standard deviation of variable y (income-MMK).

The novel coronavirus (COVID-19) pandemic has impacted on both health and different business sectors of Myanmar (The Asia Foundation, 2020). Because the informal waste recycling shops are also included in the income generating business sectors in Myanmar, it was assumed that the pandemic would also impact on this sector. To test this notion further, in this study, the effect of COVID-19 on the amount of waste collected by recycling shops was also investigated by using equation 2 (inferential statistics: two-sample paired t-test). A paired t-test can be used when the observed data are in pairs (McDonald, 2014). Due to the data collection being carried out during the COVID-19 pandemic, the respondents were requested to estimate the amount of waste collected both before and during the pandemic at the time of the interview to determine the statistical significance of variations in the amount of waste collected by them due to the pandemic.

$$t = \frac{\bar{d}}{S_d/\sqrt{n}} \tag{2}$$

Where; t is the calculated t value, $\bar{d}$ is the difference within a pair, S_d is the standard deviation of differences, and n is the sample size (Constance and Robert, 2012).

Moreover, in this study, job creation (employment to population ratio) of informal recycling shops was also calculated by using the equation 3 (Department of Population, 2015). In equation 3, employed means the average number of employees working at each recycling shop, and total population is the total population of Nay Pyi Taw in 2014.

$$\text{Employment to population ratio} = \frac{\text{Employed}}{\text{Total population}} \times 100 \tag{3}$$

3. RESULTS AND DISCUSSION

3.1 Types and amount of waste collected by informal recycling shops

Table 2 shows the summary of types and amount of waste collected by informal recycling shops before and during the COVID-19 pandemic. According to the results, it can be clearly seen that the total waste amount collected by the shops before and during the pandemic differ. This means that there was a negative impact on the recycling shops, especially in the decreasing collection of recyclable waste which led to a decrease in income. Like the pandemic's effect on the recycling shops, it also had serious negative impacts on the other business sector in Myanmar. According to the survey of the Asia Foundation on the impacts of COVID-19 on business in Myanmar, 218 enterprises out of 750 were closed

Table 2. Type and amount of waste collected by informal waste recycling shops

No.	Type of waste	Average amount of waste (Before COVID-19) (kg/day)	Percentage (%)	Average amount of waste (During COVID-19) (kg/day)	Percentage (%)
1	Plastics	510 (Min. 0-Max. 2,450)	28	219 (Min. 0-Max 2,450)	25
2	Cardboard	197 (Min. 0-Max. 1,388)	11	85 (Min. 0-Max. 694)	10
3	Metal	282 (Min. 0-Max. 2,450)	16	111 (Min. 0-Max. 1,225)	13
4	Paper	138 (Min. 0-Max. 490)	8	41 (Min. 0-Max. 163)	5
5	Aluminum	20 (Min. 0-Max. 63)	1	9 (Min. 0-Max. 82)	1
6	Glass	599 (Min. 0-Max. 3,919)	33	380 (Min. 0-Max. 2,450)	44
7	Tins and cans	38 (Min. 0-Max. 245)	2	9 (Min. 0-Max. 38)	1
8	e-waste	14 (Min. 0-Max. 105)	1	2 (Min. 0-Max. 35)	1
Total		1,798 (Min. 0-Max.1,401)	100	856 (Min. 0-Max. 892)	100

at the time of survey (between April 28 and May 10, 2020) (The Asia Foundation, 2020). It can be concluded that the income generation of these affected enterprises also declined because of the effects of the pandemic.

All the recyclable waste was collected from households, street recycling collectors, municipal staff, and other places such as restaurants and construction sites. After collecting the recycling waste, 44% and 39% of recycling shops sent their waste directly to recycling factories in Yangon and Mandalay, and big recycling shops in Nay Pyi Taw. The remaining 17% sent their collected waste to both of them. According to the Table 2, among the two (before and during the COVID-19 pandemic), the average composition of glass accounted for the highest proportion: 33% and 44% respectively. In a similar study conducted in Yangon, Myanmar, among the daily recyclable waste amount collected by waste dealers, glass occupied the highest amount of proportion for 57% (Premakumara et al., 2017).

3.2 Job opportunities and income generation of informal recycling shops

The results show that 61% of recycling shops have been working only in informal recycling, and 34% have been working together with others including taxi drivers, needlework, shops, etc. Others 4% are employed also as farmers. During the survey, the number of years that each interviewer has been working in this business was also recorded. According to the results, 48% of respondents have been working in recycling shops for 10 years and above, and 30% of respondents have 1 to 5 years of experience in this business. The remaining 13% and 9% have 6 to 9 years and less than 1 year of experience respectively.

Regarding job creation, the results show that each recycling shop created job opportunities for 14 employees on an average. In a similar study conducted in Myanmar, the average number of 13 daily-wage laborers is working at recycling business (Chelsea, 2019). A total of 1,160,242 residents are living in Nay Pyi Taw (Department of Population, 2015). Therefore, using equation 3, employment to population ratio (per recycling shop) is 0.001. If the number of employed is considered based on all estimated recycling shops (200 shops) in Nay Pyi Taw, the ratio is 0.24. In Nay Pyi Taw, the number of government employees was 87,003 (Department of Population, 2015). This makes the employment to population ratio 7.5. By comparing these two ratios, unfortunately, although the employment to population ratio of recycling shop is smaller than the ratio of government employees, it is still clear that the recycling shops are providing and generating job opportunities for the residents. Once again, Wahab and Ola (2017) also showed that job opportunities, income generation, and reduction in uncollected waste can be created by informal recycling sector.

During the survey, the respondents were requested to estimate the income of the recycling shops before the pandemic because of the difficulties to estimate the income during the pandemic as almost all the respondents operated their recycling shops only one to two weeks before interviewed. The result shows that each recycling shop earned approximately 400,000 MMK (Min. 150,000 MMK and Max. 1,000,000 MMK) net income per month. According to the Pearson's correlation, a significant positive relationship (r^2=0.65, $p<0.001$) was observed between the daily income of informal waste recycling shops and their daily collected waste before the pandemic (Figure 2). This can intuitively be understood as the more waste collected, recycling shops would earn more income.

Moreover, as a result of the paired t-test, the daily amount of waste collected by the recycling shops was significantly different ($t(22)=3.62$, $p<0.05$) before and during the pandemic. Therefore, this means that the pandemic affected the daily collected waste amount of recycling shops. As discussed above, as the income of the recycling shops was directly connected with the collected waste amount, the pandemic affected the income of the recycling shop, too. Another study also showed that the income of different enterprises was also negatively affected by the pandemic just like the income of recycling shops (The Asia Foundation, 2020).

3.3 Main challenges of informal recycling shops

During the interview almost all of the respondents answered that the main challenge they have been facing was getting an official license. Although they are very willing to get the license by paying appropriate license fees, the problem is the limitation of the current law, policy and legislation. Chelsea (2019) also showed that most of the recycling business accepted that being registered has positive impacts.

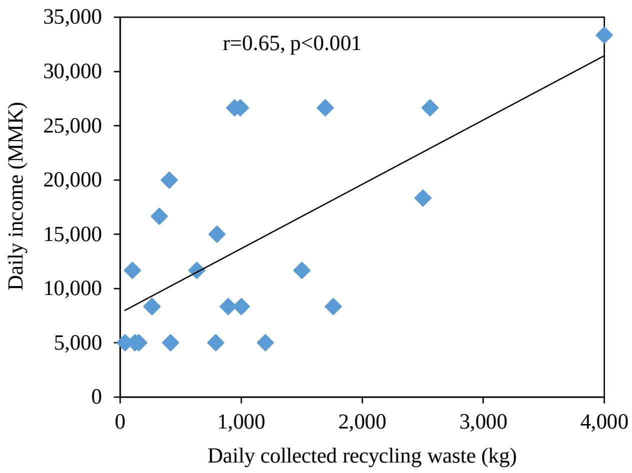

Figure 2. Relationship between daily collected recycling waste and daily income

In Myanmar, waste pickers, waste collectors and dealers are considered as informal sectors. Newspaper, metal, plastic bottles, and other waste from different places such as households and streets are gathered by waste pickers and waste collectors. Waste dealers buy these collected items from them and sell and send them on to recycling industries (Premakumara et al., 2017). They cannot borrow money from private and government banks without a license. Mostly they borrow money from microfinance institutions. The interest rates of microfinance institutions and informal lenders are higher than the interest rates of government and private banks (The Asia Foundation, 2020). To conclude, it can be said that policy and institutional factors are still weaknesses relating with informal recycling shops to run their business officially with a license because they are still recognized as an informal sector.

Apart from getting a license, the others challenges are financial problems, limited land for managing buying recyclable waste, unstable market conditions, etc. During the survey, the perceptions of respondents were polled in order to know which difficulties should be addressed step by step by decision makers relating to informal recycling shops. According to the results, as shown in Figure 3, most of the recycling shops (39%) are willing to accept the appropriate financial support to invest in their business. In a similar study, 42% of informal recycling collectors have faced inadequate fund (Wahab and Ola, 2017). Currently, the owners of shops borrow money from microfinance institutions. The second sector which needs to be improved is updating the current law or some other measure for getting safety business sectors because almost all of the respondents have experienced in unsafe situation in the past. The third challenge of recycling shops is the unstable market system because, for example, sometimes they had to buy the recycling waste at a higher rate compared with what they sold it for them. Providing land for managing collected recyclable waste and establishing a recycling factory in Nay Pyi Taw is what the respondents would like the government to improve.

Additionally, seasonal variations have also influenced the informal waste collectors, especially in their collected waste amount and income earned (Wahab and Ola, 2018). Therefore, it is also assumed that seasonal variation could affect the informal recycling shops, too. To test this idea further, the seasonal variation impact on the recycling shops was also recorded. According to the results, 74% of respondents have been affected by seasonal impacts, especially in the types and volume of recycling waste. For instance, they do not collect cardboard in the rainy season because it can easily be destroyed in the rain if it is stored outside because of limited storage area. Chelsea (2019) also stated that recycling business in Myanmar have faced the challenge dealing with limited storage area.

In order to investigate the perception of the owners of recycling shops in regard to their feelings on working in this business, their feedback was recorded. The results show that 44% of the respondents would like to quit the current work because of the above- mentioned challenges, especially when they face weak protection by law. This result is similar to the finding of another study. Wahab and Ola (2017) mentioned that 38% of informal waste collectors are willing to quit the work because of the social stigma.

The next challenge that is created by recycling shops themselves is the poor safety standards for workers. According to the survey result, although 100% of respondents answered that the employees always clean their hands with soap after work, only 30% always use protection equipment during working hours. It could be said that most of the respondents have a low level of health awareness. In another study, 55% of the informal waste collectors did not wear protective equipment during working hours (Wahab and Ola, 2017). Providing personal protective equipment is not the major concern of the owners of recycling business because they assume that it is the extra assistance to their staff (Chelsea, 2019).

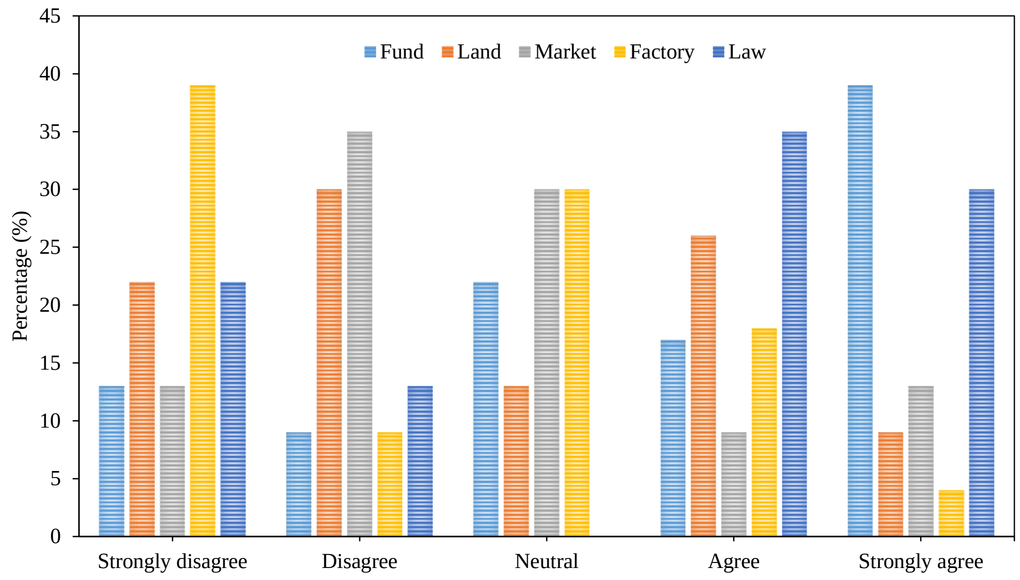

Figure 3. Main sectors needed to be improved

During the survey, in order to understand the perception of the respondents about how to mainstream the recycling shops in waste management activities, their perceptions on the participation of voluntary activities were also recorded. As a result, although 91% of respondents have not experienced on the participation of voluntary work, they are strongly willing to participate in future activities, and they requested to be invited in the future to voluntary activities. Moreover, one of the respondents recommended that, in order to create better cooperation within informal recycling sectors or, if possible, between the informal recycling sector and government, the committee of recycling shops or some special group should be organized in Nay Pyi Taw.

3.4 Recommendation

- The amount of recyclable waste collected by informal recycling shops in Nay Pyi Taw estimated in this study can be contributed to a better understanding of the role of informal recycling shops in the waste management systems.
- The government should provide some kind of special support to informal recycling shops, especially those who have lost their jobs and income because of the COVID-19 pandemic.
- The government or respective decision makers should consider tackling for getting a license as a priority because informal recycling shops have borrowed money from microfinance institutions at high interest rates instead of borrowing money from private and government banks at lower interest rates because of not having a license.
- According to the perception of the respondents, financial support and formulating appropriate legislation and laws need to be implemented as a very first step by the government because, for instance, no definitive legislation or laws to protect informal recycling shops when they face problems are also challenges.
- The government should provide appropriate land to store recyclable waste collected by informal recycling shops at reliable fees because they have faced the impacts of seasonal changes. For instance, the problem of not being able to collect cardboard in the rainy season because of insufficient storage.
- Do’s and don’ts concerning with waste management should be disseminated via television programs, magazines, newspapers, and online media (Facebook, YouTube, etc.) because employees in informal recycling shops seem to have less awareness of health protection system: they do not use the protective equipment at the time of working hours.
- The government should try to create better cooperation with informal recycling shops by organizing the committee of recycling shops or some special group of recycling shops in Nay Pyi Taw because this could contribute to mainstream the informal recycling shops in waste management schemes.
- The government should provide some technical support and capacity building programs for

improving the current status of informal recycling sectors (e.g., providing technical assistance for creating new items from waste). As a result, this could contribute to implementing goal C, proposed activities 2.8 of Myanmar National Waste Management Strategy and Action Plan (2018-2030): "Build on existing small-scale entrepreneurial recycling by integrating the informal recycling within the mainstream waste management sector".

4. CONCLUSION

This study calculates the amount of recyclable waste collected by informal recycling shops in Nay Pyi Taw before and during COVID-19. The study estimates that each recycling shop collected 1,798 kg (before the pandemic) and 856 kg (during the pandemic) of recyclable waste per day. This study also showed that the informal recycling enterprises were impacted by the pandemic.

This study indicates the challenges for informal recycling shops. Among them, getting an official license is the main challenge even though they all are willing to pay appropriate license fees because of the current legislation and policy. In addition, financial problems, limited land for managing buying recyclable waste, unstable market conditions, no factory in Nay Pyi Taw and no definitive legislation or laws are also challenges for informal recycling shops. Apart from these issues, some of the interviewed shop owners have faced the impacts of seasonal changes, too. In order to mainstream the role of informal sector into the government solid waste management system, the first step needs to promote cooperation with these sectors.

Estimating the recycling waste amount collected by informal recycling shops and recommendations based on the results of this study might provide the basic background information for policymakers, especially in order to mainstream informal sectors in the solid waste management system with consideration: they are important players in waste management schemes. Moreover, policymakers can also make a better strategy and plan to cope with and solve the waste management problems step by step, based on the findings of informal recycling shops' challenges.

ACKNOWLEDGEMENTS

We would like to express our sincerely thanks and deepest appreciation from the bottom of our heart to all of the respondents (informal recycling shops in Nay Pyi Taw) for their active responses and participation. This study would not have been finished in a timely fashion without their participation. Last but not least, we also heartily thank all of our colleagues for their support and invaluable comments.

REFERENCES

Obilor EI, Amadi EC. Test for significance of Pearson's correlation coefficient (r). International Journal of Innovative Mathematics, Statistics and Energy Policies 2018;6:11-23.

Conroy R. Sample size: A rough guide [Internet]. 2006 [cited 2020 Jun 5]. Available from: https://www.beaumontethics.ie/docs/application/samplesizecalculation.pdf.

Chelsea M. An overview of Myanmar's recycling industry: A report by building markets [Internet]. 2019 [cited 2020 Jun 20]. Available from: https:// buildingmarkets.org/ blogs /myanmar/2019/12/11/an-overview-of-myanmars-recycling-industry-a-report-by-building-markets/.

Constance AM, Robert AC. Paired-samples tests of equivalence. Communications in Statistics - Simulation and Computation 2012;41(10):1928-43.

Ceylan RF, Akpinar MG, Cherciov A, Ozkan B, Gul M. Consumer preferences of organic products for romania. International Journal of Agriculture, Forestry and Life Science 2018;2:47-55.

Department of Population. The 2014 Myanmar Population and Housing Censuses: Nay Pyi Taw. Nay Pyi Taw, Myanmar: Ministry of Labour, Immigration and Population, the Republic of the Union of Myanmar; 2015.

Environmental Conservation Department (ECD). Myanmar National Waste Management Strategy and Master Plan (2018-2030). Nay Pyi Taw, Myanmar: Ministry of Natural Resources and Environmental Conservation, the Republic of the Union of Myanmar; 2020.

Gerold A. Integrating the Informal Sector in Solid Waste Management Systems: Basic Aspects and Experiences. Germany: Frankfurt am Main; 2009.

Hoornweg D, Bhada-Tata P. What a Waste: A Global Review of Solid Waste Management. Urban Development Series; Knowledge Papers No. 15. Washington D.C., USA: World Bank; 2012.

Israel GD. Determining Sample Size. University of Florida, USA: Florida Cooperative Extension Services, 1992.

Kyessi A, Omar H, Saria J. The influence of technological factor to the sustainability of informal solid waste collection livelihood in urban areas: The case study of Kinondoni municipality. Research Journali's Journal of Economics 2017;5:1-15

McDonald JH. Handbook of Biological Statistics. 3rd ed. Maryland, USA: Sparky House Publishing, Baltimore; 2014.

Schneider P, Hung AL, Sembera J, Silva-Martinez RD. The role of the informal sector in a rurbanized environment. In: Mihai F, editor. Solid Waste Management in Rural Areas. Intech Open; 2017. p. 27-52.

Ngoc UN, Schnitzer H. Sustainable solutions for solid waste management in Southeast Asian countries. Waste Management 2009;29(6):1982-95.

Omar H. The influence of institutional factor to the sustainability of informal solid waste collectors: The case study of Kinondoni municipality-Tanzania. Global Scientific Journal 2019;7(10):1672-87.

Premakumara DGJ, Hengesbaugh M, Onogawa K, Hlaing OMT. Waste Management in Myanmar: Current Status, Key

Challenges and Recommendations for National and City Waste Management Strategies. Japan: UN Environment and Institute for Global Environmental Strategies; 2017.

Ratner B. The correlation coefficient: Its values range between +1/−1, or do they?. Journal of Targeting, Measurement and Analysis for Marketing 2009;17:139-42.

Tun MM, Juchelková D. Estimation of greenhouse gas emissions: An alternative approach to waste management for reducing the environmental impacts in Myanmar. Environmental Engineering Research 2019;24(4):618-29.

The Asia Foundation. Myanmar Business Environment Index (MBEI): COVID-19 impact on business [Internet]. 2020 [cited 2020 Jun 20]. Available from: https://asiafoundation.org/publication/myanmar-business-environment-index-covid-19-impact-on businesses/.

Wahab B, Ola B. The mode of operation and challenges of informal waste collection in Ibadan. Ibadan Journal of Sociology 2017;6:85-117.

Wahab B, Ola B. Effects of seasonal variation on informal waste collection in Ibadan, south-west Nigeria. Environment and Pollution 2018;7(1):36-45.

Analysis of Precipitation and Streamflow Data for Drought Assessment in an Unregulated Watershed

Worapong Lohpaisankrit[1*] and Jessada Techamahasaranont[2]

[1]Faculty of Engineering, Rajamangala University of Technology Isan, Khon Kaen, Thailand
[2]Faculty of Natural Resources and Agro-Industry, Kasetsart University, Sakon Nakhon, Thailand

ARTICLE INFO

Received: 31 Aug 2020
Received in revised: 1 Nov 2020
Accepted: 12 Nov 2020
Published online: 7 Dec 2020
DOI: 10.32526/ennrj/19/2020202

Keywords:
Drought index/ Cross-correlation/ Hydrological drought/ Trend analysis/ Standardized Precipitation Index (SPI)/ Upper Lam Pao watershed

*** Corresponding author:**
E-mail: worapong.lo@rmuti.ac.th

ABSTRACT

Predicting drought occurrence accurately still remains a challenging task. To fill research gaps, this study identified and analysed meteorological and hydrological droughts using the Standardized Precipitation Index (SPI) and Streamflow Drought Index (SDI), respectively, in the upper Lam Pao watershed in Thailand. The study also focused on investigating the relationships between both droughts. The SPI and SDI were computed based on observed long-term precipitation and streamflow data during the period of 1988-2017. The drought analysis was carried out by using the R packages. The location, period and severity level of drought events were graphically presented. On the basis of trend analysis, the SPI series showed slightly increasing trends, whereas no trend was found for the SDI series. This implied that the hydrological drought was influenced by not only precipitation but also other factors. The key findings indicated that there was a positive relationship between meteorological and hydrological droughts. In addition, there was a specific lag time, which may depend on physical characteristics of a basin, in drought propagating from meteorological drought to hydrological drought. Overall, the drought indices can help to predict hydrological drought events, which could be valuable information for drought monitoring and early warning systems.

1. INTRODUCTION

Drought is a recurring natural and multifaceted phenomenon, which is significantly harmful to water-use sectors in all climatic zones (Mishra and Singh, 2010). Recently, a number of major droughts have resulted in great economical losses due to crop damage, destruction of infrastructure and human settlement, and also led to disputes amongst water users (Bachmair et al., 2016). Drought events are likely to increasingly occur based on climate change projections (Van Loon et al., 2016). According to several authors (Mishra and Singh, 2010), droughts can be clustered into different categories (e.g., meteorological, agricultural, hydrological, and socioeconomic) depending on their consequences, which lead to water shortages. Normally, the development of droughts occurs in the regions where climatic conditions (e.g., precipitation) are significantly below the normal or expected conditions over a period of time. At early stages, the droughts are usually referred to as meteorological droughts. These meteorological droughts can develop into other droughts such as agricultural and hydrological droughts at a later stage (Barker et al., 2016).

One of the practical ways to assess drought events is through an index method. It derives drought indices from a variety of simple parameters to more complex functions (Mishra and Singh, 2010; Bachmair et al., 2016). Most indices for determining droughts, such as the Palmer drought severity index (Palmer, 1968) and the surface water supply index (Shafer and Dezman, 1982), in general, require a variety of data and an intensive computational effort (Van Loon, 2015; Bachmair et al., 2016). On the contrary, Standardized Precipitation Index (SPI) and Streamflow Drought Index (SDI) are simple and effective indices requiring very few input parameters and can be easily calculated. The SPI introduced by McKee et al. (1993) has been extensively used to characterise and monitor meteorological droughts

Citation: Lohpaisankrit W, Techamahasaranont J. Analysis of precipitation and streamflow data for drought assessment in an unregulated watershed. Environ. Nat. Resour. J. 2021;19(2):112-121. (https://doi.org/10.32526/ennrj/19/2020202)

(Mishra and Singh, 2010). It can be used to measure the severity and occurrence of droughts, although only precipitation data is fed as input (Barker et al., 2016). The SDI developed by Nalbantis and Tsakiris (2009) is based on the SPI developing concepts and is usually applied to characterise hydrological droughts.

A large number of studies on meteorological and hydrological droughts in many regions have been carried out by applying either the SPI or SDI method (Nalbantis and Tsakiris, 2009). For example, meteorological drought studies were conducted using the SPI method in the UK (Barker et al., 2016), Ethiopia (Belayneh et al., 2014), and Greece (Karavitis et al., 2011) and hydrological drought studies were undertaken using the SDI method in the Tigris basin, Turkey (Ozkaya and Zerberg, 2019) and the upper Yangtze River Basin, China (Hong et al., 2015). However, few published studies have used standardised indicators to explain links between meteorological and hydrological droughts due to their complexity (Lorenzo-Lacruz et al., 2013).

Owing to the complexity between meteorological and hydrological droughts, it is necessary to improve the understanding of the hydrological response to climate variations at different timescales. Thus, the present study focused on characterising meteorological and hydrological droughts on the basis of climate and hydrological data recorded in the upper Lam Pao watershed from 1988 to 2017. This watershed is an unregulated basin, where there are neither large dams nor other man-made structures located. Therefore, its hydrological data (i.e., streamflow data) represents natural flows, which are generally a useful indicator of water availability in the basin. The aims of this study were: (1) to analyse meteorological and hydrological drought evolution by using the SPI and SDI methods; (2) to determine long-term trends in drought indices at different timescales by using Mann-Kendall and Sen's slope estimator methods; and (3) to investigate the relationships between meteorological and hydrological droughts over the study period.

2. METHODOLOGY

2.1 Study area and data

The upper Lam Pao watershed has an area of approximately 2,150 km^2 with its outlet at Ban Tha Hai, where the monitoring station E65 is placed (Figure 1). Geographically, the watershed extends from latitude 16.8°N to 17.3°N and from longitude 102.6°E to 103.2°E. The Lam Pao River originates from mountainous areas in the Northwest and flows into the Lam Pao Reservoir in the Southeast. Its average annual streamflow is 749 MCM. The altitude ranges from 161 to 645 m.a.s.l. The upper Lam Pao watershed mainly covers Kumphawapi district and Nong Saeng district of Udon Thani Province, Northeastern Thailand. Average annual rainfall of the study area is 1,280 mm with mean daily temperatures ranging from 22 to 32°C. The rainy season begins in late May, lasting till October, whereas the dry season extends from November through mid-May.

Owing to being situated in a tropical monsoon climate, recurrent floods and droughts are considered to be major natural hazards. As is the case of water-use sectors, droughts have adverse impacts on water supply, agriculture, and the environment due to water shortages. Since droughts commonly occur in the watershed, it was chosen as the study area. In addition, most areas are used for rainfed crops, which are predominantly located in drought-prone areas. Therefore, the use of scientific insights can lead to better understand and predict drought because data available in the watershed meets the requirements of the index approach for drought analysis.

Meteorological data (rainfall) and hydrological data (streamflow) were collected in the period 1988-2017. Daily rainfall data of five rain gauge stations located inside and in the vicinity of the upper Lam Pao watershed were gathered from the Thai Meteorological Department (TMD). Moreover, daily water level data measured at the monitoring station E65 operated by the Royal Irrigation Department (RID) were used. Daily streamflow data were obtained from measurements of the daily water level by using local rating curves. Afterwards, both daily data were accumulated into monthly values in order to construct drought indices.

2.2 Drought indices

Studies of meteorological and hydrological droughts in the upper Lam Pao watershed were carried out by using an integrated index method for the long-term period 1988-2017. Drought indices were computed based on the monthly rainfall and streamflow data for cumulative periods of 6, 9, 12, and 18 months.

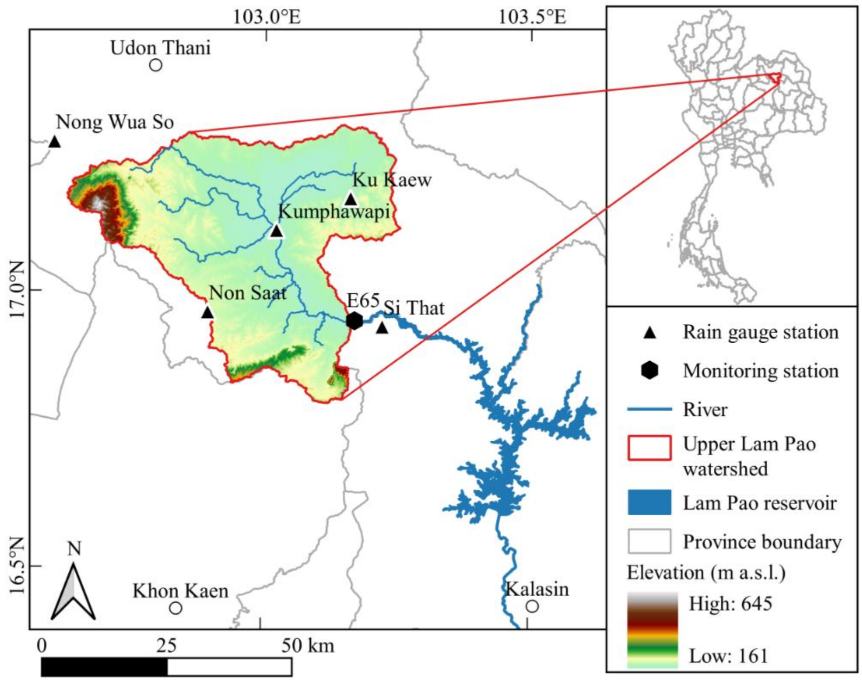

Figure 1. Map of study area with locations of rain gauge and streamflow monitoring stations.

SPI introduced by McKee et al. (1993) is a common indicator for monitoring and quantifying the intensity of meteorological drought events caused the shortage of rainfall or precipitation (Belayneh et al., 2014). This index was selected due to its simplicity and robustness (Wilhite et al., 2005), as previously mentioned. The SPI computation for any location begins by choosing a suitable probability distribution for long-term monthly precipitation data, typically a continuous period of at least 30 years. Subsequently, the cumulative probability distribution is converted into a normal distribution (McKee et al., 1993). In other words, the SPI represents a z-score variable of the standard normal distribution (Karavitis et al., 2011). The SPI can be computed as the ratio of the difference between the precipitation and the mean precipitation to the standard deviation as shown in equation (1):

$$\mathrm{SPI_i} = \frac{x_i - \overline{x_k}}{\sigma_k} \quad (1)$$

Where; $\mathrm{SPI_i}$ is Standardized Precipitation Index for the i^{th} hydrological month, x_i is seasonal rainfall (mm), $\overline{x_k}$ is long-term seasonal rainfall mean for the k^{th} reference timescale (mm), and σ_k is the standard deviation of the rainfall for the k^{th} reference timescale (mm).

SDI developed by Nalbantis and Tsakiris (2009) is a commonly used index for characterising hydrological drought events. The SDI uses the same concept as the SPI but the SDI computation is performed by replacing rainfall by streamflow series. The formula for SDI can be expressed in equation (2).

$$\mathrm{SDI_i} = \frac{Q_i - \overline{Q_k}}{\sigma_k} \quad (2)$$

Where; $\mathrm{SDI_i}$ is Streamflow Drought Index for the i^{th} hydrological month, Q_i is seasonal streamflow discharge (m^3/s), $\overline{Q_k}$ is long-term seasonal streamflow discharge mean for the k^{th} reference timescale (m^3/s), and σ_k is the standard deviation of the streamflow discharge for the k^{th} reference timescale (m^3/s).

In the present study, the drought indices (i.e., SPI and SDI) were computed using the R package “preintcon” and were based on the monthly time-series of rainfall and streamflow data, respectively. These data were ordered according to the hydrological year, which is from April to March of the following year in Thailand. The series of cumulative sums of rainfall and streamflow for 6-, 9-, 12-, and 18-month timescales were used to compute SPI-6, SDI-6, SPI-9, SDI-9, SPI-12, SDI-12, SPI-18, and SDI-18, respectively. For example, SPI-6 and SDI-6 begin from April to September, while SPI-9 and SDI-9 begin from April to December. During the computation, the series were smoothed with a moving window of k months, where k indicates the reference timescale (e.g., k=6, 9, 12, 18 months, etc.). In addition, the series were fitted to the Gamma probability distribution, which is often used by many researchers (Nalbantis and Tsakiris, 2009; Karavitis et al., 2011; Fischer et al., 2013; Boudad et al., 2018). Subsequently, the cumulative probability distribution of the series data was transformed into the normal distribution (Gumus and Algin, 2017).

The SPI values of each rain gauge station were computed over different timescales. Afterwards, the SPI values from all the five rain gauge stations were spatially averaged by using the Thiessen polygon method. These average SPI values were used to determine meteorological dry and wet periods of the study area. The SDI was obtained based on the monthly streamflow data recorded at the monitoring station E65. Since the SPI and SDI perform in a similar manner, drought classification of their results can be based on a similar criterion (Nalbantis and Tsakiris, 2009). According to McKee et al. (1993), thresholds used to categorise droughts are shown in Table 1.

Table 1. Drought classification

SPI and SDI range	Drought category
2.00 or more	Extremely wet
1.50 to 1.99	Very wet
1.00 to 1.49	Moderately wet
0.00 to 0.99	Slightly wet
-0.99 to 0.00	Mild drought
-1.49 to -1.00	Moderate drought
-1.99 to -1.50	Severe drought
-2.00 or less	Extreme drought

2.3 Trend analysis

To determine the overall direction of the SPI and SDI values at different timescales, we applied two statistical measures, namely, the Mann-Kendall test (Kendall, 1970) and the Sen's slope estimator method (Sen, 1968). which are frequently applied in environmental research (Boudad et al., 2018). In this study, the two statistical measures were calculated using the R package "trend".

2.3.1 Mann-Kendall test

The Mann-Kendall (M-K) test (Kendall, 1970) is a non-parametric statistic measure, which indicates variations of a time-series data and whether they are statistically significant. The M-K test statistic (S) and its standardised statistic ($Z_{M\text{-}K}$) are computed as follows:

$$S = \sum_{q=1}^{n-1} \sum_{p=q+1}^{n} \operatorname{sgn}(z_p - z_q) \tag{3}$$

$$z_{M-K} = \begin{cases} \frac{S-1}{\sqrt{\operatorname{Var}(S)}}, S > 0 \\ 0, S = 0 \\ \frac{S+1}{\sqrt{\operatorname{Var}(S)}}, S < 0 \end{cases} \tag{4}$$

Where; n is the number of the data values, z_p and z_q are the data values in time series p and q, respectively, for which p is greater than q, sgn is the sign functions, and Var(S) is the variance of S. A positive sign of $Z_{M\text{-}K}$ represents an increasing trend, whereas a negative sign of $Z_{M\text{-}K}$ represents a decreasing trend. In addition, the values of $Z_{M\text{-}K}$ are subjected to significance analysis. In this study, the significance level was set at α=0.05. At the 5% significance level, if the absolute value of $Z_{M\text{-}K}$ is greater than 1.96, the time-series data have a statistically significant trend.

2.3.2 Sen's slope estimator method

Similar to the M-K test, the Sen's slope estimator method developed by Sen (1968) is a non-parametric way to discover a trend in a time-series data. This method estimates the slope of a regression line that fits the time-series data on the basis of a least-squares estimate. The slope estimates of all data pairs are obtained from the following equation:

$$d_i = \frac{z_p - z_q}{p - q}, i = 1, 2, \cdots, N \text{ and } p > q \tag{5}$$

Where; d_i is a slope estimate of the time-series data, z_p and z_q are the data values in time p and q, respectively, and N is all data pairs for which p is greater than q. Afterwards, the N values of d_i are ranked from the smallest to largest and the Sen's slope estimator (SSE), which is the median of d_i, is computed as follows:

$$SSE = \begin{cases} d_{(N+1)/2} & \text{if N is odd} \\ \frac{1}{2}\left[d_{N/2} + d_{(N+2)/2}\right] & \text{if N is even} \end{cases} \tag{6}$$

A positive value of SSE indicates an increasing trend, whereas a negative value represents a decreasing trend of the time-series data.

2.4 Cross-correlation analysis

In this study, cross-correlation analysis was performed using the R package "astsa" in order to evaluate the relations between meteorological and hydrological droughts, which were based on the cross-correlations between the SPI and SDI values with varying a lag time between the two series. These cross-correlations were examined using the Pearson correlation coefficient (r) (Hipel and McLeod, 1994). The estimate of this Pearson correlation coefficient can be obtained using the following equation:

$$r = \frac{n\sum X_i Y_i - \sum X_i \sum Y_i}{\sqrt{n\sum X_i^2 - (\sum X_i)^2}\sqrt{n\sum Y_i^2 - (\sum Y_i)^2}} \quad (7)$$

Where; r is the Pearson correlation coefficient, X_i and Y_i are SPI and SDI values at time i, respectively, and n is the number of paired values of X and Y.

As previously mentioned, hydrological droughts usually develop from meteorological droughts. In order to analyse delay in drought propagation, the monthly SDI values at a given timescale were lagged behind the SPI values in monthly increments from zero lag up to a 12-month lag. Afterwards, their cross-correlations (r-values) were computed by using the equation (7).

3. RESULTS AND DISCUSSION

3.1 Meteorological and hydrological droughts

The spatial distribution maps of SPI values obtained by using the IDW method were based on rainfall data observed during the period of 30 years. Figure 2 shows, for instance, spatial-temporal variations from January 2008 to December 2017 on the basis of SPI-18 in the entire watershed and its surroundings. It can be seen from the figure that the year 2013 was the driest year in the watershed for the period of the analysis.

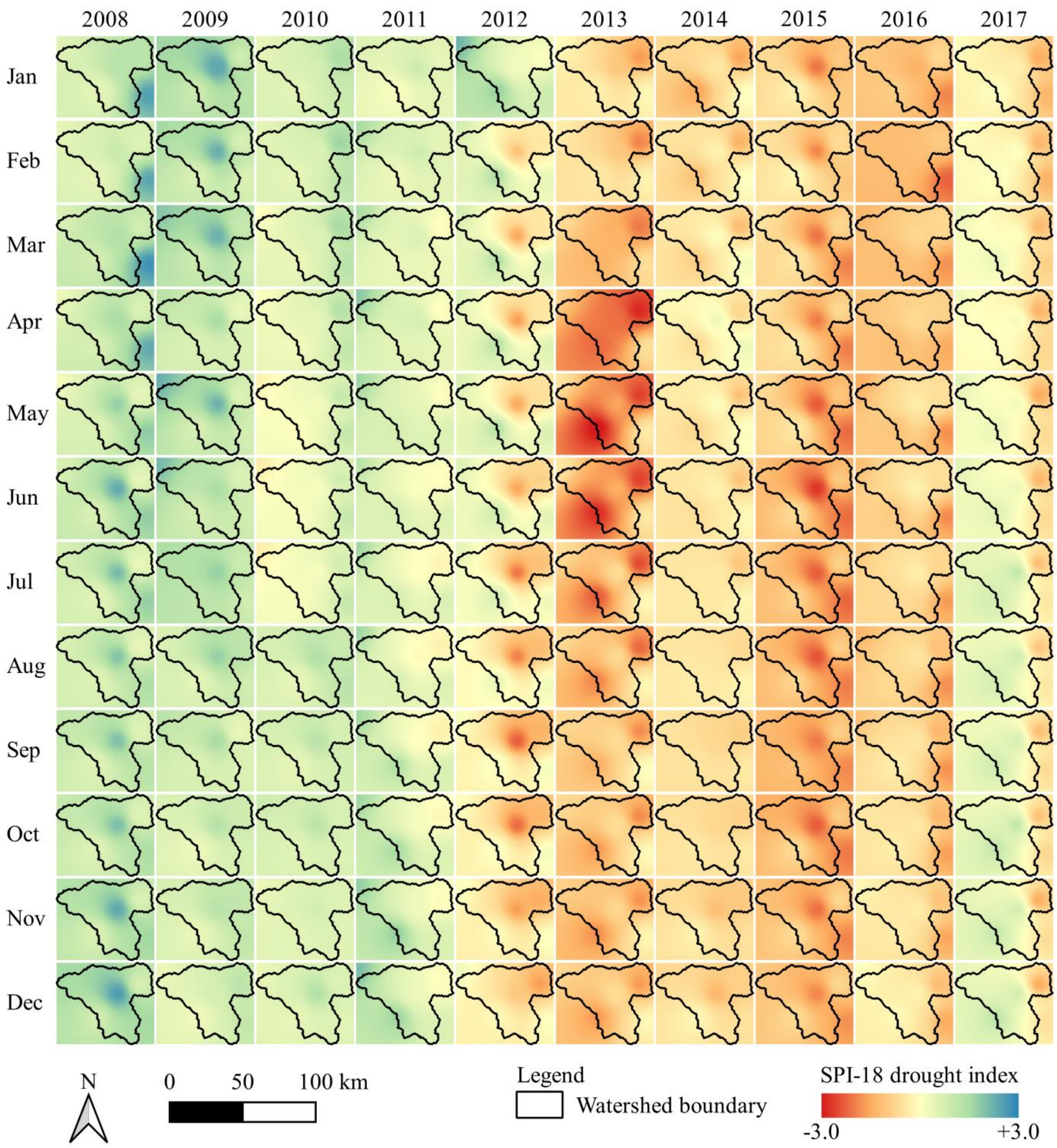

Figure 2. Spatial-temporal variations of SPI-18 drought index between 2008 and 2017.

The SPI values were classified according to McKee et al. (1993) into different levels of drought severity. Figure 3 shows an example of drought map of the upper Lam Pao watershed for the month of May 2013, which had the most critical drought condition in the entire period of the analysis. Figures 3(a) and (b) show that extreme drought events were observed in the southwest of the watershed for SPI-6 and SPI-9, respectively. In spite of that, Figures 3(c) and (d) demonstrate that extreme drought events were encountered in the southwest and northeast parts of the watershed for SPI-12 and SPI-18, respectively, with around 20% of the area affected by such events.

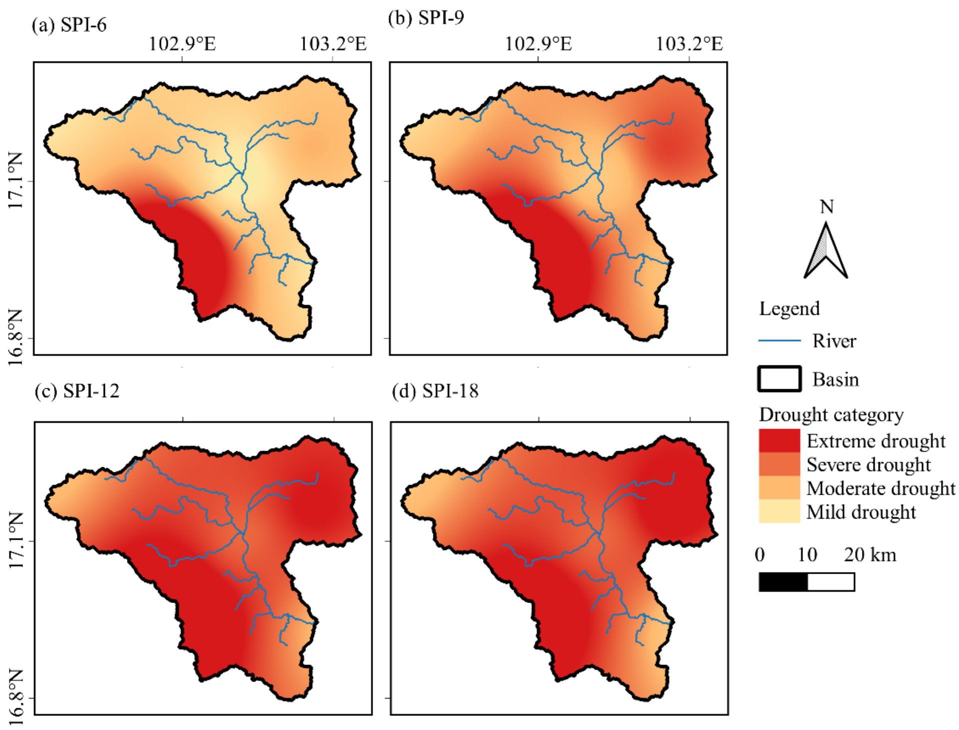

Figure 3. Spatial variations of drought based on SPI for May 2013.

The evolution of the average SPI and SDI series for each reference timescale is separately shown in Figure 4 and Figure 5, respectively. On the basis of the average SPI and SDI series, fluctuations of their values represent dry and wet periods. In a short timescale (e.g., 6 months), the average SPI and SDI series resemble tropical monsoon seasonal variations of the study watershed as shown in the figures. In the medium and long timescales (i.e., 9, 12, and 18 months), severe consecutive droughts during 1992-1994 and extreme consecutive droughts during 2012-2013 were identified by both the SPI and SDI. For example, the driest conditions occurred in the year 2013 determined with an average SPI-12 value of -1.78 for May 2013 and an SDI-12 value of -2.87 for June 2013.

3.2 Analysis of drought trends

The Z statistics of the Mann-Kendall test (Z_{M-K}) for the SPI and SDI series as well as their values of SSE are presented in Table 2. According to the Mann-Kendall (M-K) test at the 5% significance level, a trend in a time-series is accepted when the absolute value of Z_{M-K} is greater than 1.96. There were significantly increasing trends for the SPI-9, SPI-12, and SPI-18 series. In contrast, no significant trend of the SDI series was recognized by the M-K test.

Moreover, trend slopes were evaluated by using the Sen's slope estimator (SSE) method. This method produced positive values of SSE for all the SPI series, which indicated upward trends (Table 2). This result suggested that there has been no tendency for increasing meteorological droughts in recent years. The values of SSE for the SDI-6, SDI-9, and SDI-12 series showed slightly increasing trends. However, the SDI-18 series was found to have a slightly declining trend. The present study found that hydrological droughts were influenced by not only precipitation but also other factors. This finding is consistent with that of Van Loon et al. (2016), who stated that factors such as soil type, geology, and land cover can modify the hydrological response to climate variability.

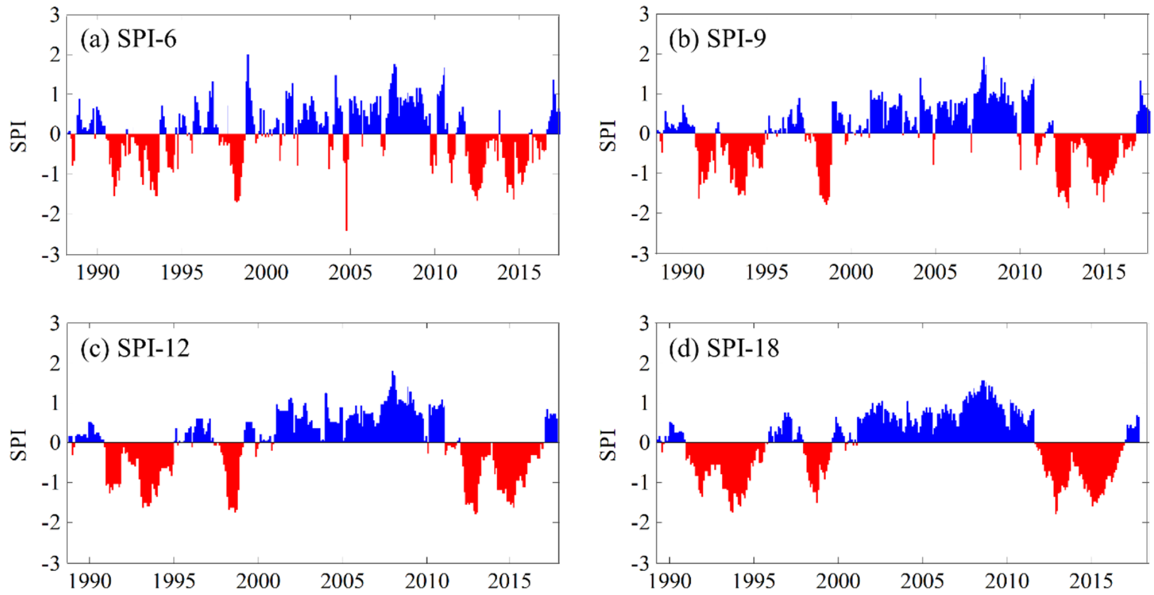

Figure 4. Temporal evolution of the average SPI of the five rain gauge stations in the accumulation periods of (a) 6, (b) 9, (c) 12, and (d) 18 months

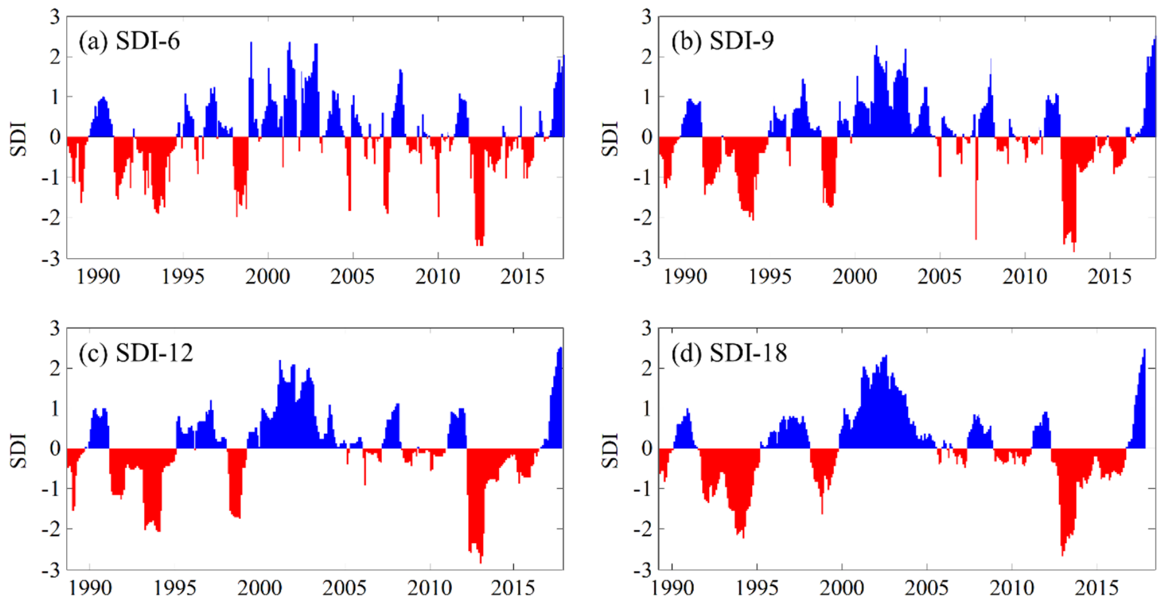

Figure 5. Temporal evolution of the SDI at the monitoring station E65 in the accumulation periods of (a) 6, (b) 9, (c) 12, and (d) 18 months.

Table 2. Z values of the M-K test (Z_{M-K}) and the Sen's slope estimator (SSE) of SPI and SDI series during the 1988-2017 (values in bold represent statistically significant trends at the 5% significance level).

Test	SPI-6	SPI-9	SPI-12	SPI-18	SDI-6	SDI-9	SDI-12	SDI-18
Z_{M-K}	1.507	**2.602**	**3.336**	**3.534**	1.801	0.739	0.150	-0.440
SSE	0.0007	0.0013	0.0016	0.0018	0.0009	0.0004	0.0001	-0.0003

3.3 Correlation between meteorological and hydrological droughts

This study found that all the average SPI series were correlated to the SDI series at the same timescale as shown in Figure 6. These results agree with the findings of other studies (Nalbantis and Tsakiris, 2009; Boudad et al., 2018), in which strong relationships between the SPI and SDI series were reported. Here, the greatest correlation was found between the SPI-18 and SDI-18 series with a correlation coefficient of about 0.692. These results need to be interpreted with caution because the average SPI series were based on available rainfall data from the five rain gauge stations located inside and outside of the study area. Figure 6(d) exhibits a good relationship between SPI-18 and SDI-18 series. However, their trend directions were found to be different. Several factors could explain these observations. Firstly, potential evaporation may be an important factor, which has an influence on drought conditions. Another possible factor is the lag time between rainfall and runoff, which can delay in drought propagating from meteorological drought to hydrological drought. The observations are in agreement with those obtained by Lorenzo-Lacruz et al. (2013) and Barker et al. (2016).

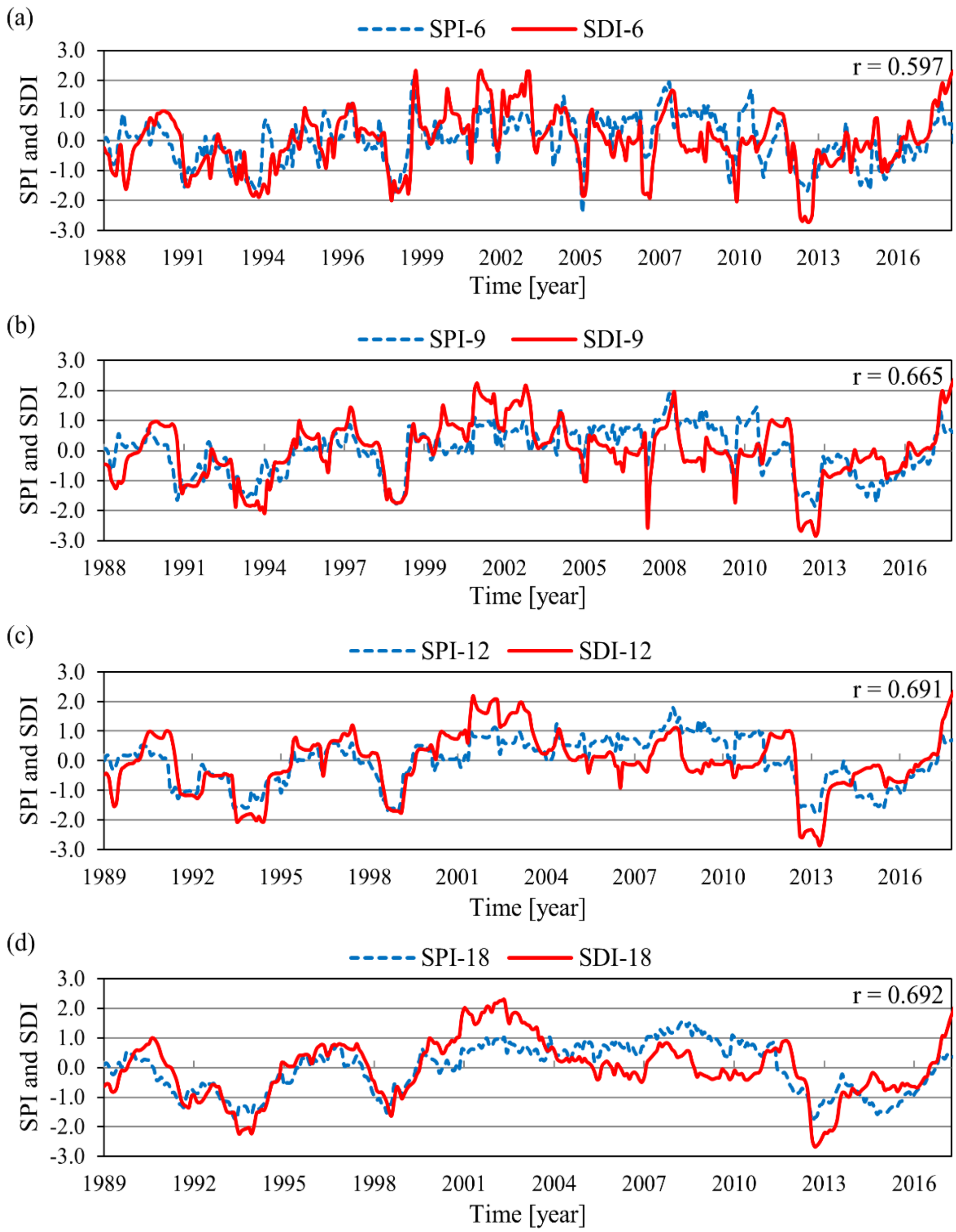

Figure 6. Average SPI values of the upper Lam Pao watershed and SDI values for the monitoring station E65 for reference timescales (6, 9, 12, 18 months). (a) SPI-6 and SDI-6 series; (b) SPI-9 and SDI-9 series; (c) SPI-12 and SDI-12 series; and (d) SPI-18 and SDI-18 series.

Furthermore, the cross-correlation test revealed that the SPI series can be used to predict hydrological drought events. Figure 7 shows the changes in the linear correlation coefficients (r-values) between the SPI series and corresponding SDI series, which were shifted after the SPI series in monthly increments from zero lag up to a 12-month lag. The peak r-values were obtained from a one-month lag between the SPI and SDI series for all the reference timescales. These results reflect those of Blagojević et al. (2013), who also found that the correlation improved as the SPI series was compared with the SDI series of the following month. Nalbantis and Tsakiris (2009) showed that a delay of one month between the two drought indices was too large for their test basin, an area of about 350 km^2. However, the 1-month lag was too small for the Seyhan-Ceyhan River basins with a total area of approximately 43,840 km^2 (Gumus and Algin, 2017). These results are likely to be related to the physical properties of the drainage basins. The finding is in line with that of previous studies (Lorenzo-Lacruz et al., 2013; Van Loon, 2015).

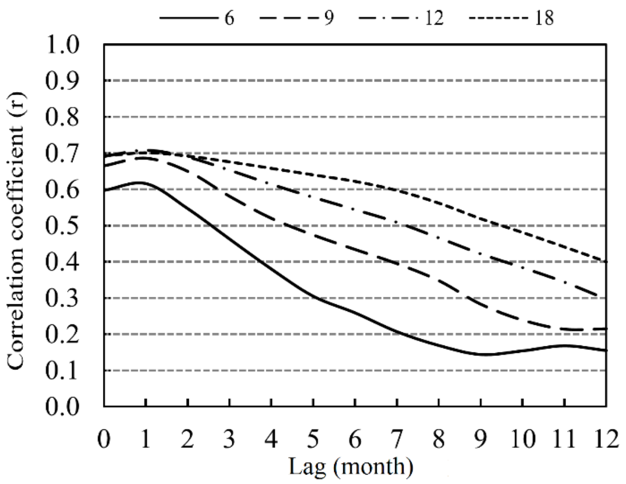

Figure 7. Correlation coefficients between SPI and SDI series at different time lags from zero up to 12 months.

In general, it seems that monitoring of meteorological and hydrological droughts can be carried out by using several drought indices (e.g., SPI and SDI). The results are suggestive of links between meteorological and hydrological droughts based on the use of the SPI and SDI. For example, the lag time between the SPI and SDI series can be useful information for improving drought monitoring and early warning systems. However, hydrological droughts may not be fully explained just by the meteorological drought indices (Van Loon, 2015). Indeed, there are other variables such as physical characteristics of the basin, soil moisture, land use as well as the relations between streamflow and groundwater that have resulted in the hydrological drought (Barker et al., 2016). In further investigations, it might be possible to use a different drought index and to establish a more complete hydrological drought index for improving drought monitoring and prediction.

4. CONCLUSIONS

This study set out to investigate meteorological and hydrological droughts in the upper Lam Pao watershed of Thailand and to explore their relations. Analysis of both droughts was performed based on the monthly values of the SPI and SDI in the period 1988-2017. The use of the SPI and SDI together with their classifications is considered a reliable tool in the assessment of meteorological and hydrological drought evolution in space and time. The Mann-Kendall test suggested that the occurrence of meteorological drought would not probably increase in recent years. However, the Sen's slope estimator method suggested an increase in the long-term hydrological drought because a slightly negative trend of SDI-18 was detected. The investigation of the relationships between meteorological and hydrological droughts presented new findings, which indicated a time lag between both droughts. The time lag may vary depending on physical characteristics of a basin. This time lag can be useful information for determining future potential hydrological droughts when rainfall data are available. In conclusion, the present study has offered a framework for the exploration of meteorological and hydrological droughts. Future studies should attempt to identify the relationships between droughts using different climatic and geophysical variables.

ACKNOWLEDGEMENTS

The authors wish to acknowledge the valuable suggestions of the editor and anonymous reviewers, which helped improve the quality of this manuscript. The first author thanks the Rajamangala University of Technology Isan for its support in implementing the study. In addition, our special thanks go to the TMD and RID for providing the data.

REFERENCES

Bachmair S, Stahl K, Collins K, Hannaford J, Acreman M, Svoboda M, et al. Drought indicators revisited. Wiley Interdisciplinary Reviews: Water 2016;3(4):516-36.

Barker LJ, Hannaford J, Chiverton A, Svensson C. From meteorological to hydrological drought using standardised indicators. Hydrology and Earth System Sciences 2016;20(6):2483-505.

Belayneh A, Adamowski J, Khalil B, Ozga-Zielinski B. Long-term SPI drought forecasting in the Awash River Basin in Ethiopia using wavelet neural network and wavelet support vector regression models. Journal of Hydrology 2014;508:418-29.

Blagojević B, Mihailović V, Gocić M, Trajković S. Streamflow drought index modelling through standard precipitation index assisted by service-oriented paradigm. In: Lamaddalena N, Todorovic M, Pereira LS, editors. Water, Environment and Agriculture. Valenzano, Italy: CIHEAM-IAMB; 2013. p. S9-2.

Boudad B, Sahbi H, Mansouri I. Analysis of meteorological and hydrological drought based in SPI and SDI index in the Inaouen Basin (Northern Morocco). Journal of Materials and Environmental Science 2018;9(1):219-27.

Fischer T, Gemmer M, Su B, Scholten T. Hydrological long-term dry and wet periods in the Xijiang River Basin, South China. Hydrology and Earth System Sciences 2013;17(1):135-48.

Gumus V, Algin HM. Meteorological and hydrological drought analysis of the Seyhan-Ceyhan River Basins, Turkey. Meteorological Applications 2017;24(1):62-73.

Hipel KW, McLeod AI. Time Series Modelling of Water Resources and Environmental Systems. Amsterdam, London, UK: Elsevier; 1994.

Hong X, Guo S, Zhou Y, Xiong L. Uncertainties in assessing hydrological drought using streamflow drought index for the upper Yangtze River Basin. Stochastic Environmental Research and Risk Assessment 2015;29(4):1235-47.

Karavitis CA, Alexandris S, Tsesmelis DE, Athanasopoulos G. Application of the Standardized Precipitation Index (SPI) in Greece. Water 2011;3(3):787-805.

Kendall MG. Rank Correlation Methods. London, UK: Griffin, 1970.

Lorenzo-Lacruz J, Vicente-Serrano SM, González-Hidalgo JC, López-Moreno JI, Cortesi N. Hydrological drought response to meteorological drought in the Iberian Peninsula. Climate Research 2013;58(2):117-31.

McKee TB, Doesken NJ, Kleist J. The relationship of drought frequency and duration to time scales. Proceedings of the 8th Conference on Applied Climatology; 1993 Jan 17-22; Anaheim: USA; 1993. p. 179-84.

Mishra AK, Singh VP. A review of drought concepts. Journal of Hydrology 2010;391(1-2):202-16.

Nalbantis I, Tsakiris G. Assessment of hydrological drought Revisited. Water Resources Management 2009;23(5):881-97.

Ozkaya A, Zerberg Y. A 40-Year Analysis of the Hydrological Drought Index for the Tigris Basin, Turkey. Water 2019; 11(4):657.

Palmer WC. Keeping track of crop moisture conditions, nationwide. Weatherwise 1968;21(4):156-61.

Sen PK. Estimates of the regression coefficient based on Kendall's Tau. Journal of the American Statistical Association 1968;63(324):1379.

Shafer BA, Dezman LE. Development of a surface water supply index (SWSI) to assess the severity of drought conditions in snowpack runoff areas. Proceedings of the 50th Annual Western Snow Conference; 1982 Apr 19-23; Reno: USA; 1982. p. 164-175.

Van Loon AF. Hydrological drought explained. Wiley Interdisciplinary Reviews: Water 2015;2(4):359-92.

Van Loon AF, Stahl K, Di Baldassarre G, Clark J, Rangecroft S, Wanders N, et al. Drought in a human-modified world. Hydrology and Earth System Sciences 2016;20(9):3631-50.

Wilhite DA, Svoboda MD, Hayes MJ. Monitoring drought in the United States. In: Boken VK, Cracknell AP, Heathcote RL, editors. Monitoring and Predicting Agricultural Drought. Oxford, USA: Oxford University Press; 2005. p. 121-31.

Environment and Natural Resources Journal 2021; 19(2): 122-131

Spatial Zonation of Landslide Prone Area Using Information Value in the Geologically Fragile Region of Samdrup Jongkhar-Tashigang National Highway in Bhutan

Thongley Thongley and Chaiwiwat Vansarochana*

Faculty of Agriculture, Natural Resource and Environment, Naresuan University, Thailand

ARTICLE INFO

Received: 15 Jul 2020
Received in revised: 28 Oct 2020
Accepted: 16 Nov 2020
Published online: 9 Dec 2020
DOI: 10.32526/ennrj/19/2020171

Keywords:
Information value/ Kappa index/ Area under the curve

*** Corresponding author:**
E-mail: chaiwiwatv@gmail.com

ABSTRACT

Samdrup Jongkhar-Tashigang National Highway (SJ-TG NH) in Bhutan experiences several landslides every year. However, there are no studies on the landslides which will assist in highway realignment. This study developed the landslide susceptibility mapping (LSM) using the information value (IV) and check the reliability of the IV. The workflow consists of landslide inventory, factor preparation, LSM development, and its validation. During the landslide inventory, a total of 130 landslides were identified from satellite image interpretation, google earth image, and field investigation. The landslide inventory was divided into a training dataset (70%) and a validation dataset (30%). Then, nine factors were used to construct a spatial database. The accuracy was conducted using the area under curve (AUC) and the reliability of the model was performed using the kappa index. The AUC for the success rate (0.7700) falls under a good category and the prediction rate (0.6798) falls under the moderate category. The kappa index (0.3407) for the IV falls under the fair reliability category. The LSM was classified into very safe (16.42%), safe (30.64%), moderately (27.67%), risky (16.18%), and high risky zones (9.09%) based on the natural break. The LSM will guide decision-makers in the realignment of the road.

1. INTRODUCTION

A landslide is the downward movement of the materials from the surface of the earth which are caused by several natural phenomena as well as induced by anthropogenic activities (Kahlon et al., 2014). The Himalayan region is considered as the youngest mountains and geo-dynamically active causing instability in the region (Chauhan et al., 2010). The number of landslides in the region is increasing every year due to deforestation, intense developmental activities, and unplanned human settlement (Chauhan et al., 2010). The landslides cause serious concern due to the loss of life, damage to the infrastructure, natural resources, etc. and pose a serious problem for future developmental activities (Kanungo et al., 2008). According to a global risk analysis report published by the world bank, landslides stood as the seventh most dangerous natural disaster and it claimed the lives of 18,200 people between 1980 to 2000 (Dilley et al., 2005). The study of landslide risk and hazard has become one of the major topics for geoscientists and engineers in recent years due to increasing awareness of its socio-economic impacts and the urbanization in mountainous areas (Aleotti and Chowdhury, 1999).

There are several methods to assess landslides which are broadly categorized into a qualitative approach and a quantitative approach. Both approaches works on the principle of past and present to the future which means the past and present landslide events will help in predicting the future landslides. The qualitative approach such as Analytical Hierarchy Process and Weighted Linear Combination works entirely based on the knowledge of the experts (Aleotti and Chowdhury, 1999). The quantitative approach is data-driven, and it is classified into a deterministic and statistical approach. The deterministic approach is appropriate for the smaller area due to its requirement for an exhaustive geotechnical test (Aleotti and

Citation: Thongley, Vansarochana C. Spatial zonation of landslide prone area using information value in the geologically fragile region of Samdrup Jongkhar-Tashigang national highway in Bhutan. Environ. Nat. Resour. J. 2021;19(2):122-131. (https://doi.org/10.32526/ennrj/19/2020171)

Chowdhury, 1999). In recent years, the statistical approach in conjunction with GIS has become more popular for the LSM due to high predictive power, cheap, easy calculation, and ability to handle the large data (Mandal and Mandal, 2018). Among the various statistical approaches, this study uses information value (IV) for the landslide assessment.

Bhutan lies in the Himalayan region with an area of 38,394 km^2 sandwiched between China and India. Bhutan is prone to several natural disaster hazards due to its location in the fragile geological setting and active seismic zone (Keunza et al., 2004). The rugged terrain and heavy monsoon precipitation intensify the landslide risk in the country. The Samdrup Jongkhar-Tashigang National Highway (SJ-TG NH) in Bhutan experiences several landslides during the monsoon season. However, the government keeps on maintaining the same route without changing the alignment and the same problem persists every year. The development of infrastructure along the highway will further destabilize the area. The unstable area may erode natural resources such as minerals, forests, threaten wildlife, and pollute water (Geertsema et al., 2009). The landslide also threatens properties, agricultural lands, and human lives.

There is no landslide risk map to guide the decision-makers for the re-alignment of the road, even though some portion of the 180 km SJ-TG NH is located in the most landslide-prone areas. Therefore, the main objective of this study is to develop, assess, and validate the LSM along the SJ-TG NH in Bhutan using the information value (IV) model. This study also aimed at checking the reliability of the IV model using the kappa index.

2. METHODOLOGY

The overall methodology of the research is shown in Figure 1. The workflow consists of landslide inventory, influencing factor preparation, developing LSM, and its validation.

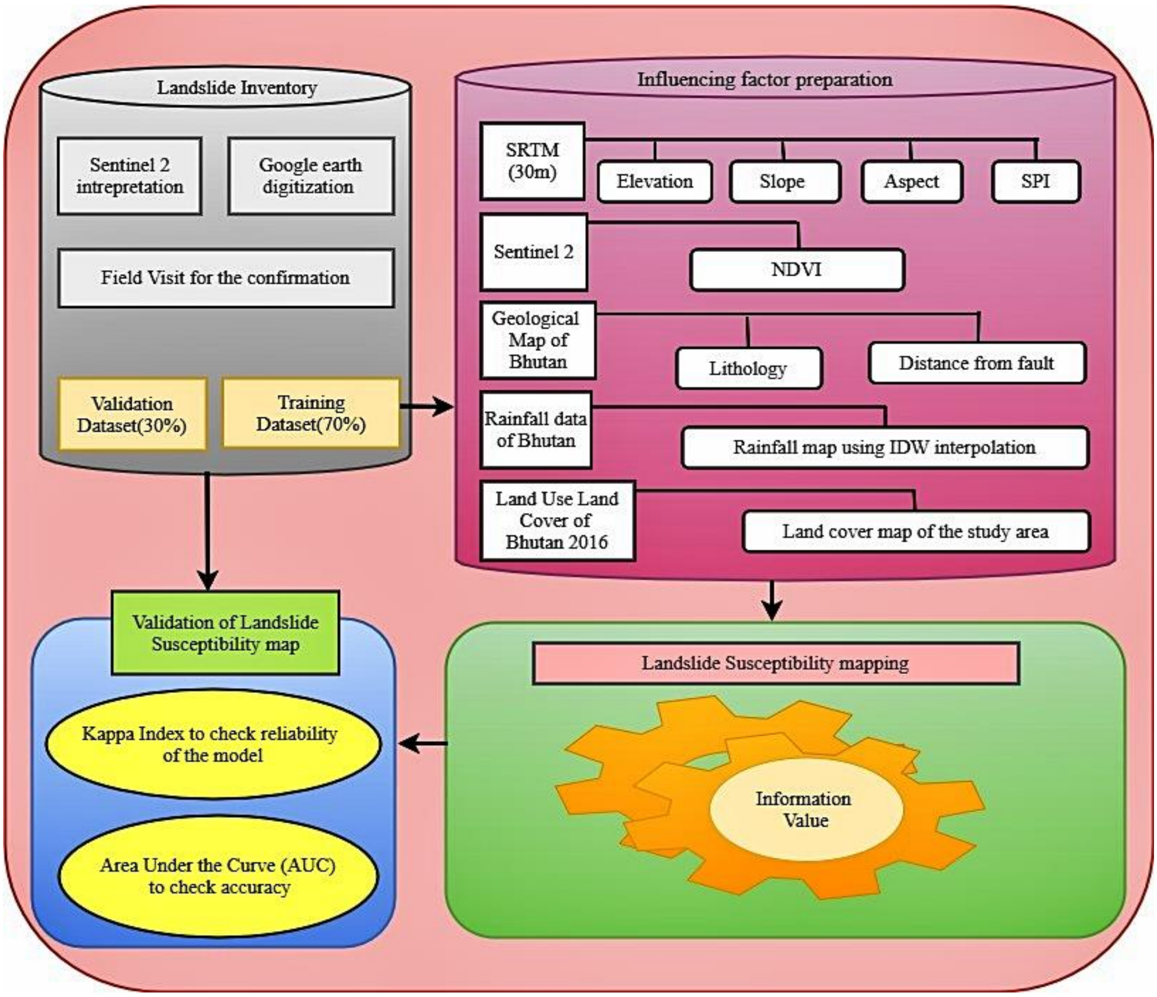

Figure 1. Flowchart of preparing the landslide susceptibility mapping

2.1 Study area

The study area (Figure 2) is located along the SJ-TG NH in Bhutan with a buffer distance of 3 km on both sides of the highway. Geographically, the study area is located between 26°48'0"N to 27°21'0"N latitude and 91°27'30"E to 91°30'0"E longitude with altitude ranging from 156 to 3,700 m.a.s.l. The highway stretches approximately 180 km connecting the Eastern districts of Bhutan. SJ-TG NH is the only highway connecting the four Eastern districts with the rest of the places of Bhutan. Moreover, the highway is the main door to the international border of Assam State of India. The area experiences several landslides every year due to its topographic nature and geological setting. The detail of lithology in the study area is given in Table 1.

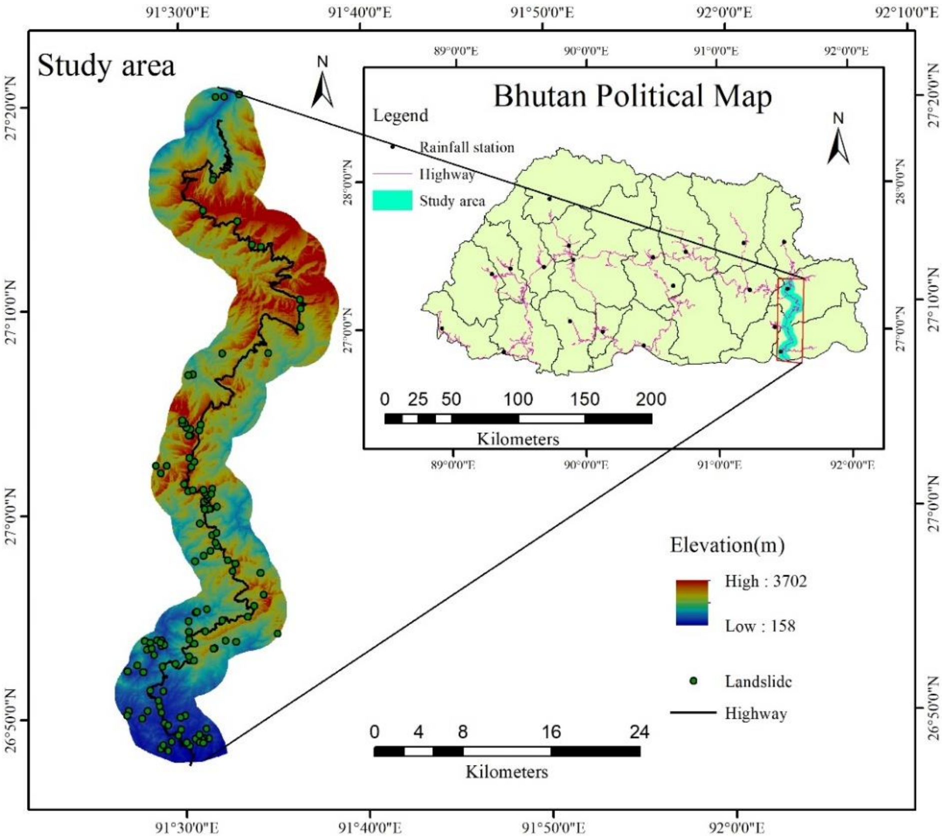

Figure 2. Study area showing the elevation, landslide locations, and rainfall stations

Table 1. Detail description of the lithology of the study area

Code	Lithological description
Tsm	Medium to coarse grained sandstone and pebble to cobble conglomeratic sandstone.
Tsl	Massive weathering siltstone and shale, interbedded with tan to gray, fine-grained, lithic-rich sandstone.
Pzg	Gray, medium grained, feldspathic, lithic-rich sandstone interbedded with dark gray to black, thin to medium-bedded, carbonaceous siltstone, shale, slate, and argillite, and rare black coal beds
Tsu	Medium to coarse grained sandstone and pebble to cobble and boulder conglomerate, interbedded siltstone.
GHlo	Massive weathering, granite-composition orthogneiss; generally, exhibits leucosomes and abundant feldspar augen. Paragneiss, schist, and quartzite intervals locally split out.
pCs	Light gray to white, tan-weathering, very fine grained, medium to thick-bedded, cliff forming quartzite. Interbeds of thin to thick bedded, green, muscovite biotite schist and phyllite with diagnostic sigmoidal quartz.
pCd	Dominated by schist and phyllite. Quartzite is thin to medium quartzite bedded, and medium gray limestone.
Pzd	Green-gray, pebble to cobble, slate-matrix diamictite
GHlml	Dominantly amphibolite-facies metasedimentary rocks, including quartzite, and biotite-muscovite-garnet schist and paragneiss often exhibiting kyanite, sillimanite, or staurolite, and partial melt textures
Tgr	Massive to foliated, syn-Himalayan leucogranite plutons
Pzj	Gray, biotite rich, locally garnet bearing schist, interbedded with biotite lamination, lithic clast-rich quartzite.

2.2 Landslide inventory mapping

The landslide inventory map shows the spatial distribution of the landslide location, types, and timing of the event of the existing landslides (Achour et al., 2017). The landslide inventory is used to find the relationship between the landslide events and its factors (Saha et al., 2005). In this study, landslide inventory was done using the google earth, satellite image interpretation, and field verification using handheld GPS. The SJ-TG NH experiences all types of landslides with the majority of translational slides and debris flow. A total of 130 landslides (Figure 2) were identified of which 91 landslides were used for the training dataset and the remaining 39 landslides were used for validation datasets.

2.3 Landslide influencing factor preparation

The landslide influencing factors used for this study were elevation, slope, aspect, stream power index (SPI), normalized difference vegetation index (NDVI), distance from the fault, lithology, rainfall map, and land cover map. The SRTM DEM (30 m) was used to derive elevation, slope, aspect, and SPI. The NDVI was prepared using sentinel 2. The geological map of Bhutan (1:500,000) prepared by Long et al. (2011) was used to extract the fault and lithological map of Bhutan. The detail of lithology is elaborated in Table 1. The average annual rainfall map was prepared using inverse distance weighting interpolation from 20 rainfall stations (Figure 2) across Bhutan from 1996 to 2017. The rainfall data was shared by the National Center of Hydrology and Meteorology. The land cover map was extracted from the Bhutan land cover map 2016 and it was prepared by the Department of Forests and Park Services. The factors were shown in Figure 3.

2.4 Information value (IV)

The information value (IV) model was developed by Yin and Yan (1988) for the prediction of slope instability. The IV creates a spatial relationship between the landslide event (landslide inventory) and its factors (Achour et al., 2017). If the IV value is positive, the landslide possibility is higher and vice versa (Chuanhua and Xueping, 2009). As per Chuanhua and Xueping (2009), IV is calculated using equation 1.

$$IV = \ln \frac{\frac{Npix(Si)}{Npix(Ni)}}{\frac{SNpix(Si)}{SNpix(Ni)}} \qquad (1)$$

Where; IV is the information value of the factor’s class, Npix(Si) is the number of pixels containing landslides in a factor’s class, Npix(Ni) is the number of pixels in a factor’s class, SNpix(Si) is the number of pixels that containing landslides in the entire study area, and SNpix(Ni) is the total number of pixels in the entire study area.

The resulting value of the IV is used for the reclassification of the factors. The reclassified factors were summed up using equation 2 to obtain the LSM.

$$LSM = F1 + F2 + \dots Fn \qquad (2)$$

Where; F represents reclassified factors using the weight from the information value.

3. RESULTS AND DISCUSSION

3.1 Relationship between the factors and the landslide event

The result of the landslide susceptibility assessment using the IV for the individual classes of the factors is given in Table 2. The chances of the landslide are higher for the higher IV.

From Table 2, it is noticed that the IV decreases with an increase in elevation. The lowest elevation class (158-741) corresponds to the highest IV (0.738) while the highest elevation class (2480-3702) corresponds to the lowest IV (-1.351). This shows that the lower elevation of an area experiences more landslides compared to the higher elevation. This may be due to higher precipitation and fragile geology in the lower elevation. A similar trend of results was shown by Chen et al. (2014).

In contrast to elevation, the IV increases with increases in the slope angle indicating more landslide probability in the steeper slope. The IV for slope angle 0°-14.67° is -0.412 while the IV for slope angle 37.29°-46.03° is 0.657. During the site investigation, the result confirmed that the steeper slopes experienced relatively more landslides. Singh and Kumar (2018) also noticed that the steeper slope is more prone to landslides.

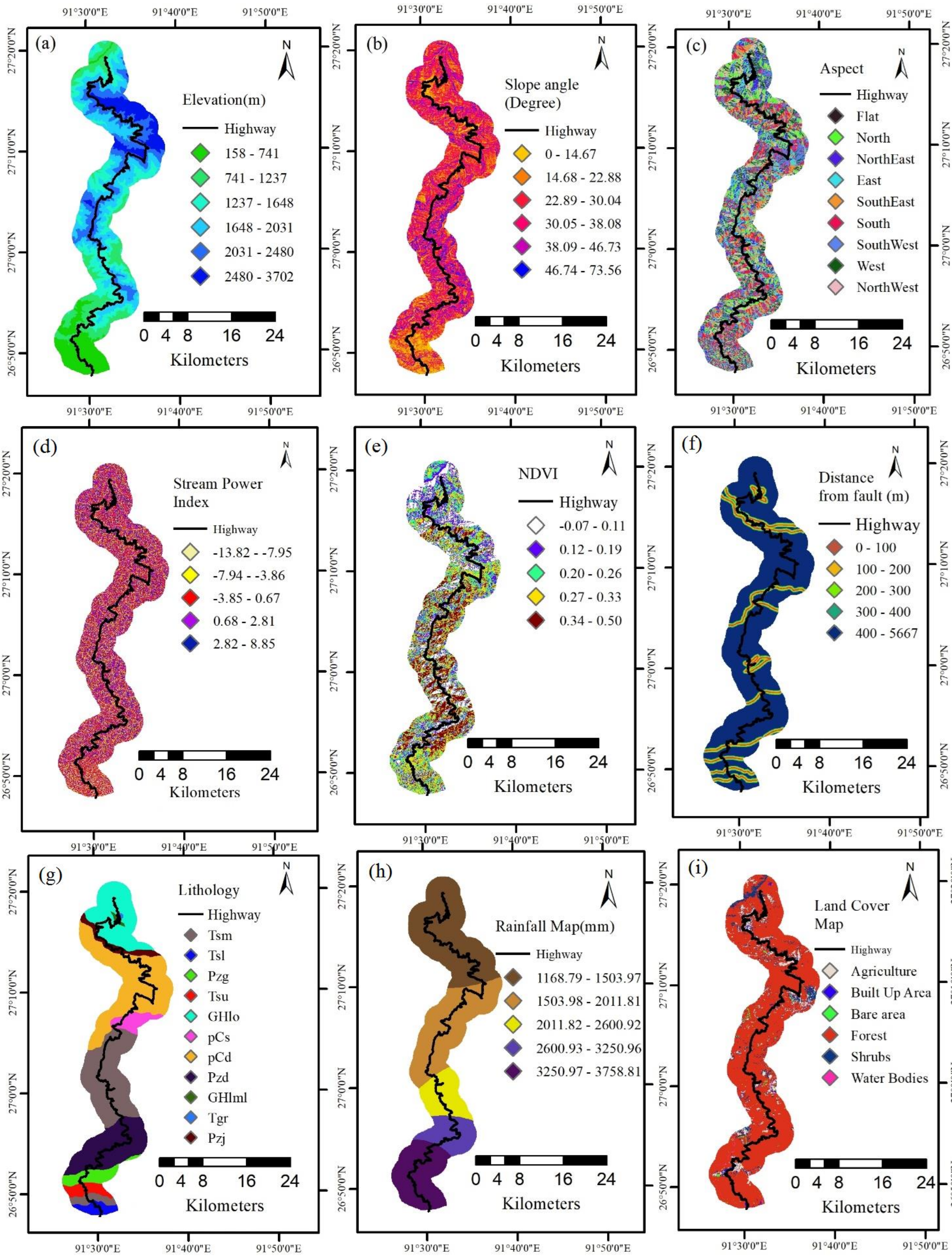

Figure 3. Factors (a) elevation, (b) slope angle, (c) aspect, (d) stream power index, (e) NDVI, (f) distance from fault, (g) lithology, (h) rainfall map, and (i) land cover map

Table 2. Relationship between the landslide event and the factors using the information value

Factor	Class	No of pixel in class	% of the pixel in class	No of landslide	% of landslide	IV
Elevation (m)	158-741	72131	12.079	23	25.275	0.738
	741-1,237	87104	14.586	15	16.484	0.122
	1,237-1,648	126532	21.189	16	17.582	-0.187
	1,648-2,031	146385	24.513	21	23.077	-0.06
	2,031-2,480	114326	19.145	14	15.385	-0.219
	2,480-3,702	50687	8.488	2	2.198	-1.351
Slope (degree)	0-14.67	59424	9.951	6	6.593	-0.412
	14.68-22.88	114980	19.254	13	14.286	-0.298
	22.89-30.04	144336	24.170	15	16.484	-0.383
	30.05-37.28	139679	23.390	18	19.780	-0.168
	37.29-46.03	98687	16.526	29	31.868	0.657
	46.04-73.56	40059	6.708	10	10.989	0.494
Aspect	Flat	7	0.001	0	0.000	0.000
	North	83659	14.009	4	4.396	-1.159
	Northeast	58950	9.872	7	7.692	-0.249
	East	56862	9.522	9	9.890	0.038
	Southeast	70077	11.735	20	21.978	0.627
	South	83741	14.023	30	32.967	0.855
	Southwest	90412	15.140	11	12.088	-0.225
	West	75084	12.573	8	8.791	-0.358
	Northwest	78373	13.124	2	2.198	-1.787
SPI	-13.82 to -7.95	46929	7.859	5	5.495	-0.358
	-7.94 to -3.86	113194	18.955	18	19.780	0.043
	-3.85 to 0.67	187826	31.453	30	32.967	0.047
	0.68 to 2.81	186860	31.291	28	30.769	-0.017
	2.82 to 8.85	62356	10.442	10	10.989	0.051
NDVI	-0.07-0.11	82147	13.756	14	15.385	0.112
	0.12-0.19	127449	21.342	24	26.374	0.212
	0.20-0.26	140709	23.563	30	32.967	0.336
	0.27-0.33	140934	23.601	20	21.978	-0.071
	0.34-0.50	105926	17.738	3	3.297	-1.683
Distance from the fault (m)	0-100	32903	5.510	12	13.187	0.873
	100-200	27860	4.665	11	12.088	0.952
	200-300	29991	5.022	3	3.297	-0.421
	300-400	24410	4.088	4	4.396	0.073
	400<	482001	80.715	61	67.033	-0.186
Lithology	Tsm	143711	24.066	37	40.659	0.524
	Tsl	14975	2.508	6	6.593	0.967
	Pzg	25318	4.240	2	2.198	-0.657
	Tsu	17511	2.932	7	7.692	0.964
	GHlo	90638	15.178	5	5.495	-1.016
	pCs	22264	3.728	6	6.593	0.570
	pCd	162213	27.164	27	29.670	0.088
	Pzd	99416	16.648	1	1.099	-2.718
	GHlml	2477	0.415	0	0.000	0.000
	Tgr	675	0.113	0	0.000	0.000
	Pzj	17967	3.009	0	0.000	0.000

Table 2. Relationship between the landslide event and the factors using the information value (cont.)

Factor	Class	No of pixel in class	% of the pixel in class	No of landslide	% of landslide	IV
Rainfall (mm/year)	1,168.79-1,503.97	202545	33.918	7	7.692	-1.484
	1,503.98-2,011.81	163862	27.440	13	14.286	-0.653
	2,011.82-2,600.92	62304	10.433	26	28.571	1.007
	2,600.93-3,250.96	59427	9.952	9	9.890	-0.006
	3,250.97-3,758.81	109027	18.257	36	39.560	0.773
LULC	Agriculture	39374	6.593	1	1.099	-1.792
	Built up area	4292	0.719	4	4.396	1.811
	Bare area	4130	0.692	1	1.099	0.463
	Forest	507583	84.999	78	85.714	0.008
	Shrubs	39286	6.579	7	7.692	0.156
	Water bodies	2500	0.419	0	0.000	0.000

In the case of the slope aspect, the IV is higher for the south-facing slope and the south-east facing slope. This reveals that the south-facing slopes encounter more landslides. This may be due to the orographic effect of the giant Himalayan Mountain which blocks the air from the Indian Ocean, condense it, and finally precipitate on the south-facing slopes. Saha et al. (2005) also observed that the south-facing slopes encounter more landslides in the Himalayan Region.

Regarding the SPI, the IV does not follow the orderly trend with the SPI value. However, it is noticed that the IV is slightly higher for the higher SPI classes. The SPI shows the erosive power of the flowing water. Higher SPI indicates higher erosive power and increases the risk of landslides.

On the other hand, the IV gradually decreased with an increase in NDVI value and the result is agreed with the result of Ba et al. (2017). The higher NDVI indicates healthy vegetation and vice versa. The decrease in IV with an increase in NDVI signifies that there is less probability of landslide in the healthy vegetated area.

Similarly, the IV decreases with an increase in distance from the fault. This clearly shows the possibility of landslide decreases as we go further from the fault and a similar result was noted by Achour et al. (2017). This is due to the weak lithology along the fault and the stability increases as we go away from faults.

The detail of lithology is explained in Table 1. The order of the highest to the lowest IV for the various lithology are Tsl, Tsu, pCs, Tsm, pCd, Pzg, GHlo, and Pzd with the IV 0.967, 0.964, 0.570, 0.524, 0.088, -0.657, -1.016, and -2.718, respectively, while GHlml, Tgr, and Pzj do not influence the landslides with zero IV.

The lowest IV (-1.484) corresponds to the lowest rainfall class (1,168.79-1,503.97). Although the IV does not follow the systematic trend with rainfall intensity for this study, it is observed that the IV increases with an increase in rainfall intensity, and the result resembles the result of Ba et al. (2017). This shows rainfall is one of the triggering factors for the landslides.

Regarding land use, the relationship between the IV and land use is still debatable in many studies. In this study, the highest IV (1.811) corresponds to the built-up area, followed by bare area (0.463), shrubs (0.156), forest (0.008), and agriculture (-1.792). The built-up area disturbs the natural topography and weakens the slopes which ultimately increase the landslides risk.

3.2 Landslide susceptibility mapping

The LSM using statistical analysis works on the principle of past and present landslide events to the future landslide zonation (Aleotti and Chowdhury, 1999). The LSM was developed using the IV which is a part of statistical analysis. The final LSM (Figure 4) is generated by reclassifying the factors using the IV from Table 2 and summing up all the reclassified factors using equation 2. The final LSM needs to classify for the better visualization and zonation of the landslide risk (Jaafari et al., 2014). The natural break classification was selected for this study due to its distinct breakpoint between the groups (Toshiro, 2002). The LSM was classified into five classes which include very safe (16.42%), safe (30.64%), moderately (27.67%), risky (16.18%), and high risky zones

(9.09%). The cost of the repeated maintenance and clearing of the highway due to landslide is much higher than the initial cost of highway construction in the long run. This research will guide the decision-makers to avoid a very high-risk landslide zone during the realignment of the highway.

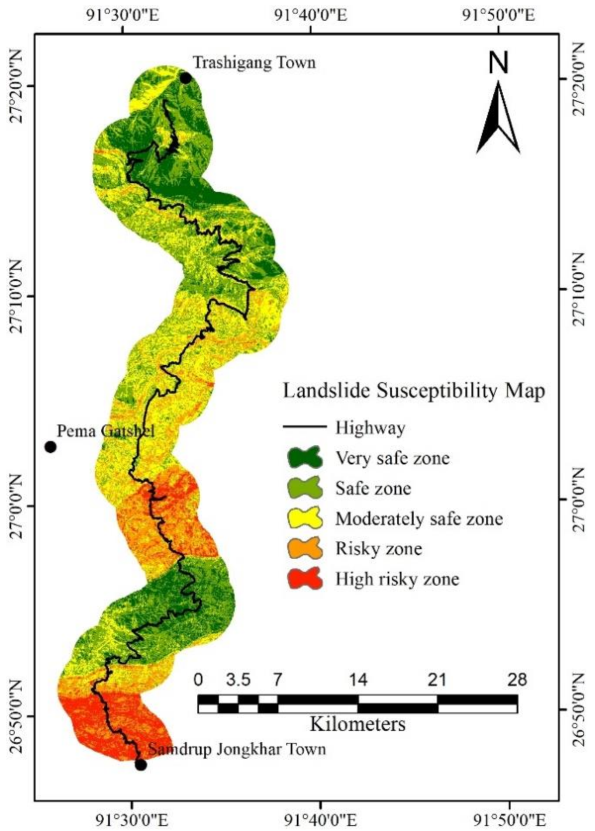

Figure 4. Landslide susceptibility map along Samdrup Jongkhar-Tashigang highway

3.3 Evaluation of the reliability of the information value for the landslide susceptibility mapping

The reliability of the model was performed by the kappa index and its value ranges from -1 (non-reliable) to 1 (reliable). As per Shirzadi et al. (2017), the kappa index is calculated based on equation 3 to equation 5.

$$\text{Kappa} = \frac{P_{obs} - P_{exp}}{1 - P_{exp}} \quad (3)$$

$$P_{obs} = \frac{TP+TN}{n} \quad (4)$$

$$P_{exp} = \frac{(TP+FN)(TP+FP)+(FP+TN)(FN+TN)}{n^2} \quad (5)$$

Where; P_{obs} (observed agreements), P_{exp} (expected agreements), and n (total pixel of the training dataset), TP (true positive), TN (true negative), FP (false positive), and FN (false negative).

As per Landis and Koch (1977), the kappa value is interpreted as shown in Table 3. For this study, the Kappa value of the IV model is 0.3407 and it falls under the fair category for the reliability of the IV model. The fair category of the model shows the fair capability of the IV model to perform LSM.

Table 3. Interpretation of the Kappa statistics scale

Kappa statistics	Strength of agreement
≤0.00	Poor
0.00-0.20	Slight
0.21-0.40	Fair
0.41-0.60	Moderate
0.61-0.80	Substantial
0.81-1.00	Almost perfect

3.4 Validation of landslide susceptibility mapping

The landslide map was validated using the area under the curve (AUC) of the receiver operating characteristic (ROC) curve. The AUC value ranges from 0.5 to 1 with AUC value 1 indicating perfect prediction (Tien Bui et al., 2019). The ROC curve was plotted using 1-specificity on the x-axis and sensitivity on the y-axis (Tien Bui et al., 2019). The sensitivity and specificity were calculated using equation 6 and equation 7

$$\text{Sensitivity} = \frac{TP}{TP+FN} \quad (6)$$

$$\text{Specificity} = \frac{TN}{TN+FP} \quad (7)$$

Where; TP (true positive), TN (true negative), FP (false positive), and FN (false negative).

The success rate curve was generated using the training dataset (70%, 91 landslides location) while the prediction rate is developed using the validation dataset (30%, 39 landslides). The success rate shows how well the resulting landslide map was classified using the existing landslides while the prediction rate indicates the predictive power of the landslide map (Jaafari et al., 2014).

From the validation result, the success rate was 0.7700 (Figure 5(a)) while the prediction rate was 0.6798 (Figure 5(b)). As per Shirani et al. (2018), the AUC is interpreted as excellent (0.9-1.0), very good (0.8-0.9), good (0.7-0.8), moderate (0.6-0.7), and poor (0.5-0.6). From the scale, the success rate (0.7700) falls under a good category while the prediction rate (0.6798) falls under the moderate category.

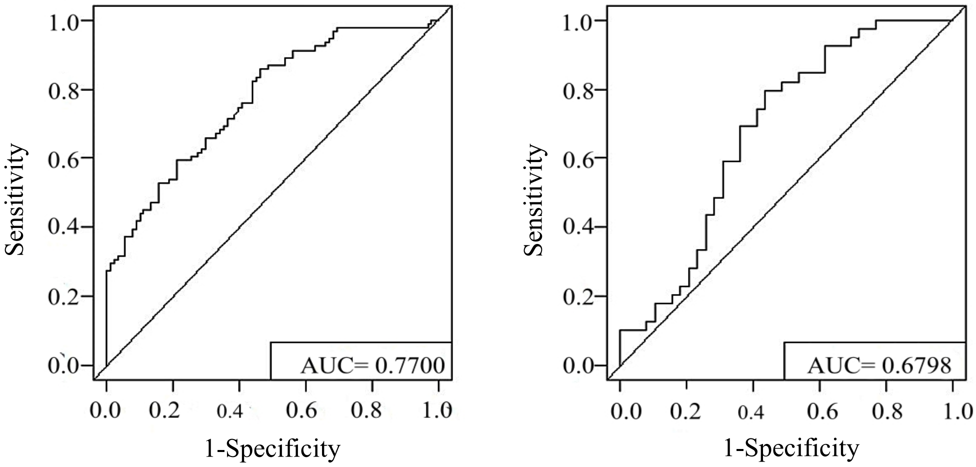

Figure 5. Validation (a) success rate curve, (b) prediction rate curve

4. CONCLUSIONS

This paper presents the LSM developed using the IV along the SJ-TG NH in Bhutan. The reliability of the LSM was checked using the Kappa index and its value of 0.3407 falls under the fair category (0.2-0.4) (Landis and Koch, 1977). Similarly, the LSM has a predictive power of 0.6798 and the prediction rate falls under a moderate category (0.6-0.7) (Shirani et al., 2018). The LSM of the SJ-TG NH is expected to help decision-makers and engineers with the realignment at the critical landslide sites. It is recommended to avoid a very high-risk landslide zone which covers 9.09% of the total area during the realignment of the highway or any other infrastructure development.

This study covers a large area with minimal accuracy using the IV model. The geotechnical study is feasible for a smaller area with higher accuracy (Lei and Jingfeng, 2006). Therefore, it is recommended to do a geotechnical test in the selected sites of the study area to further validate and confirm the reliability of the LSM.

REFERENCES

Achour Y, Boumezbeur A, Hadji R, Chouabbi A, Cavaleiro V, Bendaoud EA. Landslide susceptibility mapping using analytic hierarchy process and information value methods along a highway road section in Constantine, Algeria. Arabian Journal of Geosciences 2017;10(8):194.

Aleotti P, Chowdhury R. Landslide hazard assessment: Summary review and new perspectives. Bulletin of Engineering Geology and the Environment 1999;58(1):21-44.

Ba Q, Chen Y, Deng S, Wu Q, Yang J, Zhang J. An improved information value model based on gray clustering for landslide susceptibility mapping. ISPRS International Journal of Geo-Information 2017;6(1):18.

Chauhan S, Sharma M, Arora MK. Landslide susceptibility zonation of the Chamoli Region, Garhwal Himalayas, using logistic regression model. Landslides 2010;7(4):411-23.

Chen W, Li W, Hou E, Zhao Z, Deng N, Bai H, et al. Landslide susceptibility mapping based on GIS and information value model for the Chencang District of Baoji, China. Arabian Journal of Geosciences 2014;7(11):4499-511.

Chuanhua Z, Xueping W. Landslide susceptibility mapping: A comparison of information and weights-of-evidence methods in Three Gorges Area. Proceeding of the International Conference on Environmental Science and Information Application Technology; 2009 July 4-5; Wuhan: China; 2009.

Dilley M, Chen RS, Deichmann U, Lerner-Lam AL, Arnold M. Natural Disaster Hotspots: A Global Risk Analysis. The World Bank; 2005.

Geertsema M, Highland L, Vaugeouis L. Environmental Impact of landslides. Landslides-Disaster Risk Reduction: Springer; 2009. p. 589-607.

Jaafari A, Najafi A, Pourghasemi H, Rezaeian J, Sattarian A. GIS-based frequency ratio and index of entropy models for landslide susceptibility assessment in the Caspian forest, Northern Iran. International Journal of Environmental Science and Technology 2014;11(4):909-26.

Kahlon S, Chandel VB, Brar KK. Landslides in Himalayan Mountains: A study of Himachal Pradesh, India. International Journal of IT, Engineering and Applied Sciences Research 2014;3:28-34.

Kanungo D, Arora M, Gupta R, Sarkar S. Landslide risk assessment using concepts of danger pixels and fuzzy set theory in Darjeeling Himalayas. Landslides 2008;5(4):407-16.

Keunza K, Dorji Y, Wangda D. Landslides in Bhutan. Country Report. Thimpu. Bhutan: Department of Geology and Mines, Royal Government of Bhutan; 2004. p. 8.

Landis JR, Koch GG. The measurement of observer agreement for categorical data. Biometrics 1977:159-74.

Lei Z, Jingfeng H. GIS-based logistic regression method for landslide susceptibility mapping in regional scale. Journal of Zhejiang University-Science A 2006;7(12):2007-17.

Long S, McQuarrie N, Tobgay T, Grujic D, Hollister L. Geologic map of Bhutan. Journal of Maps 2011;7(1):184-92.

Mandal S, Mandal K. Bivariate statistical index for landslide susceptibility mapping in the Rorachu River Basin of Eastern

Sikkim Himalaya, India. Spatial Information Research 2018;26(1):59-75.
Saha AK, Gupta RP, Sarkar I, Arora MK, Csaplovics E. An approach for GIS-based statistical landslide susceptibility zonation-with a case study in the Himalayas. Landslides 2005;2(1):61-9.
Shirani K, Pasandi M, Arabameri A. Landslide susceptibility assessment by dempster-shafer and index of entropy models, Sarkhoun Basin, Southwestern Iran. Natural Hazards 2018;93(3):1379-418.
Shirzadi A, Bui DT, Pham BT, Solaimani K, Chapi K, Kavian A, et al. Shallow landslide susceptibility assessment using a novel hybrid intelligence approach. Environmental Earth Sciences 2017;76(2):60.
Singh K, Kumar V. Hazard assessment of landslide disaster using information value method and analytical hierarchy process in highly tectonic Chamba Region in bosom of Himalaya. Journal of Mountain Science 2018;15(4):808-24.
Tien Bui D, Shahabi H, Omidvar E, Shirzadi A, Geertsema M, Clague JJ, et al. Shallow landslide prediction using a novel hybrid functional machine learning algorithm. Remote Sensing 2019;11(8):931.
Toshiro O. Classification Methods for Spatial Data Representation. London, UK: Center for Advanced Spatial Analysis University College London; 2002.
Yin K, Yan, T. Statistical prediction model for slope instability of metamorphosed rock. Proceedings of the 5th International Symposium on Landslides; 1988 Jul 10; Lausanne: Switserland; 1988. p. 1269-72.

Reducing Production of CO_2 and CH_4 from Peaty Paddy Soils through Applying Slag in South Sumatera, Indonesia

Anicetus Wihardjaka*, Elisabeth Srihayu Harsanti, Ali Pramono, and Mas Teddy Sutriadi

Indonesian Agricultural Environment Research Institute, Central Java, Indonesia

ARTICLE INFO

Received: 1 Jul 2020
Received in revised: 6 Nov 2020
Accepted: 23 Nov 2020
Published online: 18 Jan 2021
DOI: 10.32526/ennrj/19/2020138

Keywords:
Carbon dioxide/ Methane/ Peaty paddy soil/ Steel slag

*** Corresponding author:**
E-mail: awihardjaka@gmail.com

ABSTRACT

The change of anthropogenic peatlands to agricultural lands could have negative impacts, namely soil subsidence due to oxidation processes, and reduce the stock of soil organic carbon due to the increase of greenhouse gases (CO_2 and CH_4) emissions which contribute to global warming. Stability of converted peatlands could be increased through amelioration of soil by applying steel slag. A laboratory experiment was conducted with using factorial complete randomized design with ten combination treatments, including slag application, of peat soil samples collected from paddy fields in South Sumatera. This study determined the effect of steel slag application on reducing greenhouse gas (CO_2 and CH_4) production from cultivated peatland soils. The first factor of experimental treatment was peaty soil from 5 different locations, and the second factor was the application of steel slag. The highest production potentials of CH_4 and CO_2 were shown by peaty paddy soils from Kayu Agung and Plaju, respectively, while the lowest fluxes were shown by Indralaya's peaty paddy soil. Peaty paddy soil from the Indrajaya site produced the lowest CO_2 and CH_4 compared with other sites. Application of steel slag ameliorant reduced CH_4 and CO_2 emissions by 19.24% and 18.95%, respectively, on average. Slag ameliorant also reduced acidity of peaty paddy soils.

1. INTRODUCTION

The area of peat land in Indonesia is 14.9 million hectares (ha), most of which are distributed in Sumatera, Kalimantan and Papua (Wahyunto et al., 2014). Of the total area of peat, around 50.1% of the land is covered by forests, 10.5% by oil palm, 5.7% by other cereal crops and 2.3% by rice fields. About 44.6% of Indonesia peatland had been degraded (Masganti et al., 2014). Peat soils are degraded when the organic C content decreases from 38.91-57.24 g/kg to 30.62-41.83 g/kg and are a source of greenhouse gases (GHGs) emissions (Masganti et al., 2014). Peat also plays an important role as a long-term sink of GHG (Roulet et al., 2007). Improper management of peat is a source of greenhouse gas (GHG) emissions that contributes to global warming and climate change (Miettinen and Liew, 2010; Leng et al., 2019).

Tropical peatlands are a source of carbon deposits (70 Gt C) and nitrogen. Carbon stocks (C) in tropical peatlands vary with a range of 30-70 kg C/m^3 or 300-700 mg C/ha per meter of peat depth, while the C content in mineral soils at depths of 0-20 or 25 cm does not exceed 250 mg C/ha (Agus and Subiksa, 2008). Peatlands in Sumatera and Kalimantan are estimated to have a C stock varying in the range 2,000-3,000 Mg C/ha, which are potential sources of high C emissions. Organic matter in peat soil is naturally decomposed slowly and continuously. Drained peat accelerates decomposition rates, soil subsidence and carbon loss (Crozier et al., 2000; Hooijer et al., 2012). Carbon loss from peats used for agricultural cultivation ranges from <40 mg to <60 mg CO_2/ha/year on 70 cm of groundwater (Hooijer et al., 2012). The high water retention in peatland limits or impedes decomposition rate of soil organic matter, and lowering of peat water table increases organic matter mineralization and this subsequently enhances carbon losses (Leng et al., 2019)

The management of land use change of peatlands for agricultural activities greatly influences the rate of decomposition. Draining of organic soils for agricultural purposes increases the emissions of greenhouse gases (CO_2, CH_4, and N_2O) compared to

Citation: Wihardjaka A, Harsanti ES, Pramono A, Sutriadi MT. Reducing production of CO_2 and CH_4 from peaty paddy soils through applying slag in South Sumatera, Indonesia. Environ. Nat. Resour. J. 2021;19(2):132-140. (https://doi.org/10.32526/ennrj/19/2020138)

undrained peat (Kasimir et al., 2018). Without appropriate management, peats are easily degraded and become a source of GHG emissions. In the reductive conditions of soil, the decomposition rate of organic matter is slow and produces a lot of poisonous organic acids and high methane (Rezanezhad et al., 2016), whereas in oxidative conditions the decomposition rate is rapid and much CO_2 is released (Nakonieczna and Stepniewska, 2014; Evans et al., 2019). The rate of decomposition under anaerobic or aerobic conditions affects the balance of CO_2 versus CH_4 production in peat rice soils (Rumbang, 2015). The rate of decomposition of peat determines the level of peat maturity or changes in the level of fibers content in peat soil (Sulistyono, 2000).

The peat utilization for lowland rice cultivation influences the dynamics of GHG emissions mainly carbon dioxide (CO_2) and methane (CH_4). CO_2 and CH_4 emissions contribute to the global greenhouse effect by 55% and 15%, respectively (Mosier et al., 1994; Olivier et al., 2017). The effect of CH_4 in the atmosphere on global warming is 21 times greater than CO_2 (IAARD, 2011). The methane concentration of 1.3 ppm in the atmosphere causes an increase in global temperature by 1.3°C. Anthropogenic global methane emissions in 2010 were 6,875 million mg of CO_2-e which is predicted to increase by 15% to 7,904 million mg of CO_2-e in 2020 (Global Methane Initiative, 2017).

Indonesia has committed to reduce GHG emissions from the sectors of peat, energy, waste, forestry, industry and agriculture by 26% independently or 41% with international cooperation. Based on Presidential Regulation No. 61/2011, the target for reducing GHG emissions from sustainable peat management is 103.98 million mg of CO_2-e (Ministry of Environment and Forestry, 2017).

Increased productivity of peat can be improved through amelioration, among others, by utilizing industrial waste such as slag. The iron and steel industry produces 20% of slag waste per ton of steel production which has the potential to negatively impact the environment and public health (Perdana and Sukandar, 2016). Slag waste management is based on the concept of reduce, reuse, recycle and recovery approaches. During this time, slag waste has been used as a mixture of cement construction materials and asphalt mixtures for road construction (Yahya, 2013; Perdana and Sukandar, 2016). Slag is an iron or steel smelting industrial waste in the form of small chunks obtained from the side results of steel making in a high temperature furnace. Steel slag has been reported to contain 40-43% CaO, 31-36% SiO_2, 13-15% Al_2O_3, and 4-6% MgO (Munir and Handayani, 2012). Slag is rich in lime (CaO), silicic acid (SiO_2), phosphoric acid (P_2O_5), magnesia (MgO), Mn, and Fe. These properties of the slag can be exploited to make use as a fertilizer (Das et al., 2019). Fertilizers made of slag are categorized as slag silicate fertilizer, lime fertilizer, slag phosphate fertilizer, and iron matter of special fertilizer (Das et al., 2019). The objective of this paper was to determine the effect of steel slag ameliorant on the production rates of CO_2 and CH_4 from peaty paddy soils.

2. METHODOLOGY

2.1 Soil sampling and experimental design

The research activities were carried out at the greenhouse gas laboratory, Indonesian Agricultural Environment Research Institute in Pati Regency, Central Java Province in October-December 2017. The peaty paddy soils were taken at the center of wetland rice in South Sumatera, namely Plaju, Musi Banyuasin District (104.78694°E, -2.98569°S), Jejawi, Ogan Komering Ilir/OKI District (104.79293°E, -3.06313°S), Kayu Agung, OKI District (104.80498°E, -3.32292°S), Teluk Gelam, OKI District (104.73877°E, -3.46498°S), and South Indralaya, Ogan Ilir District (104.64241°E, -3.26908°S), as shown in Figure 1. The undisturbed soils were taken with a ring sampler from a PVC pipe diameter 14 cm at a depth of 30 cm, according to standard sampling. Soil in the pipe are closed and wrapped in black plastic to avoid oxidation.

The factorial experiment was arranged in a completely randomized design replicated three times, with peaty soil samples from South Sumatera as the first factor treatment covering peaty soil from Plaju, Jejawi, Kayu Agung, Teluk Gelam, South Indralaya; and the application of steel slag as a second factor treatment consisting of without applying steel slag and with applying 1 mg steel slag/ha. Steel slag is broadcasted on peaty soil surface.

Peat taken from Plaju and Jejawi is a shallow peat (less than 50 cm depth) and categorized as peaty land that has been utilized for wetland cultivation, while that taken in Kayu Agung, Teluk Gelam and Indralaya is medium peat dominated by vegetation of *alang-alang*/cogon grass (*Imperata cylindrica* L.), *gelam* (*Maleleuca* sp.), and partly used for palm oil plantations.

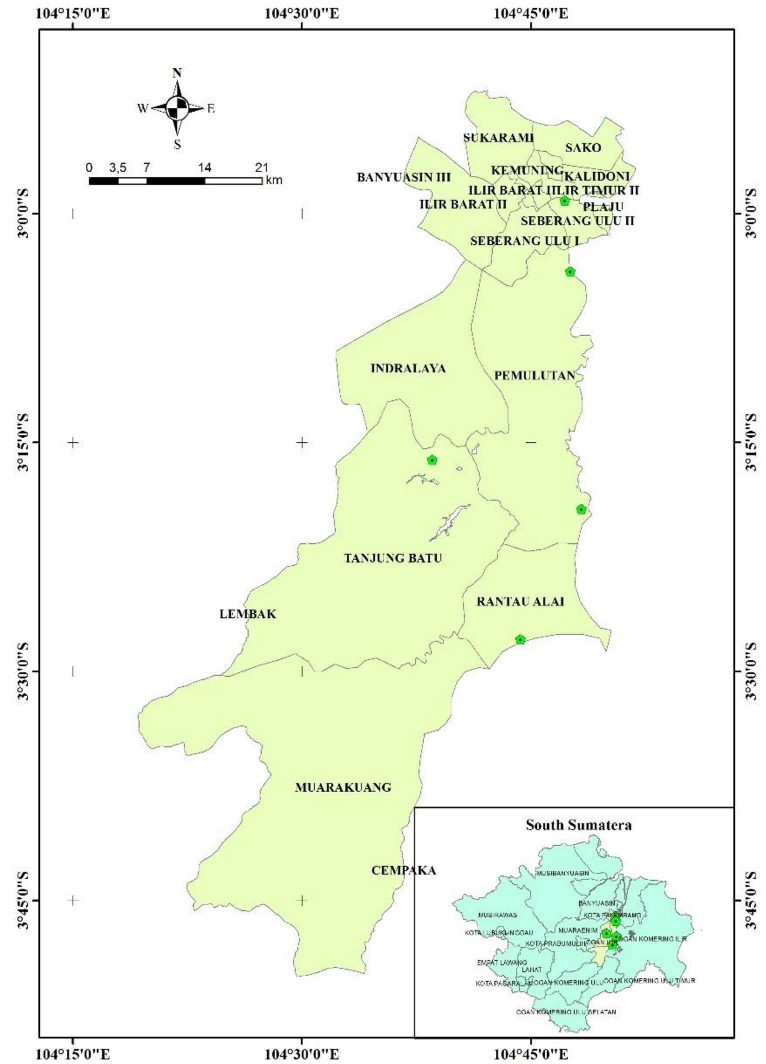

Figure 1. Map of peaty paddy soil sampling in South Sumatera

Characteristics of soil samples were analyzed at the Bogor Soil Research Institute Laboratory, while the analysis of GHG production rates was carried out in the GHG laboratory at Indonesian Agricultural Environment Research Institute. Analysis of physical and chemical properties of peaty soil covered fiber content, organic C (Walkley and Black method), total N (Kjeldahl method), available P (Bray 1 method), exchangeable K (Morgan method), cation exchangeable capacity and exchangeable cation (NH_4OAc 1 N saturation method), Al^{3+} and H^+ (KCl 1 N method), Fe, Mn, Cu, Zn (DTPA method), density (gravimetric method), fulvic, and humic acid content (extraction NaOH + $Na_2P_2O_7$ method).

2.2 Experimental implementation

Incubation was carried out in the laboratory. Peaty rice soils in PVC pipes were maintained in water saturation conditions and prepared for treatments. The top of the pipe was closed with a cover equipped with rubber septum, thermometer, and channel for gas N_2 intake. N_2 gas flowed at 250 mL/min into ring sampler, and gas samples were taken using a syringe vol-10 mL (t_0). After incubation for 24 h (t_{24}), the gas sample was taken again. Additional gas sampling was carried out every two days for 30 days with steps like the first step. Gas samples taken from the trap hood were injected in a gas chromatography (GC) device with different detectors. The CH_4 concentration was measured by a GC tool equipped with flame ionization detector (FID), while CO_2 concentration was analyzed using a GC tool with a thermal conductivity detector (TCD). The production rate of methane and carbon dioxide was determined using the equation used by Lantin et al. (1995), as follows:

$$E = (C_{24} - C_0) \times \frac{Vh}{20} \times \frac{mW}{mV} \times \frac{273.2}{(273.2+T)} \quad (1)$$

Where; E=production of CH_4 or CO_2 (mg/g soil); C_0=concentration of CH_4 or CO_2 at t_0 (ppm); C_{24}=concentration of CH_4 or CO_2 at 24 h after incubation (ppm); Vh=headspace volume in incubation glass (mL); mW=molecule weight of CH_4 or CO_2 (g); mV=molecule volume of CH_4 or CO_2 (22.4 L at standard temperature and pressure in mol/L); T=averaged temperature in incubator (°C)

2.3 Data analysis

The collected data were analyzed by analysis of variance using the SAS program followed by a real honest difference test (Tukey test) at 5% level to determine significant differences between treatments.

3. RESULTS AND DISCUSSION

3.1 Flux of methane and carbon dioxide

The highest methane flux is seen in peaty paddy soils from Kayu Agung compared to other locations (Figure 2). The lowest CH_4 flux was seen in peaty paddy soils from Indralaya followed by from Plaju, while the magnitude of methane flux on peaty soil from Gelam and Jejawi is between Indralaya/Plaju and Kayu Agung.

The application of slag can generally decrease methane production from peaty paddy soils, except in Teluk Gelam site (Figure 2). The decrease in CH_4 production is possible due to the oxidants role in steel slag such as Al_2O_3, SiO_2, CaO, MgO (Munir and Handayani, 2012), which can oxidate CH_4 to CO_2. Slags are rich in oxides of iron, aluminum, manganese, and silica that act as alternative electron acceptors in an anoxic soil and their application suppress CH_4 emissions by stimulating iron for reducing methanogenic bacterial activity (Das et al., 2019). Slag reduces potentially methane emission by 0.6-56.0% from rice fields, depend on the slag type, rate of application, soil type, and agronomic practices (Das et al., 2019). Amelioration of peaty paddy soils with steel slag produces flux with a range of 0.0002-0.0654 mg CH_4/g soil, while CH_4 production without applying steel slag ranges 0.0002-0.0787 mg/g soil during 55 days of incubation. The application of steel slag in anaerobic soil conditions does not affect the activity of methanogenic bacteria in the formation and release of methane gas.

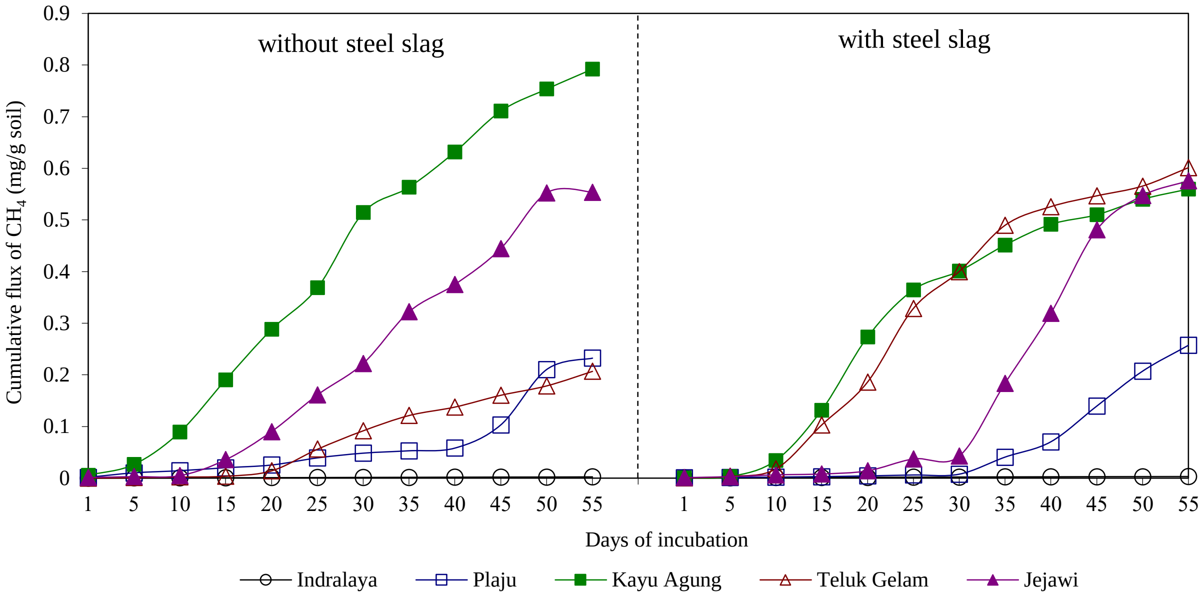

Figure 2. Cumulative fluxes of methane from peaty paddy soils in South Sumatra

The magnitude of methane production in peaty soils from Kayu Agung is related to peat condition that reacts rather acid-neutral, while the high flux in peat from Jejawi and Plaju may be due to the higher organic matter content (Table 1). The methane flux in peat from Indralaya is low during incubation which was caused by high soil acidity and oxidative condition that was more dominant than the reductive condition, so these conditions are not favourable for methanogenesis process.

Table 1. Characteristics of peaty paddy soil from South Sumatra

Site	pH-H_2O	C-total (g/kg)	N-total (%)	C/N	P_2O_5 HCl 25% (mg/ kg)	K_2O HCl 25% (mg/kg)	Exchangeable cations (cmol/kg)				CEC (cmol/kg)	BS (%)	Humic acid (g/kg)	Fulvic acid (g/kg)
							Ca	Mg	K	Na				
Indralaya	4.19	9.71	0.51	19	129	28	3.99	2.07	0.30	0.99	30.99	24	1.91	0.43
Plaju	5.12	11.17	0.72	16	19	14	3.96	3.49	0.18	1.56	31.04	30	2.56	0.51
Kayu Agung	5.65	6.80	0.49	14	34	49	3.43	1.70	0.25	0.29	19.70	29	1.41	0.68
Teluk Gelam	5.15	4.94	0.31	16	15	58	3.96	1.99	0.12	0.38	18.12	36	1.05	0.67
Jejawi	4.98	10.90	0.84	13	66	39	10.43	3.80	0.33	0.50	34.38	44	2.27	0.39

Note: CEC=cations exchange capacity, BS=base saturation

Peaty soil from South Sumatra generally reacts acid-slightly acid (pH>4), where the peaty pH value from Kayu Agung approaches neutral, while peaty from Indralaya reacts more acid than from Jejawi, Plaju, Teluk Gelam, and Kayu Agung (Table 1). The total C content of peat in South Sumatra is generally high. Peat from Teluk Gelam has the lowest total C content. Thin or shallow peaty soils from South Sumatra have generally been used for agricultural crops cultivation, so the organic material has been mineralized with a C N ratio less than 20. The content of P and K extracted with HCl 25% in South Sumatra peat ranges from 15-129 and 14-58 mg/kg, respectively. Exchangeable cations and cation exchange capacity (CEC) from Jejawi are relatively higher than from other sites. The magnitude of peaty CEC is possible due to more functional groups in organic matter. According to Liang et al. (2006), the oxidized functional groups in black carbon will increase cation exchange capacity in soils.

Figure 3 shows the fluctuations in production rate of CO_2 from South Sumatra peat. The lowest CO_2 flux was seen in peaty paddy soils from Indralaya followed by peat from Kayu Agung, while the highest CO_2 flux was seen in peaty rice soils from Plaju. Peat from Jejawi and Plaju has a thin layer with relatively high fulvic acid and humic acid content, so that the potential of mineralization rate is higher when soils cannot be maintained in its reductive conditions.

Peat contains functional groups such as carboxyls and phenols which are weak acids. The source of peat damage is caused by carboxyl and phenolic groups. Carbon emissions generally occur in aliphatic groups which are easily degraded by microbes to produce CO_2 and CH_4. The application of steel slag generally decreases CO_2 production from peaty wetlands (Figure 3). Steel slags contain oxides and polyvalent cations such as Al, Fe, Mn which can form coordination bonds with organic ligands where polyvalent cations form the core of coordination and bind monomeric organic acids to form complex compounds. Carboxyl functional groups are high in low pH peat. Applying slag can stabilize the bonds of organic acids and polyvalent cations and increase pH values (Husen and Agus, 2011). The oxidant contents of CaO, MgO, Al_2O_3, SiO_2 in steel slag enhances CO_2 production due to the oxidants role in oxidizing methane in peaty paddy soils. Amelioration of peat paddy soils with steel slag gives flux with a range of 2.17-3.42 mg CO_2/g soil, while CO_2 production without steel slag ranges from 1.99 to 4.64 mg/g soil for soil sample incubated for 70 days. Application of steel slag to peat wetlands significantly reduces the potential for CO_2 production. Addition of ameliorants that contain high valence cations may form a ligand complex with the simple organic acids and thus reduce the rate of peat decomposition (Husen and Agus, 2011).

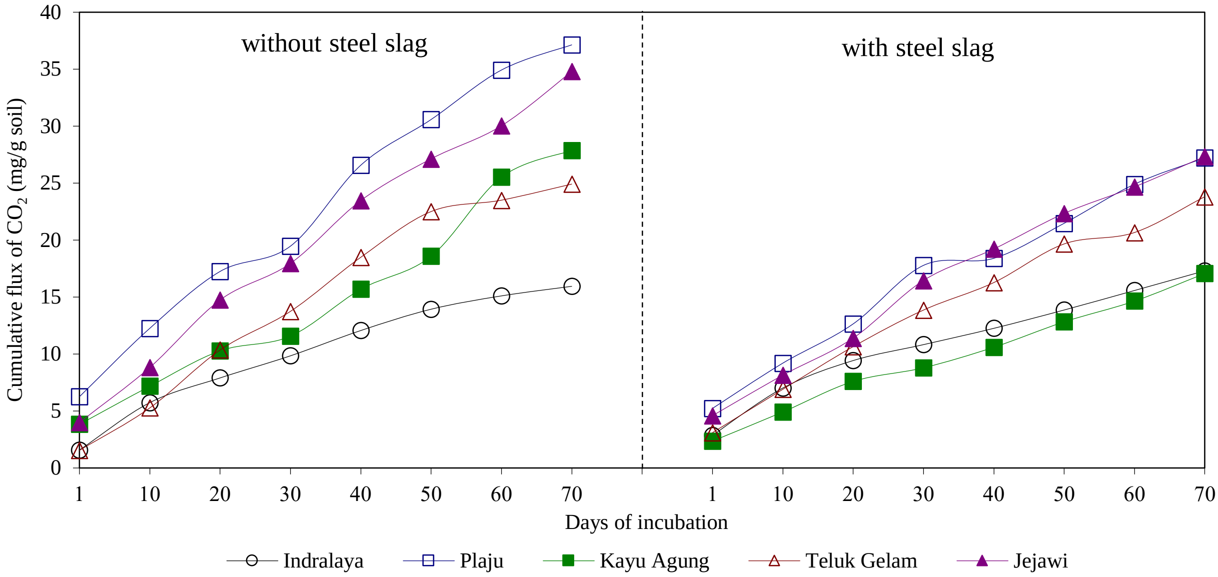

Figure 3. Cumulative flux of carbon dioxide from peaty paddy fields in South Sumatra

3.2 Production of methane and carbon dioxide

The low production of greenhouse gases (CO_2+CH_4) from Indralaya's peat paddy fields indicates that conversion of peat land to lowland rice cultivation has caused decomposition of organic matter which has resulted in a decrease in carbon availability in the peat soil. In peat soil from Plaju, CH_4 flux is low but CO_2 flux is high, this reflects that the peat soil is sensitive to aerobic conditions, so the decomposition process of organic matter will produce CH_4 higher than CO_2. In contrast, the peat soil from Kayu Agung shows high CH_4 flux and low CO_2 flux, this indicates organic matter decomposition under anaerobic conditions' potential to produce CH_4 higher than CO_2. It was also probable that the CH_4 was emitted from nonmicrobial sources of CH_4 production such as lignin and humic acids (Wang et al., 2013). This might have happened under tropical temperature as peat soils are high in organic matter besides being natural polyelectrolytes with substances such as humic and fulvic acids as its major components (Choo and Ahmed, 2017).

The potential for CH_4 and CO_2 productions from peaty paddy fields in the five locations in South Sumatra is significantly different with p value <0.05 (Table 2). The application of steel slag only significantly affects CO_2 production with p value of 0.0601 (Table 3). The application of steel slag into peat paddy fields tends to reduce the production rate of CH_4 and CO_2 after 70 days of incubation. The steel slag reduced production of CH_4 and CO_2 by an average of 19.24% and 18.95%, respectively. We presumed that the content of polyvalent cations in steel slag plays an important role in the complexation of organic acids which decreases production of CO_2 and CH_4 and increases soil pH.

Table 2. Potential production of greenhouse gas and acidity from five sites of peaty paddy fields in South Sumatra

Treatment	CH_4 flux (mg/g soil)	CO_2 flux (mg/g soil)	pH value
Indralaya	0.0002^{a}	1.74^{a}	3.80^{a}
Plaju	0.0178^{ab}	4.02^{b}	4.29^{a}
Kayu Agung	0.0657^{b}	2.81^{ab}	5.52^{b}
Teluk Gelam	0.0257^{ab}	3.05^{ab}	5.15^{b}
Jejawi	0.0574^{ab}	3.88^{b}	4.59^{ab}
p value	0.0430	0.0068	0.0060

Means in same column followed by same letter are significantly different according to Tukey test at 0.05 level.

Table 3. Effect of steel slag application on production of methane, carbon dioxide and acidity of peaty paddy fields in South Sumatra

Treatment	CH_4 flux (mg/g soil)	CO_2 flux (mg/g soil)	pH value
Without steel slag	0.0369^a	3.42^a	4.12^a
With steel slag	0.0298^a	2.78^a	5.22^b
p value	0.4210	0.0621	0.0001

Means in same column followed by same letter are significantly different according to Tukey test at 0.05 level.

The average production of CO_2 in peat soils with steel slag applied ranged from 2.17-3.42 mg CO_2/g soil which is relatively lower than without steel slag application which ranged from 1.99-4.64 mg CO_2/g soil. With steel slag applied in peaty wetlands, the average of CH_4 production ranged between 0.0002-0.0501 mg CH_4/g soil, while without steel slag CH_4 production ranged between 0.0002-0.0660 mg CH_4/g soil. Generally, peaty paddy fields from Kayu Agung and Jejawi produced high CH_4 flux compared to the other three locations, while the highest CO_2 flux can be seen in Plaju and Jejawi locations. The lowest production of CO_2 and CH_4 is generally seen at the Indrajaya site.

3.3 Peat acidity

Peat has very low pH values, ranging from 3 to 4 depending on the peat properties. Peat requires additional lime such as calcitic or dolomitic lime to adjust the pH to a value around 5.5 (Prasad et al., 2020). Slag has been used widely in acidic soils to neutralize soil acidification (Das et al., 2019). Application of ameliorant on peat soil has an important role on improving fertility status of peat soil via increasing soil pH, reducing organic acids and toxic ions, and also increasing nutrients availability (Septiyana et al., 2016). The diversity of peat paddy fields significantly influences the soil acidity (p=0.006) as presented in Table 2. The application of steel slag also significantly determines the change in soil acidity (p=0.000), but its interaction with peat paddy fields does not significantly affect changes in soil pH. Thus, steel slag significantly decreases the acidity of peat paddy fields compared to without using steel slag. The pH values of peat without using steel slag ranged from 3.14-5.99 while pH values with steel slag ranged from 4.19-6.12. The average pH values of peatland without and with steel slag was 4.12 and 5.22, respectively. The slag fertilizer utilized in agriculture is effective to neutralize soil acidity (Das et al., 2019).

The content of Ca and Mg in steel slag plays a role in reducing soil acidity. Increased soil pH helps plants easily absorb other nutrients. There is a positive correlation between Ca and Mg and pH value. Slag application is not only to increase the pH value but also supply Ca and Mg which are essential plant nutrients required for plant growth (Prasad et al., 2020).

Steel slag has the opportunity and prospect to be used as fertilizer or ameliorant because of the essential cations needed for the growth and development of plants such as silicate, calcium, magnesia, iron, phosphor. Slag is high in lime, silicic acid, phosphoric acid, magnesia, manganese, and iron. The properties of the slag can be exploited to make use of fertilizer. Mostly in Japan, Korea, and China, slag has been intensively utilized as raw materials for fertilizer production, such as silicate fertilizer, lime fertilizer, slag and phosphate fertilizer to improve crop productivity, alleviate soil acidification, mitigate GHG emissions, and stabilize heavy metals (Das et al., 2019). The addition of slag-based silica fertilizer increase Si 0.16-47.2% in rice grain yield and could improve crop yield up to 47.2%. High yields in response to silicate fertilizer occurs because Si preferentially deposits in the epidermal cell wall and increase the physical strength of leaves and leaf-sheaths and helps plants to sustain yield by counteracting various biotic and abiotic stresses (Das et al., 2019).

Utilization of steel slag as fertilizer or ameliorant is constrained by its heavy metal content. Slags contain traces of heavy metals, but the concentrations of heavy metals might not be enough to pose environmental risks (Das et al., 2019). Before being applied on agriculture, the content of heavy metals in the fertilizer must be reduced to the permissible concentration based on regulations for hazardous heavy metals in order to be safe for the environment and human health.

4. CONCLUSION

Amelioration of peat paddy fields using steel slag tends to reduce the production rate of CO_2 and CH_4, and soil acidity. The application of steel slag reduced the production of CO_2 and CH_4 by 18.95 and 19.24%, respectively. The application of steel slag decreases production of CO_2 and CH_4 and increases soil pH. The potential production of methane from peaty paddy fields in South Sumatra, stated sequentially from the lowest, is Indralaya<Plaju< Teluk Gelam<Jejawi<Kayu Agung, while the potential for CO_2 production in peat rice fields is from Indralaya<Kayu Agung<Teluk Gelam<Jejawi<Plaju. Steel slag has the prospect to be utilized as a raw material of fertilizer or ameliorant to mitigate GHG emission from peaty soils and substitute for limestone to neutralize soil acidity and improve crop productivity.

ACKNOWLEDGEMENTS

In this chance, authors acknowledge to Ms. Titi Sopiawati and Mr. Yono who help in analyzing GHGs concentrations in laboratory. As main contributors, Anicetus Wihardjaka and Ali Pramono are equal contributors in preparing this work since arranging experimental design until writing of manuscript, while Elisabeth Srihayu Harsanti and Mas Teddy Sutriadi are as supporting contributors that help in analyzing data statistically and correcting manuscript, respectively.

REFERENCES

Agus F, Subiksa IGM. Peatlands: Potency for Agriculture and Environmental Aspects. Bogor: IAARD-World Agroforestry Centre; 2008.

Choo LNLK, Ahmed OH. Methane emission from pineapple cultivation on a tropical peatland at Saratok, Malaysia. Sustainable Agriculture Research 2017;6(3):64-74.

Crozier CR, DeLaune RD, Patrick Jr. WH. Methane production in Mississippi deltaic plain wetland soils as a function of soil redox species. In: Lal R, Kimble J, Levine E, Stewart BA, editors. Soils and Global Change. Boca Rahon, Florida: CRC Press; 2000. p. 247-55.

Das S, Kim GW, Hwang HY, Verma PP, Kim PJ. Cropping with slag to address soil, environment, and food security. Frontiers in Microbiology 2019;10:1320.

Evans CD, Williamson JM, Kacaribu F, Irawan D, Suardiwerianto Y, Hidayat MF, et al. Rates and spatial variability of peat subsidence in Acacia plantation and forest landscapes in Sumatra, Indonesia. Geoderma 2019;338:410-21.

Global Methane Initiative. Global Methane Emissions and Mitigation Opportunities [Internet]. 2017 [cited 2019 Dec 15]. Available from: http://www.globalmethane.org/.

Indonesian Agency for Agricultural Research and Development (IAARD). Road Map of Agricultural Strategies Facing Climate Change. Jakarta: Indonesian Agency for Agricultural Research and Development; 2011.

Hooijer A, Page S, Jauhiainen J, Lee WA, Lu XX, Idris A, et al. Subsidence and carbon loss in drained tropical peatlands. Biogeosciences 2012;9:1053-71.

Husen E, Agus F. Microbial activities as affected by peat dryness and ameliorant. American Journal of Environmental Science 2011;7(4):348-53.

Kasimir A, He H, Coria J, Norden A. Land use of drained peatlands: Greenhouse gas fluxes, plant production, and economics. Global Change Biology 2018;24(8):3302-316.

Lantin RS, Aduna JB, Javeliana AM. Methane Measurements in Rice Fields. Los Banos, Manila, Philippines: International Rice Research Institute; 1995.

Leng LY, Ahmed OH, Jalloh MB. Brief review on climate change and tropical peatlands. Geoscience Frontiers 2019;10:373-80.

Liang B, Lehmann J, Solomon D, Kinyangi J, Grossman J, O'Neill B, et al. Black carbon increases cation exchange capacity in soils. Soil Science Society of America Journal 2006;70: 1719-30.

Masganti, Wahyunto, Dariah A, Nurhayati, Yusuf R. Characteristic and potential utilization of degraded peatlands in Riau Province. Jurnal Sumberdaya Lahan 2014;8(1):59-66.

Miettinen J, Liew SC. Status of peatland degradation and development in Sumatra and Kalimantan. Ambio 2010; 39:394-401.

Ministry of Environment and Forestry. Nationally Determined Contribution (NDC) and Progress. Ministry of Environment and Forestry; 2017. p. 49.

Mosier AR, Bronson KF, Freney JR, Keerthisinghe DG. Use nitrification inhibitors to reduce nitrous oxide emission from urea fertilized soils. In: CH_4 and N_2O: Global Emissions and Controls from Rice Field and Other Agricultural and Industrial Sources. Tsukuba, Japan: NIAES; 1994. p. 187-96.

Munir M, Handayani NI. Recycling of sludge wastes from industry of iron slag as mixture materials in environmentally friendly steel industry. Jurnal Riset Teknologi Pencegahan Pencemaran Industri 2012;2(1):1-10.

Nakonieczna AS, Stepniewska Z. Aerobic and anaerobic respiration in profiles of Polesie Lubelskie peatlands. International Agrophysic 2014;28:219-29.

Olivier JGJ, Schure KM, Peters JAHW. Trends in global CO_2 and total greenhouse gas emissions: 2017 report. PBL Netherlands Environmental Assessment Agency; 2017.

Perdana AL, Sukandar. Heavy metals leachability from iron and steel slag utilization as aspalt concrete - wearing course aggregate. Jurnal Teknik Lingkungan 2016;22(1):1-10.

Prasad M, Chrysargyris A, McDaniel N, Kavanagh A, Gruda NS, Tzortzakis N. Plant nutrient availability and pH of biochars and their fractions, with the possible use as a component in a growing media. Agronomy 2020;10(1):1-17.

Rezanezhad F, Price JS, Quinton WL, Lennartz B, Milojevic T, van Cappellen P. Structure of peat soils and implications for water storage, flow and solute transport: A review update for geochemists. Chemical Geology 2016;429:75-84.

Roulet NT, Lafleur PM, Richard PJH. Contemporary carbon balance and late holocene carbon accumulation in a northern peatland. Global Change Biology 2007;13:397-411.

Rumbang N. A study of carbon dioxide emission in different types of peatland use in Kalimantan. Agricultural Science 2015;18(1):9-17.

Septiyana, Sutandi A, Indriyati LT. Effectivity of soil amelioration on peat soil and rice productivity. Journal of Tropical Soils 2017;22(1):11-20.

Sulistyono NBE. Role of Fe(III) Cation on Production of Carbon Dioxide (CO_2) and Methane (CH_4) [dissertation]. Bogor, University of IPB; 2000.

Wahyunto, Nugroho K, Ritung S, Sulaeman Y. Indonesian peatland map: Method, certainty, and uses. Proceedings of the Sustainable Management of Degraded Peatlands to Mitigate

GHGs Emissions and Economical Value Increase; 2014 Aug 18-19; Jakarta: Indonesia; 2014.

Wang B, Hou L, Liu W, Wang Z. Non microbial methane emissions from soils. Atmospheric Environment 2013;80: 290-8.

Yahya M. Utilization of Industrial Waste Steel (Blast Furnace Iron Slag) as Building Materials Case Study: PT. Barawaja Makassar. Proceedings of Thirty-First International Conference on Solid Waste Technology and Management; 2016 Apr 3-6; Philadelphia: USA; 2013. p. 11-7.

Landslide Risk Analysis on Agriculture Area in Pacitan Regency in East Java Indonesia Using Geospatial Techniques

Aditya Nugraha Putra[1*], Istika Nita[1], Muhammad Rifqi Al Jauhary[1], Shofie Rindi Nurhutami[1], and Mohd Hasmadi Ismail[2,3*]

[1]*Department of Soil Science, Faculty of Agriculture, University of Brawijaya, Malang, Indonesia*
[2]*Department of Forestry Science and Biodiversity, Faculty of Forestry and Environment, Universiti Putra Malaysia, 43400 UPM, Serdang, Selangor, Malaysia*
[3]*Geospatial Information Science Research Centre, Faculty of Engineering, Universiti Putra Malaysia, 43400 UPM Serdang, Selangor, Malaysia*

ARTICLE INFO

Received: 9 Jul 2020
Received in revised: 20 Nov 2020
Accepted: 16 Dec 2020
Published online: 20 Jan 2021
DOI: 10.32526/ennrj/19/2020167

Keywords:
Landslides/ Land use/ Agriculture/ Geographic information system/ Remote sensing

*** Corresponding author:**
E-mail: aditya.n.putra@ub.ac.id; mhasmadi@upm.edu.my

ABSTRACT

Pacitan is one of the regencies in East Java Province, dominated by hills and mountain landforms covering 85% of its area. Since 2011, more than 16 landslides have occurred significantly in this area. These disasters have engulfed more than 350 ha of agricultural land in Pacitan. This study analyzed the risk of future landslides due to land use change. The parameters used were rainfall, slope, topography, geology, soil, and land use which were assessed and weighed by the Paimin method. Land-use classification from Landsat 8 OLI in 1998, 2008, and 2018 were analyzed using regression formula to calculate the trend of change in 2030. Land use was also classified from the land capability classification (LCC) and regional spatial planning (RSP) as land use options in 2030. The results showed that land use changed over time due to the changes in landslide hazards, which increased three-foldfrom 1998 to 2018 and will peak tremendously in 2030. There are 29.47 ha of agricultural land in 2018 that have a high potential landslide hazard if no intervention is made. The accuracy for prediction of the 2018 data mapping was 82%. The LCC strategy suggests land use planning to reduce a high level of the landslides.

1. INTRODUCTION

The landslide is defined as the movement of a mass of rock, debris, or earthflow (Cruden, 1991). The landslide is one of the natural disasters with severe damages (Jiao et al., 2019), especially in mountainous areas and there is a tendency forlandslides to increase in the era of climate change (Dagdelenler et al., 2015; Kirschbaum et al., 2015) and natural resource exploitation activities, including in the Asia Region. Globally, from 2004 to 2016, there were 4,800 landslides with 56,000 fatalities. Furthermore, Frounde and Petley (2018) suggested that 300 million people are affected by this disaster. Based on BNPB (2019) data from 1998 to 2020, there were 5,157 landslides in Indonesia. In Indonesia, tectonic conditions form faults, volcanic rocks are easily fragile, and supported by the climate in Indonesia, which is wet tropics, so the potential for landslides is high. This condition is supported by the recent changes in land use and the high erosion triggered by rainfall which causes landslides to increase (Fan et al., 2017; Naryanto et al., 2019). Indonesia is ranked in the top three countries with the highest percentage (32%) of landslide fatalities (Frounde and Petley, 2018; Hidayat et al., 2019). Especially in Pacitan, landslides occurred more than 16 times from 2011 to 2020. Landslides are one of the most common natural risks that threaten the safety and property of mountain farmers (Conforti et al., 2014). This disaster causes soil erosion (Panagos et al., 2018), which can directly result in cropland abandonment. Meanwhile, landslides may damage farmland irrigation systems and increase the difficulty of cropland management (Zhao et al., 2018), which can indirectly result in cropland abandonment. Based on Geological Map of 1:100,000, Pacitan Regency is identified to have a sufficient number of faults that can potentially cause landslides. This condition is exacerbated by the

Citation: Putra AN, Nita I, Jauhary MRA, Nurhutami SR, Ismail MH. Landslide risk analysis on agriculture area in Pacitan Regency in East Java Indonesia using geospatial techniques. Environ. Nat. Resour. J. 2021;19(2):141-152. (https://doi.org/10.32526/ennrj/19/2020167)

topography of which 85% is formed from hills and small mountains with a slope of more than 40% (Nita et al., 2020). Landslides hit Pacitan and cause damage to paddy fields covering more than 350 ha. Therefore, the potential for disaster-prone areas in Pacitan Regency have become a strict concern because the topography is mostly mountains and hills with slopes with varying levels of slope (Faturahman, 2018).

The efforts to prevent landslides are carried out by post-incident handling, and a small part uses geographic information systems and remote sensing to predict or mitigate it. These prevention efforts aim to reduce the consequences of disaster risk, both through physical development and awareness as well as to enhance the ability to deal with the threat of disaster called mitigation. Disaster mitigation is very important as the main point in disaster management. One of the most important things in disaster mitigation is the provision of information and maps of disaster-risk areas for each type of disaster (Sulistyo, 2016). Using a training point area from existing landslides, the expert can assess the hazard of the area by identifying areas with similar geological and geomorphological conditions. The possibility of landslides will occur in the future by correlating several main factors causing landslides with the distribution of landslides in the past (Hidayah and Dzakiya, 2018; Hidayat et al., 2019).

The information and maps of landslide-risk areas can be obtained by estimating landslide disasters to reduce the impact and losses due to disasters. One of the ways that can be done in this mitigation effort is to evaluate areas with the potential for landslides by using geographic information systems (GIS) and remote sensing by using the parameters that cause these disasters. Nusantara and Setianto (2015) suggested that remote sensing technology, GIS and global positioning systems (GPS) that are used together can predict the landslide risk in Piyungan and Plered Districts, Bantul Regency, Special Region of Yogyakarta with a good level of prediction accuracy of 70.5%. Landslide monitoring using remote sensing has proven to be an effective method for getting a general picture quickly and accurately (Arif et al., 2017; Jaya, 2005; Mohd et al., 2019; Sulistyo, 2016).

This study also used the Paimin method to analyze the level of landslide susceptibility. The preparation of landslide susceptibility is one of the most practical approaches to landslide hazard assessment and proper management tasks. Although there are many models developed for the landslide susceptibility map, there is no universal guideline for selecting a model to better model landslide susceptibility map. One of the main approaches to developing hazard reduction strategies is to create a landslide susceptibility map (Nohani et al., 2019). This method begins with the preparation of information in thematic maps about the level of vulnerability. This information is then used for the preparation of management plans in the form of a matrix or map of proposed activities such as forest and land rehabilitation. Proposed activities to determine the type of activity can be in line with the direction for land use or regional spatial planning (RSP). Alignment of the level of vulnerability with the function of the area to determine the planned location of activities is carried out using GIS tools, namely by overlapping the map of the level of vulnerability with the map of the function of the area (Paimin et al., 2012).

This study aims to analyze the landslide risks in Pacitan Regency in 1998 and 2018, projecting future landslide disasters through land capability classification (LCC), regional spatial planning (RSP), and business as usual (BAU). The data from 1998-2018 are used to predict land use in 2030 and analyzed the potential for landslides in Pacitan Regency, especially agricultural lands and their land-use scenarios.

2. METHODOLOGY

2.1 Description of the study area

This study was conducted in Pacitan Regency, East Java Province, with an area of 138,987.16 ha (Figure 1). Pacitan Regency is in the border area between East Java Province, and Central Java Province, with an area coordinate of 110°55'-111°25' East Longitude and 7°55'-8°17' South Latitude. Most of it is mountainous and rocky and had a few rocky canyons. The geography covers about 88% of the regency area because Pacitan is located in the Sewu Mountains. The highest mountain in Pacitan is Mount Lima in Kebonagung, and Mount Gembes in Bandar as the Spring of Grindulu River. The study is located about 946 m.a.s.l. It was in the Southern Mountains of Java Island which consists of coastal areas, plains, hills, and mountainous areas with flat to undulating landforms. Generally, the land in Pacitan was divided into two categories, calcium-rich in the south, and fertile land in the north. The soil consisted of Litosols association, red Mediterranean lithosol, tuff and volcanic compounds, reddish lithosol complexes, and grey alluvial, clay sediments containing many potential

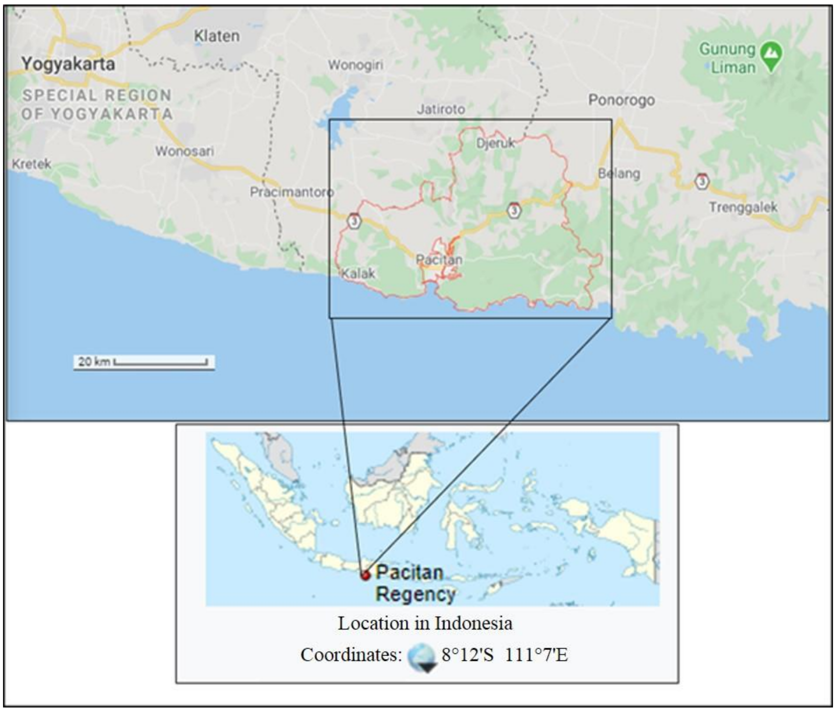

Figure 1. Location of the study area

minerals. Based on data from the Regional Disaster Management Agency of Pacitan Regency, there were at least 14 landslides disasters in Pacitan Regency in 2011-2013 (Avridianto, 2016).

2.2 Tools and materials

The tools used in this study consisted of stationery for compiling reports. Then a set of computers, ArcGIS 10.6 software (Putra and Nita, 2020), PCI Geomatica software, all of these were used for making maps of the survey location regencies. The global positioning system (GPS) tools, a set of survey tools (survey set), a camera, and observation sheets, were used for soil sampling at the research location. While the materials used consisted of Indonesian Topography Maps of 1:25,000, digital elevation model map with a resolution of 8.25 m, climate data, landform maps, and geological data, water management data, and watershed maps.

2.3 Research stages

Landslide risk analysis in Pacitan Regency consisted of several survey activities. It was started with a pre-survey consisting of preparing tools and materials, arranging for research permits at the research location, and processing initial materials to compile a survey location map and determining the location for taking soil samples. Then proceed with the preliminary survey stages and the primary survey with ground check activities to take intact and disturbed soil samples. Then, the post-survey stage was carried out to analyze the soil samples, research data, and validation process. The research flow diagram is presented in Figure 2. The study started with preparing tools and material, especially in collecting the secondary data such as Indonesian Topography Maps (RBI), digital elevation model (DEM), climatology data, landform data, geological map (Samodra et al., 1992), water management data, and watershed map.

The pre-processing materials consisted of radiometric correction activities to improve image quality, eliminate noise, and determine the portion of the image to be examined using PCI Geomatica. Then the haze cloud removal was carried out to remove the fog or dust contained in satellite imagery. Land use classification at different time scales used Landsat imagery of 30 m × 30 m resolution. Landsat image analysis was carried out to classify the different land uses, namely forests; agroforestry; drylands; settlements; water bodies; and other land uses. Landuse change analysis was carried out using Landsat 5 TM imagery for 1998, Landsat 7 ETM for 2008, and Landsat 8 OLI for 2018. Because the reporting period was quite long (10 years), the Landsat imagery used was also different. The classification method used in Landsat image processing was the unsupervised classification method. The results of image analysis for three different years were used to

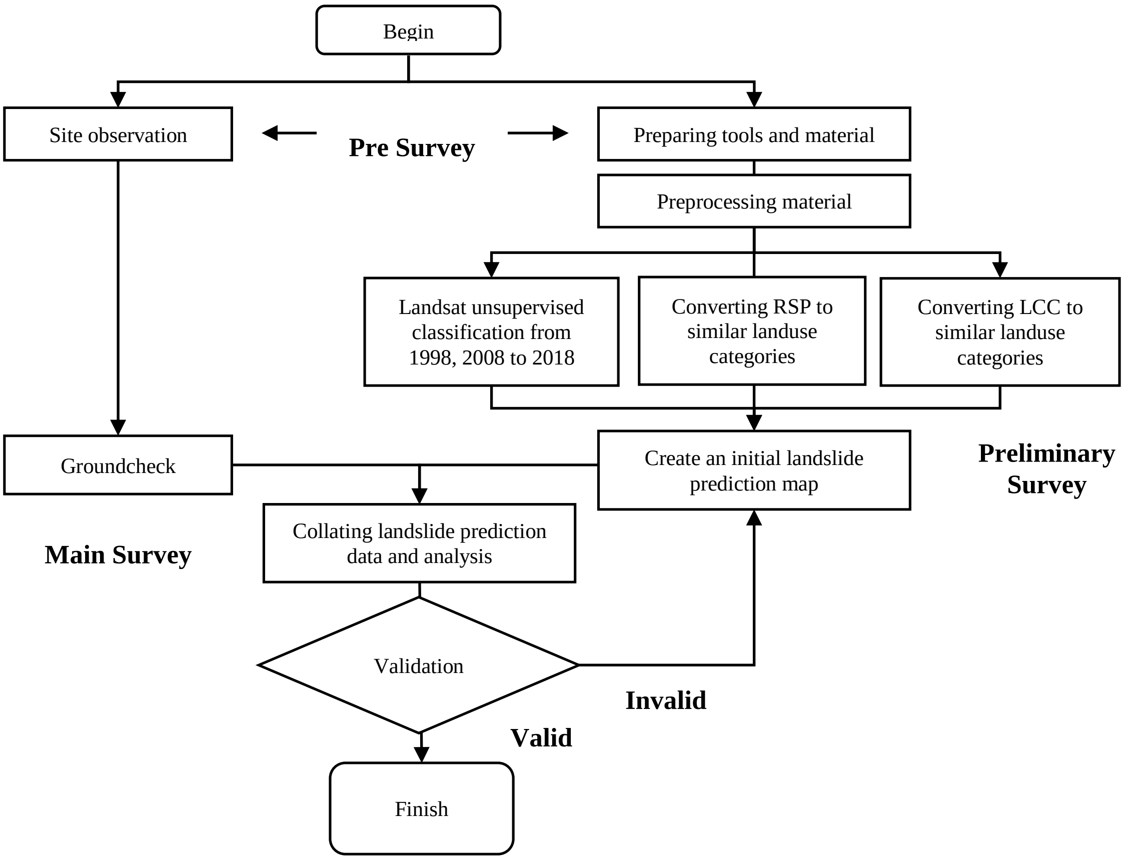

Figure 2. The flow chart of the study

determine business as usual (BAU), which contained predictions of the risk of landslides in 2030 concerning changes in disaster patterns and land use simulations according to land capability classification.

The parameters were divided into natural factors causing landslides (three consecutive days of cumulative annual rainfall, land slopes, rock types, faults/claws, and soil depth to impermeable layers) and management factors (land use and infrastructure as well as a settlement if the land slopes were below 25%). The land use share management factor was a parameter modified by including three main scenarios: land capability classification (LCC), regional spatial planning (RSP), and business as usual (BAU). Land capability classification illustrated the intensity of land that can use without damage. The analytical method followed the land capability analysis method by Arsyad (1989). The lands were classified using roman letters from class I to class VIII. Meanwhile, the subclass was a limiting factor or damage hazard consisting of erosion (e), excess flooding or flood risk (w), rooting area or sufficient soil depth (s), and climate (c).

In this study, the researcher employed the Paimin et al. (2012) method, which has been approved. Paimin et al. (2012) explained that scores and weights carried out the novelty analysis on increasing parameters. Remote sensing and GIS analysis was conducted using Geomatica and ArcGIS 10.3 software to process the primary data. The scoring and weighting scores were carried out according to the compiled value categories (Paimin et al., 2012). The arithmetic overlay operation was carried out with a weighted overlay based on a predetermined weight (Figure 3).

This study focused on the weighted overlay using parameters that have been scored so that the final stage was analyzed using Algebra Map of the weighted overlay results. The analysis results were validated to ensure the data that needed to be proven correct by observing and knowing the actual situation or presence in the field (ground check). The data collection and observation of slopes, sensitivity, and level of erosion, depth of soil, rock, and vegetation were compiled. The confusion matrix was used to validate overall accuracy data. The parameters for the preparation of landslide prediction maps included; (1) natural parameters of three consecutive days, namely cumulative annual rainfall, land slopes, rock types, faults, and soil depths to impermeable layers; and (2)

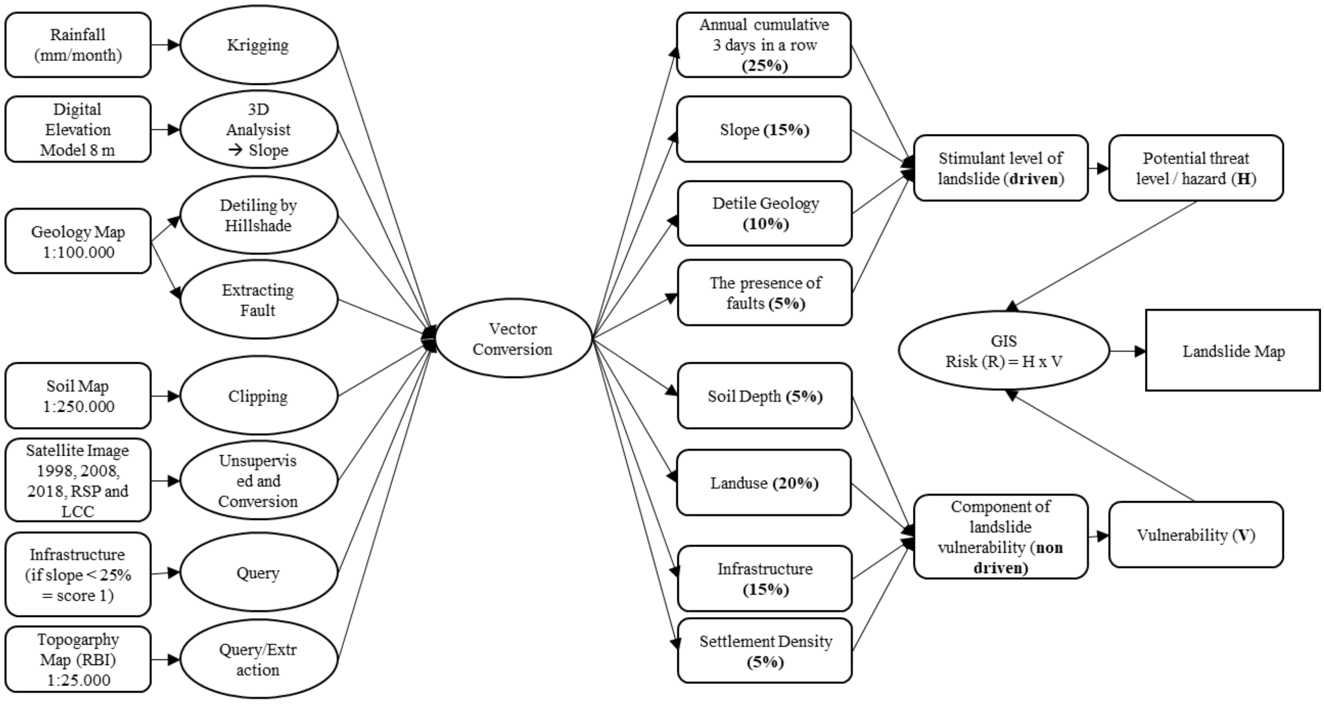

Figure 3. Model analysis of the landslide risks modified from Paimin et al. (2012)

management factors of the land use as well as infrastructure and settlement if the land slope was below 25%. An analytical model of a landslide prediction analysis in an area was carried out by performing vector data, which was then overlaid to obtain a landslide prediction analysis using remote sensing and GIS.

3. RESULTS AND DISCUSSION

3.1 Land use change and business as usual (BAU) analysis

The changes in forest land use have increased from 1998 to 2018 so that in 2030, it is estimated that forest land use will increase to 22.45 ha (Figure 4). In contrast to forests, plantations had decreased significantly from 44.74 ha in 1998 to 39.79 ha in 2018. Thus, the pattern of decline that occurs in 2030 will reduce the area of agroforestry to 36.44 ha. In addition to forests, other land uses that have increased are predicted to reach 6.82 ha in 2030, shrubs around 42.54 ha, and dryland farming around 7.93 ha in 2030. These increases affect the decline in plantations and affect the decrease in paddy and coastal areas with a prediction of 22.77 ha and 64 ha. Precisely, in paddy fields and dry fields, the decrease in paddy land areas followed by an increase in drylands in 2008, 2018, and predictions in 2030. This change is assumed to be more influenced by land management and plant species selection. The next change that may occur is that paddy fields are very large to change their private functions, given the location of paddy fields around the district center with adequate public facilities, centralized offices, and suitable topography for use in settlements. This condition causes areas close to public facilities to become densely populated areas. Besides, the increase in population every year in an area followed by the need for shelter is the main reason many changes in land use for settlements, one of them is paddy fields (Yasta and Yarmaidi, 2019). Moreover, paddy fields, dry fields, and settlements are very close to the Grindulu River, the main and the largest river in Pacitan Regency, which is directly connected to the sea.

3.2 Analysis of land use according to regional spatial planning (RSP)

The regional spatial planning (RSP) in Pacitan Regency consists of cultivated and protected areas. The classification of land use in Pacitan Regency is based on a protected area development plan, consisting of protected forest areas, karst areas, border areas, areas around springs, areas of nature reserves and cultural reserves, areas risk to natural disasters, and other protected areas. The cultivation area consists of allotment areas for production forests, community

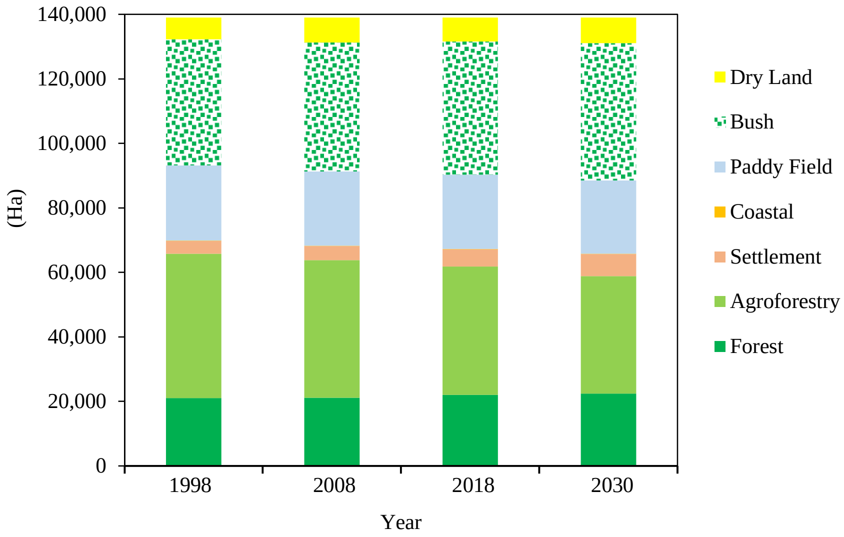

Figure 4. Chart of land use change in Pacitan Regency

forests, agriculture, fisheries, mining, industry, tourism, settlements, mainstays, and a safe area for flight operations at Iswahyudi Air Force Base. Most of the land use plans in Pacitan Regency until 2028 will be designated as community forests. This is because Pacitan Regency has a various community forest area. The second-largest land use is cultivated land, namely green open areas, agriculture, and settlement. Table 1 shows an area of regional spatial planning (RSP) in the Pacitan Regency and its conversions.

Table 1. Regional spatial planning (RSP) in Pacitan Regency and its conversion

Land use plan	Area (ha)	Conversion to
Public forest area	65,951.00	Forest
Nature/cultural reserves	1,254.13	Forest, production forest, and agroforestry
Production forest	1,484.39	Production forest and agroforestry
Agriculture	13,033.00	Paddy fields and dryland farming
Settlement	16,253.31	Settlement
Green open space/reserve land	26,720.37	Settlement and agroforestry
Other	14,291.00	Various land use

3.3 Land use analysis according to the land capability classification (LCC)

Land capability classification carried out in Pacitan Regency is a systematic evaluation of land characteristics and is grouped into various categories based on the potentials and obstacles in land use (Arsyad, 1989). The land characteristics assessed are slope, erosion, solum depth, texture (top and bottom layers), permeability, drainage, drought risk, and salinity. Based on the land capability grouping, a land capability map is compiled according to land capability classification (LCC), as shown in Table 2.

Table 2. Types of land use based on the capability and area classification in Pacitan Regency

Land use	Area (ha)
atural forest	31,832.20
Production forest	61,816.90
Agroforestry	1,909.35
Settlement	5,856.06
Paddy fields	6,805.09
Bush	2,061.13
Dryland farming	28,709.27
Total area (ha)	138,990.00

3.4 Landslides risk potential

The differences in land use in 1998, 2008, 2018, 2030, regional spatial planning (RSP), and land capability classification (LCC) affect disasters' potential. The potency levels in 1998, 2008, and 2018 increase at high levels and assume to be very high due to land-use changes. The changes in land use will affect runoff so that when it rains, some falling water will seep into the ground and some will pool in the soil surface, depending on the conditions at the ground level. In addition, land use affects the shelf life of water in the soil. Based on land changes that have occurred, the prediction of future land-use changes is based on the patterns that occurred. Furthermore, this land-use is called business as usual (BAU). The results of the BAU analysis shows that if there are no interventions in the current land-use change patterns in Pacitan Regency, there will be an increase in the level of potential landslides from low to moderate, high to high, and high to very high in 2030 (Table 3).

The landslide risk class in 2030 (BAU) will have an impact on lowering the moderate class if intervened by the regional spatial planning (RSP) in Pacitan Regency. However, on the other hand, it also affects increasing moderate to very high classes. The land-use planning based on the RSP increases the potential for landslides compared to business as usual (BAU). The regional spatial planning (RSP) should pay attention to the land capability classification (LCC), which is proven to be able to reduce the landslide class from high to medium and low to very low. The results of the overall accuracy calculation show that the reliability of the data reaches 82%. There are 12 data errors based on the assumption that data inequality is at a very low level. Figure 4 shows the pattern of potential changes in landslide risks in 1998 to 2018 and predictions for 2030 based on BAU, RSP, and LCC. Meanwhile, Figure 5 shows the landslide risk map in Pacitan Regency

Table 3. The results of the potential landslides in Pacitan Regency in ha

Level	1998	2008	2018	2030 (BAU)	RSP	LCC
High	15,878	21,349	67,801	112,219	44,223	9,094
Moderate	48,911	48,617	26,388	9,194	24,467	54,613
Low	55,016	52,650	36,479	14,898	40,859	47,652
Very low	19,182	16,656	8,319	2,676	29,380	27,628
Total	138,987 ha					

Explanation: BAU=business as usual; LCC=land capability classification; RSP=regional spatial planning

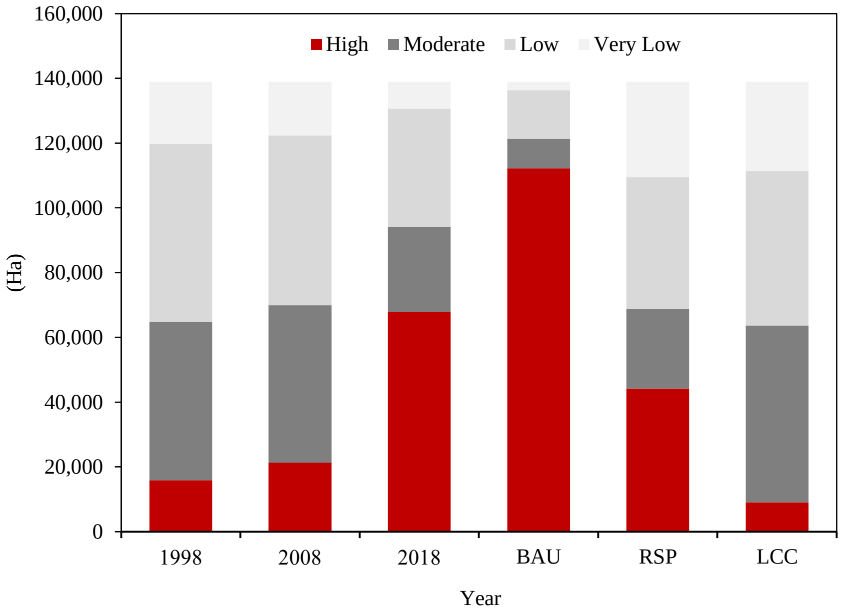

Figure 5. The pattern of landslides potential in Pacitan Regency

3.5 Discussion

Landslide is influenced by human activities, geographical conditions, topographical conditions, river channel conditions, rainfall, and land-use changes. Pacitan Regency is one of the regencies located in the Southern part of Java, and morphologically almost 50% of its area is mountains with slopes (>40%) (Budiono, 2012). In Pacitan Regency, the landslides risk in 1998, 2008, and 2018 continues to increase at moderate to high landslide risk levels. This condition happens because of changes in land use in the area. The differences in land use in 1998, 2008, 2018, 2030, RSP, and LCC will affect the landslides in the Pacitan Regency (Figure 6).

The changes not only lead to growth and can reduce the landslide risk, but also land-use changes can also increase the landslide risk. It is predicted that through business as usual (BAU), in 2030, there will be an increase in the landslide risk from low to moderate and medium to high. This will happen if there is no intervention in the pattern of land-use change in the Pacitan Regency. The high-risk landslide level happens in the forest (16%), agroforestry (27%), settlement (1%), paddy field (11%), bush (39%) and dry land (6%). There are around 29,473 ha of agricultural land in 2018, which has a high landslide risk and will increase if no intervention made. Landslides can occur due to natural conditions and the influence of human activities. This is based on Naryanto et al. (2019) statement that landslides occur due to two main factors: controlling and triggering factors.

Controlling factors affect the condition of the material itself, such as geological conditions, slope, lithology, faults, and burly of rocks. Triggering factors cause the movement of these materials, such as rainfall, earthquakes, slope foot erosion, and human activities. Landslides can occur at any time and cause various unintended consequences in the form of physical, social, economic, and environmental impacts. Landslides cause extensive damage to property and infrastructure and the loss of human lives almost every year (Hidayah and Dzakiya, 2018). Additionally, landslides cause many losses that will felt by residents, both directly and indirectly. Some of the losses are damaging to the infrastructure, damage to agricultural areas, disruption to watersheds, and disease spread. The high level of loss experienced by the community due to natural disasters can cause a lack of public information about the possibility of disasters occurring nearby so that public awareness of disaster response becomes very minimal. The historical data shows that 95% of disasters in East Java are related to hydro-meteorological disasters such as floods, landslides, and strong winds (BNPB, 2019). This number can increase if we consider climate change in the East Java Region. In 2018, the potential for damage due to landslides in Pacitan Regency, especially on the dry land, paddy field, and agroforestry was 29,473 ha.

Based on the study conducted by Hidayah and Dzakiya (2018) about analysis geological and geophysical data for landslide hazard zone prediction with the weight of evidence method in Pacitan Regency, East Java to predict the potential landslide using weight of evidence method. The geological data used lithological data, structural data, contour data, and alteration data. The results from this data analysis are six evidence maps, such as NE-SW lineament, NW-SE lineament, host rock, heat source, kaolinite alteration, and iron oxide alteration maps. The geophysical data analysis the distribution of rock density to interpretation the landslides. The evidence maps are analyzed by weight of evidence method to produce a good map where the validity is tested using conditional independence (CI), the pairwise and overall tests. Then, the analyses have a posterior probability map of the landslide. The checking field validates the posterior probability map (potential mineral maps). The posterior probability map (after validation) or favourable map predicts approximately favourable zone and non-favourable zones. Favourable zones of potential landslide hazard zonation divides into three classes: high-potential hazard, moderate hazard, and low hazard. The analysis of the susceptibility map developed shows that the high susceptibility is mostly concentrated in the northern and west parts of the study area. The local environmental conditions are very favourable to trigging (a combination of a slope gradient >25°; relief delivered; strong fracturing; extremely degraded soils or dissected; the presence of forest and vegetation or not properly maintained). High hazard is about 140 km^2, the moderate hazard is about 238 km^2, and the low hazard is about 194 km^2. The biggest landslide in Pacitan Regency increases at moderate and high levels.

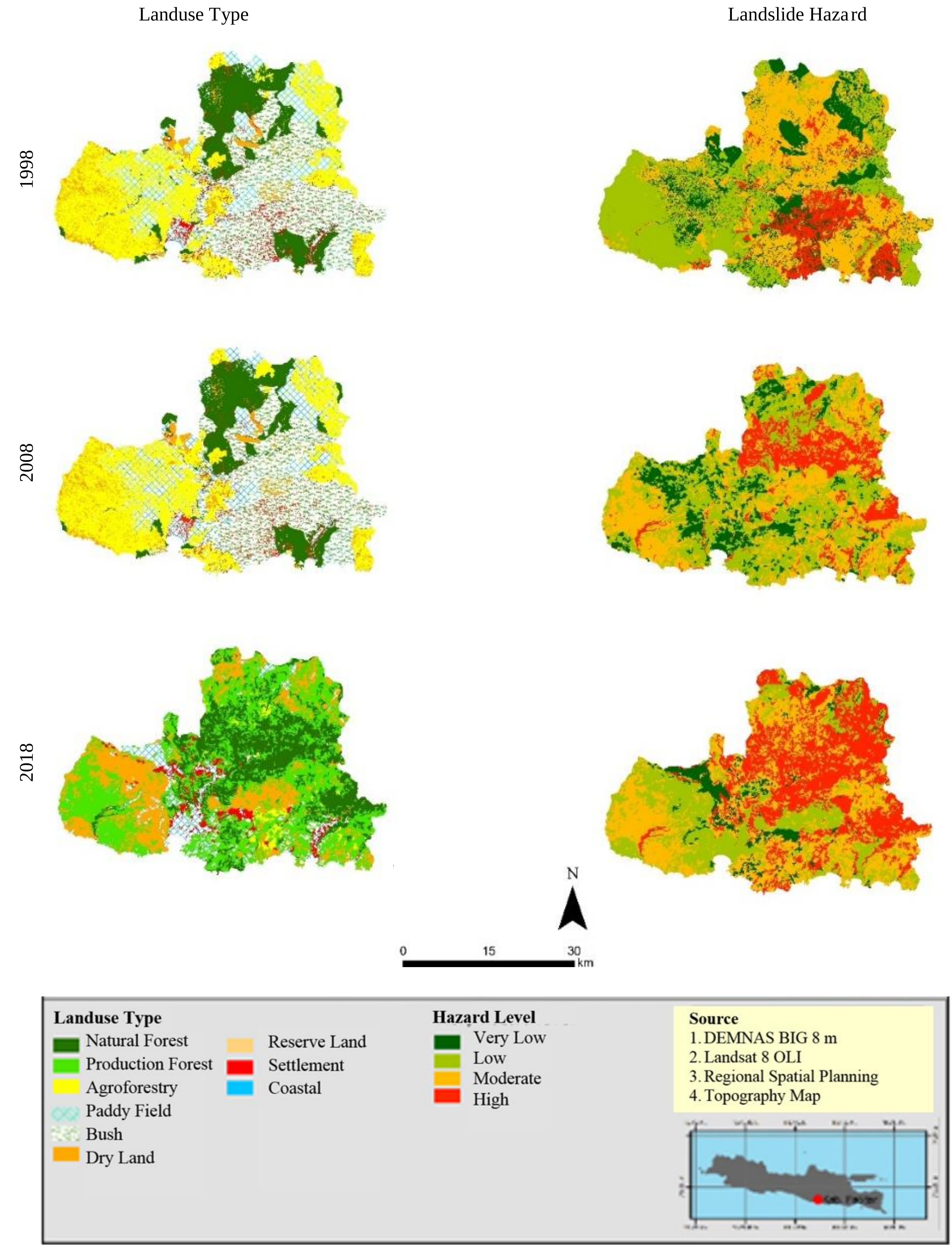

Figure 6. Landslide risk maps in Pacitan Regency

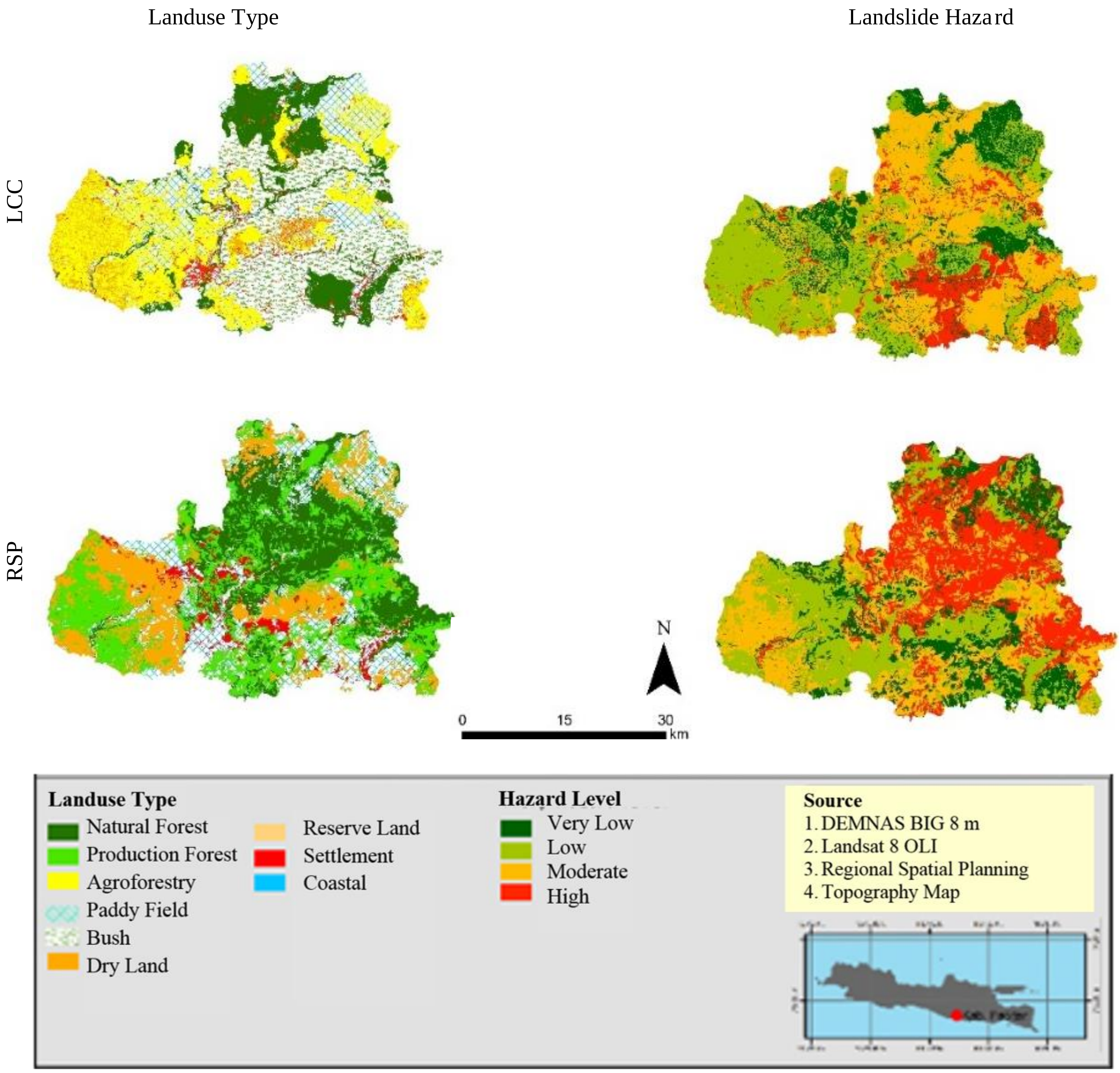

Figure 6. Landslide risk maps in Pacitan Regency (cont.)

Based on the study conducted by Sipayung et al. (2014), a vulnerability of landslides was used (Paimin et al., 2009) to determine the degree of landslide vulnerability using the natural factors, namely the formula for cumulative daily rainfall for three consecutive days (25%), soil slope (15%), geology/rocks (10%), presence of layers/faults (5%), and soil depth (5%). Meanwhile, the management factors included land use (20%), infrastructure (15%), and settlement density (5%). From the results of empirical equations, testing potential predictions of landslide events in Citarum watershed show quite good predictions. The above empirical equation applies to the category of moderate, high, and very high vulnerability levels. In order to obtain better prediction, additional parameters such as fault, rock geology, infrastructure, and additional landslide event data can be considered.

A study by Susanti et al. (2017) regarding the vulnerable landslides in Banjarnegara Regency using Paimin et al. (2009) method showed that the information on the vulnerable landslides dominated by "somewhat vulnerable". Thus, to increase the level of accuracy of landslide susceptibility classes in Banjarnegara, it is necessary to modify the setting of landslide vulnerability parameters, especially the classification of slopes and the area affected by disasters. The research accuracy in the Pacitan area is 82%.

The improvement of the accuracy has also been modified to regulate landslide vulnerability such as faulting, rock geology, infrastructure, and even adding mudslide event data of the affected area. As for the natural factors that cause landslides, according to Paimin et al. (2009), the parameters in the landslide vulnerability assessment process is the geological condition and regolith depth. One of the geological conditions is the type of soil that has a significant effect on landslides (Setiadi, 2013). Solle and Ahmad (2016) also said that soil with clay mineral content, especially kaolinite and vermiculite in water-saturated condition, will become unstable. Regarding this matter and based on the results of the field survey, it is known that most of the soil types in Pacitan are Ultisol and Inceptisol. This condition causes the area to be a vulnerable area of landslide. Priyono (2012) conveyed that the lands in the development period, such as Inceptisol is a type of soil prone to landslide.

In this study, the landslide increases at moderate and high levels due to changes in land use. The interaction between forest coverage and landslides is complex (Haigh et al., 1995). Land-use change is an essential factor in the occurrence and movement of rainfall triggered landslides (Glade, 2003; Karsli et al., 2009; Kingsburry, 1994). The presence of landslides is directly related to variations in land use (Glade, 2003). There is currently no consensus on the effect of covered vegetation on slope stability. Some studies have found that plants may not contribute to slope stability (Wu and Sidle, 1995), while other researchers argued that vegetation roots increase slope stability (Jakob, 2000; Karsli et al., 2009). The higher proportion of forest cover, the lower the amount of soil eroded by rainfall. Thus, lumbering a slope can accelerate its movement to failure and extend its area. Since it takes 30-35 years or longer for a slope to recover naturally, slope land development will cause a slope to lose equilibrium which is more easily inducing slope failure during torrential rain.

4. CONCLUSION

The prediction of landslide risk in Pacitan using the Paimin modification method has an accuracy rate of 82%. The most influential factor is land use. If there is no intervention (BAU) for land use in Pacitan Regency, the risk of high-level landslides will increase to 65.51%. However, suppose there is land use intervention, according to RSP. In that case, landslide incidence will decrease as indicated by a decrease in the level of risk, namely at a low level (12%) and a very low level (253.17%). The regional spatial planning (RSP) should consider the land capability classification (LCC), which is proven to be able to reduce the landslide classes from high to medium and low to very low. It means that the high risk of landslides is reduced if the intervention refers to the LCC, which reaches 86.59%.

ACKNOWLEDGEMENTS

This research was funded by the Beginner Researchers Grant by Research and the Community Service University of Brawijaya. Researchers convey many thanks to reviewers who have provided suggestions to improve the writing.

REFERENCES

Arif N, Projo D, Hatono H. Raster-based qualitative spatial erosion modeling (case study in das serang, kulonprogo district. Journal of Environmental Science 2017;15(2):127-34.

Arsyad S. Soil and Water Conservation. Bogor, Indonesia: Institut Pertanian Bogor Press; 1989.

Avridianto DF. Landslides risk level in ketro village, tulakan sub-district, Pacitan District. Swara Bhumi 2016;1(2):18-27.

Badan Nasional Penanggulangan Bencana (BNPB). Indonesian Disaster Information Data [Internet]. 2016 [cited 2020 Jul 21]. Available from: http://dibi.bnpb.go.id/.

Budiono UF. White Book of Pacitan District Sanitation Chapter I. Preliminary. Pacitan, Indonesia: Pacitan Distric Government. 2012.

Conforti M, Pascale S, Robustelli G, Sdao F. Evaluation of prediction capability of the artificial neural networks for mapping landslide susceptibility in the Turbolo River catchment (northern calabria, italy). Catena 2014;113(2-3):236-50.

Cruden DM. A simple definition of a landslides. Bulletin of the International Association of Engineering Geology 1991; 43(1):27-9.

Dagdelenler G, Nefeslioglu HA, Gokceoglu C. Modification of seed cell sampling strategy for landslide susceptibility mapping: An application from the eastern part of the gallipoli peninsula (canakkale, turkey). Bulletin of Engineering Geology and the Environment 2015;75(2):575-90.

Fan W, Wei X, Cao Y, Zheng B. Landslide susceptibility assessment using the certainty factor and analytic hierarchy process. Journal of Mountain Science 2017;14(5):906-25.

Faturahman BM. Strategy of emergency response of flood and landslide disaster in pacitan regency. Jurnal Ilmu Administrasi Media Pengembangan Ilmu dan Praktek Administrasi 2018;15(2):133-47.

Frounde MJ, Petley DN. Global fatal landslide occurrence 2004 to 2016. Natural Hazards and Earth System Sciences 2018;18:2161-81.

Glade T. Landslide occurrence as a response to land use change: A review of evidence from New Zealand. Catena 2003;51(3-4):297-314.

Haigh MJ, Rawat JS, Batarya SK, Rai SP. Interactions between forest and landslide activity along new highways in the kumaun himalaya. Forest Ecology and Management 1995;78(1-3):173-89.

Hidayah RA, Dzakiya N. Analysis geological and geophysical data for landslide prediction hazard zone with weight of evidence method in pacitan district east java. Journal of Applied Geospatial Information 2018;2(1):117-23.

Hidayat R, Sutanto SJ, Hidayah A, Ridwan B, Mulyana A. Development of a landslide early warning system in indonesia. Geosciences 2019;9(10):451.

Jakob M. The impacts of logging on landslide activity at clayoquot sound, british columbia. Catena 2000;38(4):279-300.

Jaya I. Landslide detection techniques using multi-time spot imagery, case studies in Teradomari, Tochio and Shidata Mura, Niigata, Japan. Journal of Tropical Forest Management 2005;10(1):31-48.

Jiao Y, Zhao D, Ding Y, Liu Y, Xu Q, Qiu Y, et al. Performance evaluation for four gis-based models purposed to predict and map landslide susceptibility: A case study at a world heritage site in southwest china. Catena 2019;183:104221.

Karsli F, Atasoy M, Yalcin A, Reis S. Effects of land-use changes on landslides in a landslide-prone area (ardesen, rize, ne turkey). Environmnet and Monitoring Assesment 2009;156(1-4):241-55.

Kingsburry PA. Preliminary Assessment of the Johnson Hill Landslide, Palliser Bay. Contract Report 94.205. North Island, New Zealand: Wellington Regional Council; 1994.

Kirschbaum D, Stanley T, Zhou Y. Spatial and temporal analysis of a global landslide catalog. Geomorphology 2015;294:4-15.

Mohd MH, Rahman MAA, Azman FNUZ, Jusoh A. Landslide susceptibility mapping at lebir and galas river basins after extreme flood event using weights of evidence. Journal of Sustanability Science and Management 2019;14(2):103-15.

Naryanto HS, Soewandita H, Ganesha D, Prawiradisastra F. Analysis of the causes of the occurrence and evaluation of landslides in Banaran Village, Pulung District, Ponorogo Regency, East Java Province. Journal of Environmental Science 2019;17(2):272-82.

Nita I, Putra AN, Fibrianingtyas A. Analysis of drought hazards in agricultural land in Pacitan Regency, Indonesia. Journal of Soil Science and Agroclimatology 2020;17(1):7-15.

Nohani E, Moharrami M, Sharafi S, Khosravi K, Pradhan B, Pham BT, et al. Landslide susceptibility mapping using different gis-based bivariate models. Water 2019;11(7):1402.

Nusantara YP, Setianto A. Landslide hazard mapping using the frequency ratio method in piyungan and pleret sub-districts, bantul district, yogyakarta special area. Proceedings of 8th Academia-industry Lingkage National Earth Seminar; 2015 Oct 15-16; Graha Sabha Permana, Yogyakarta: Indonesia; 2015.

Paimin, Pramono IB, Purwanto, Inrawati DR. Watershed Management Planning System. Jakarta, Indonesia: Ministry of Forestry, Forestry Research and Development Agency, Research and Development Center for Conservation and Rehabilitation; 2012.

Paimin, Sukresno, Pramono IB. Flood and Landslide Mitigation Techniques. Balikpapan, Indonesia: Tropenbos International Indonesia Programme; 2009.

Panagos P, Standardi G, Borrelli P, Lugato E, Montanarella L. Cost of agricultural productivity loss due to soil erosion in the European Union: From direct cost evaluation approaches to the use of macroeconomic models. Land Degradation and Development 2018;29:471-84.

Priyono KD. A study of clay mineral in the occurences of landslide disaster area at kulonprogo mountains yogyakarta special province. Geography Forum 2012;26(1):53-64.

Putra AN, Nita I. Reliability of using high-resolution aerial photography (red, green and blue bands) for detecting available soil water in agricultural land. Journal of Degraded Minning and Lands Management 2020;7(3):2221-32.

Samodra H, Gafoer S, Tjokrosapoetro S. Geological map sheet pacitan, java, scale 1: 100.000. Bandung, Indonesia: Geological Research and Development Center; 1992.

Setiadi T. Designing a geographic information system for mapping landslide prone areas, mitigation and disaster management in Banjarnegara District. Kes Mas 2013;7(1):33–43. (in Indonesian)

Sipayung SB, Cholianawati N, Susanti I, Aulia SR, Maryadi E. Development of empirical equation model in predicting the occurrence of landslide at watershed of citarum (west java) based on thetrmm satellite data. Journal of Sains Dirgantara 2014;12(1):12-21.

Solle MS, Ahmad A. Identification of soil, rock and tectovolcanisme on landslides intensity in tondano watershed. Journal of Geological Resource and Engineering 2016;6:271-82.

Sulistyo B. The role of geographic information systems in mitigating landslides. Proceedings of the National Seminar on Disaster Mitigation in Regional Development Planning; 2016 Mar 28; Agricultural Faculty, Bengkulu University, Bengkulu: Indonesia; 2016.

Susanti PD, Harjadi B, Miardini A. Vulnerability analysis as a basis for landslide mitigation in banjarnegara regency. Journal of Watershed Management Research 2017;1(1):49-59.

Wu W, Sidle RC. A distributed slope stability model for steep forested basins Water Resources Research 1995;31(8):2097-110.

Yasta RD, Yarmaidi Y. Analysis of changes in the use of paddy fields to settlements in the north pagelaran district. Journal of Geographic Research 2019;7(3):1-11.

Zhao L, Zuo S, Deng D, Han Z, Zhao B. Development mechanism for the landslide at xinlu Village, Chongqing, China. Landslides 2018;15:2075-081.

Brick Sector and Air Quality: An Integrated Assessment towards 2020 Challenge of Environment Development

Shazia Pervaiz[1*], Muhammad Ameer Nawaz Akram[2], Filza Zafar Khan[3], Kanwal Javid[4], and Younis Zahid[1]

[1]*Enviornemntal Protection Agency Punjab, Lahore, Pakistan*
[2]*State Key of Laboratory of Information Engineering in Surveying, Mapping and Remote Sensing, Wuhan University, China*
[3]*Pakistan Council of Scientific and Industrial Research Laboratories Complex, Lahore, Pakistan*
[4]*Department of Geography, Government College University, Lahore, Pakistan*

ARTICLE INFO

Received: 6 Sep 2020
Received in revised: 9 Dec 2020
Accepted: 4 Jan 2021
Published online: 26 Jan 2021
DOI: 10.32526/ennrj/19/2020203

Keywords:
Brick kilns of Punjab/ COVID-19 and Punjab air quality/ Smog/ Zig-Zag technology

*** Corresponding author:**
E-mail: shaziapervaiz@gmail.com

ABSTRACT

Brick sector is a mainstay of the urban economy of Punjab. The traditional technology of brick making emits a lot of toxic gases and smoke particulates into air. Hence, the Government of the Punjab, Pakistan announced a ban on low technology brick kiln operations during winter season by the end of December 2020. Initially, the existing set up of brick kilns and air pollution levels were evaluated before and during lockdown period using spatial application. Further, environmental parameters such as aerosols, carbon monoxide, ozone, sulfur dioxide and carbon dioxide were determined to analyze the air quality, including metrological factors. Results of the study exhibited that the upper and central regions of Punjab are the major hubs of brick kilns. So, the level of air quality was inconsistent in the study period due to the existence of large mushrooms of brick kilns. Further, despite lockdown the highest concentration of carbon monoxide was recorded in the eastern side of the province, such as Kasur, Lahore, and Sheikhupura. The level of aerosols also fluctuated and shifted its trends in the central and southern part of the province. While SO_2 and CO_2 level declined and revealed a satisfactory level of air quality during shutdown. On the other hand, no significant relation to metrological factors, such as rain, is involved in the pollution reduction. Conclusively, the findings of the present study encourage the government agencies to realign the stringent control measures to improve the quality of air in the winter months using the experience of quarantine in 2020.

1. INTRODUCTION

Brick making (Hossain et al., 2019) is an ancient industry of the world (Maithel and Uma, 2000) and its evolution is recorded around 6,000-7,000 BC (Momčilović-Petronijević et al., 2018). Although brick furnaces are established all over the world (Bandyopadhyay et al., 2006), the highest production (90%) is associated with South Asia (Weyant et al., 2014; Tusher et al., 2018). Among South Asian countries, Pakistan ranked 3rd (Figure 1) in brick manufacturing (Naveen, 2016; Khan et al., 2019) and contributes 3.50% share from 18,000 kilns. In addition, 1.5% is the prime input of this sector (Kataria et al., 2018) in the country's Gross Domestic Product (GDP).

Despite its contribution to the country's GDP and social well-being, the brick industry has remained an unregulated and undocumented sector (Iqbal, 2006) which fulfills the rural-urban bricks demand. However, the operational brick kilns in the country are working on classical low-cost Bull's Trench Kilns (BTK) technology and considered one of the major causes of smog formation. The old kilns technology has adverse impacts on the environment (Bhanarkar et al., 2002), biodiversity (Gupta and Narayan, 2010), and air (Wahid et al., 2014). In addition, brick kilns are the emission discharging workplaces causing gastrointestinal, respiratory, skin, reproductive, and psychosocial diseases (Figà-Talamanca, 2006; Shaikh et al., 2012). Further, Coronavirus have been reported

Citation: Pervaiz S, Akram MAN, Khan FZ, Javid K, Zahid Y. Brick sector and air quality: An integrated assessment towards 2020 challenge of environment development. Environ. Nat. Resour. J. 2021;19(2):153-164. (https://doi.org/10.32526/ennrj/19/2020203)

to have a positive correlation with air pollutants and the virus can transmit through atmospheric aerosols (Comunian et al., 2020).

Before the pandemic, the Government of Punjab banned the operation of old technology brick kilns to control smog and issued the notification for the conversion of old kilns into new technology. But due to COVID-19 lockdown, all economic and social activities were suspended and conversion process from traditional kilns to Zig-Zag system got paralyzed and fractured the socio-economic level of the province. Therefore, considering the above situation, the objectives of the present study were (i) To provide a comprehensive spatial overview of the brick kilns located in Punjab, Pakistan; (ii) To highlight the air pollutants concentration with special focus on all districts of the Punjab; and (iii) To compare the air pollutants level of February 2020 with the lockdown period (April 2020).

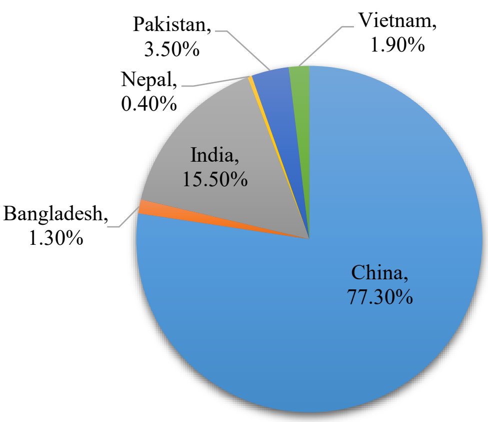

Figure 1. Brick manufacturing in South Asian Countries (Rupan, 2017)

2. METHODOLOGY

2.1 Site description

In Pakistan, 10,347 brick kilns out of 18,000 kilns are established in Punjab (PBC, 2016) and approximately 3.1 million workers are associated with brick manufacturing units in the province. The study site (Javid et al., 2020) presented in Figure 2 comprises of thirty-six districts of Punjab where clusters of estimated brick kilns are contributing to the country's GDP. In Punjab, 38% of bricks supply is produced from the upper and central parts of the districts such as Lahore, Gujranwala, Sheikhupura, Gujrat, Sialkot, Sargodha, Jhelum, and Rawalpindi. While the rest of the districts are contributing 29% share to the country's economy.

In Punjab, brick making is characterized by old modes of brick production which is seasonal and mainly starts in winter season (Khaliquzzaman et al., 2020) (October-November) and lasts until rainy season. The brick manufacturers utilize coal, manure and firewood as fuel which emits hazardous air pollutants which has detrimental impact on environment and human health (Das and Gangopadhyay, 2011).

In Punjab, prior to COVID-19, the province was facing the worst episode of smog (Pervaiz et al, 2020a) when the first coronavirus case was reported on 26th February, 2020 (Badshah et al., 2020) and the percentage of confirmed cases increased rapidly. As the COVID situation got critical, the Government of Punjab Pakistan took control measures against COVID-19 to curb the virus and suspended all economic and social activities. The suspension of human activities not only provided the opportunity to lower the level of air pollution globally (Ramasamy, 2020) but also improved the quality of air in Punjab (Pervaiz et al., 2020a) and smog prone city 'Lahore' (Pervaiz et al., 2020b). On the other hand, the COVID-19 lockdown shut down the brick kilns and affected the socio-economic level (Unni, 2020) badly. Due to this lockdown phase, the forced measures are thought provoking for the government to balance the brick sector and air quality simultaneously to achieve the sustainable development goals.

2.2 Brick kilns classification in Punjab

Brick manufacturing units are like baking ovens (Schmidt, 2013) which are designed to harden the brick material such as clay, soil, and mud. In Punjab, the following intermittent and continuous kilns (Rajarathnam et al., 2014) are operating:

- Hoffman Kiln
- Fixed Chimney Bull's Trench Kilns
- Vertical Shaft Brick Kiln (VSBK)
- Zig-Zag Kiln

2.3 Air quality assessment of Punjab

In order to evaluate the air quality, The modern-era retrospective analysis for research and applications, version 2 (MERRA-2) images were used to analyze aerosol, carbon monoxide, ozone, sulfur dioxide and carbon dioxide concentration in the atmosphere of the two months, February and April 2020. In addition, all data were procured from the world view National Aeronautics and Space

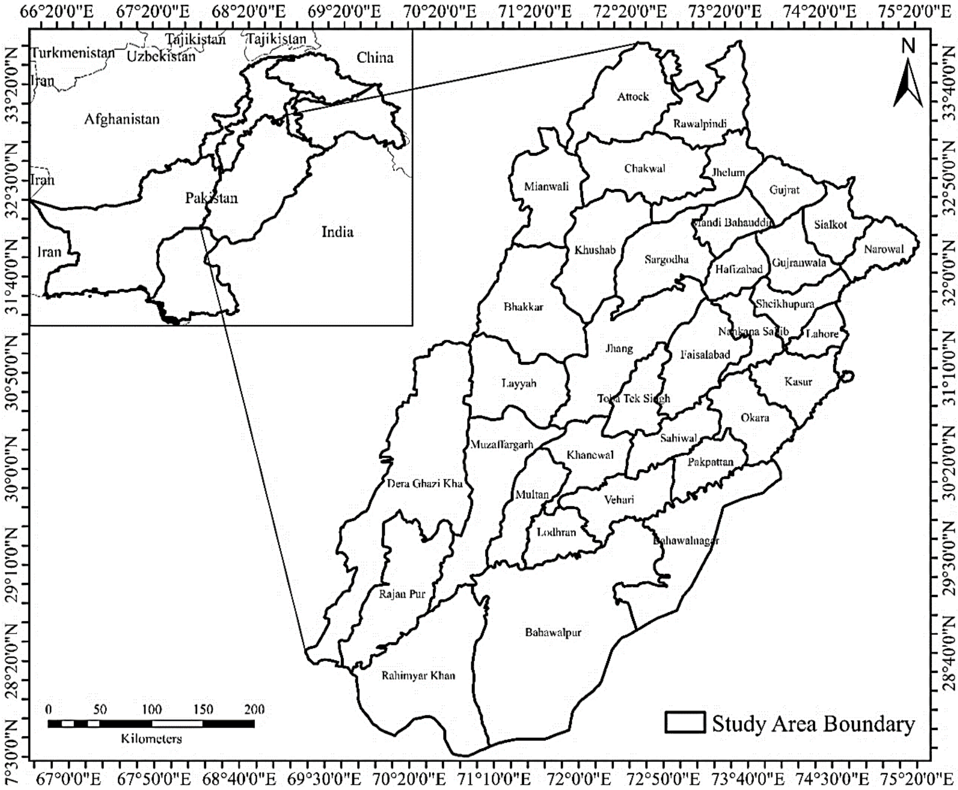

Figure 2. Map of the study site

Administration (NASA) site and processed in ArcGis 10.5 to interpret results. However, the description of spatial data is aggregated in Table 1. In addition metrological factors data of February and April, 2020 was taken from Pakistan Metrological Department (PMD).

Table 1. Description of spatial data

Data set name	Resolution (km)	Month
Total column ozone dobsons (TO_3)	0.5 × 0.625	February and April 2020
Co emission (kg/m^2/s)	0.5 × 0.625	February and April 2020
Aerosol optical depth Analysis (AOD)	0.5 × 0.625	February and April 2020
So_2 surface mass concentration (kg/m^3)	0.5 × 0.625	February and April 2020
Net ecosystem CO_2 exchange (NEE)	9 × 9	February and April 2020

3. RESULTS AND DISCUSSION

3.1 Brick kiln scenario in Punjab

Brick kilns (Kamal et al., 2014; Sikder et al., 2020) of Punjab support the country socio-economically. The brick industry flourished in the province due to the availability of abundant raw material, coal (Shahzad and Ali, 2018). Figure 3 represents the distribution of brick furnaces in the province, Punjab. The data reveals that Faisalabad is dominant in all districts by having maximum number of brick kilns as shown in Figure 3.

In addition, 10 out of 36 districts of the Punjab have big clusters of brick kilns such as Faisalabad, Kasur, Multan, Vehari, Bahawalpur, Gujranwala, Gujrat, Rahim Yar Khan, Sargodha, and Sialkot (Figure 3). Among all districts, Faisalabad (Mehmood et al., 2018) and Kasur are the main hubs of brick kilns (Kataria et al., 2018). Based upon the recent results, it can be clearly perceived that the smallest brick markets are situated in Chiniot and Attock, having less than 100 kilns. Furthermore, Figure 3 shows the recent estimate of kilns' population has exceeded 200 units in 18 districts of Punjab. Furthermore, the existing old brick kiln technology consumes 160 kg of coal for firing 1,000 bricks on average (Raza et al., 2014) and emits various pollutants. So, disaggregating results further, it is revealed that fairly large set up of brick sector in the province is one of the main causes of

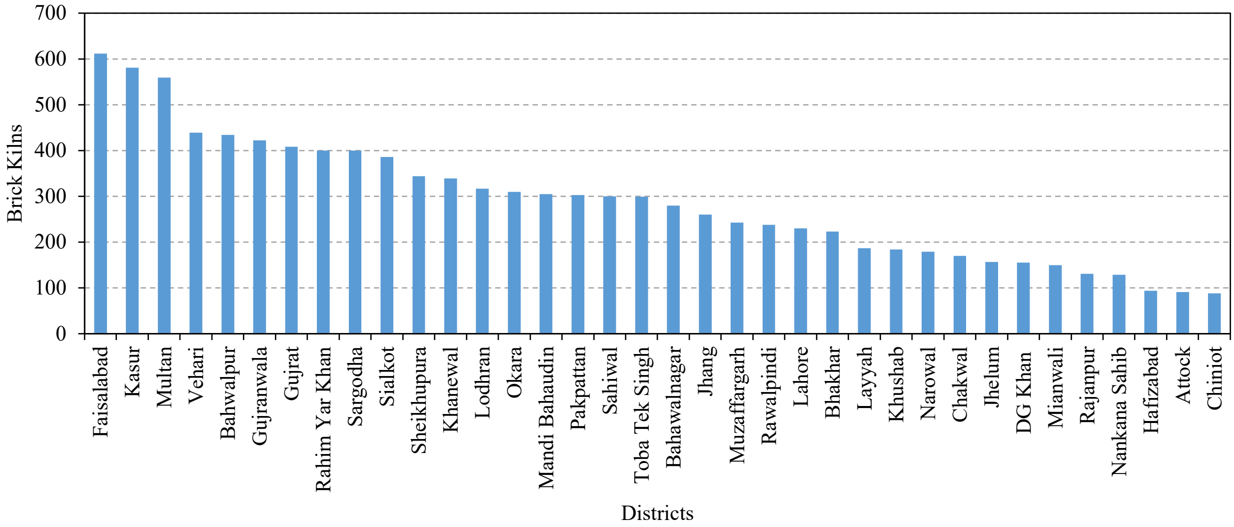

Figure 3. Brick kilns in Punjab (PBC, 2016)

stagnant air. Thus, functioning of old technology kilns in future by delaying in setting up new Zig-Zag system will accumulate emission and increase the proportion of pollutants in the air. Considering further results, it is observed that the brick factories are established in all districts of the province to meet the demand of building material.

3.2 Brick kilns in Punjab

In Punjab, bricks manufacturers are still using old technology for brick manufacturing (Nazir et al., 2011) which is the stationary source (Haque et al., 2018) of air emission (Ismail et al., 2012; Achakzai et al., 2017). As the data of Figure 4 represents the high intensity of old technology kilns are operating in the province which is the largest contributor of air pollutants. The air pollutants level regarding old technology brick kilns are associated with the use of different types of fuel (Sanjel et al., 2016), such as coal (Kumar et al., 2016), old tyres (Gomes and Hossain, 2003; Joshi and Dudani, 2008), agricultural residues (Hameed et al., 2018), bagasse (Kazmi et al., 2016), wood (Tahir and Rafique, 2009; Skinder et al., 2014), industrial waste (Peter et al., 2018), biomass (Zhong et al., 2019), and manure (Blackman, 2000).

So, the fuel consumed in old technology brick kilns pumps out the harmful noxious gases such as sulfur dioxide (SO_2), carbon dioxide (CO_2) (Nepal et al., 2019), carbon monoxide (CO) (Guttikunda et al., 2013), particulate matters (PM) (Aslam et al., 1994; Suresh et al., 2016), volatile organic compounds (VOCs) (Salve et al., 2007), oxides of nitrogen (NOx) (Khan and Vyas, 2008), sulfur (SOx), carbon (COx) (Sanjel et al., 2016), polycyclic aromatic hydrocarbons (PAHs) (Saikia et al., 2016), dioxin (Khan et al., 2015), and furans (Hilten et al., 2008). In addition, stack and fugitive emissions (Rajarathnam et al., 2014; Chen et al., 2017) are discharged from old technology brick kilns during the different process (Darain et al., 2016) such as firing (Sanjel et al., 2017), loading and unloading bricks (Khan et al., 2018), coal crushing (Kumbhar et al., 2014; Pokhrel and Lee, 2014), and cleaning ash of trench (Mondal et al., 2017).

In addition, lack of basic information and technical knowledge of kiln owners, and using substandard kiln technology and cheap fuel to obtain high profit margin are the dominant factors to pollute air. Further, from the perspective of above results it is revealed that in winter the smog is highly dependent on the old technology brick kilns which show their existence in largest number in Punjab.

Whereas, Figure 5 shows that the most of the kilns are closed/abandoned in Attock, Mandi Bahauddin, Sheikhupura, Bhakkar and Muzafargarh. While a very small number of kilns are closed in Rajanpur, Layyah, Vehari, Pakpatan, Bahawalpur, Narowal, and Gujranwala. Das (2015) study has highlighted the reasons to run the brick furnaces on rented land, such as being cost-effective for brick makers. The reasons behind closed and abandoned brick units in Punjab are expired leased contracts and degradation of land (Zhang and Fang, 2007).

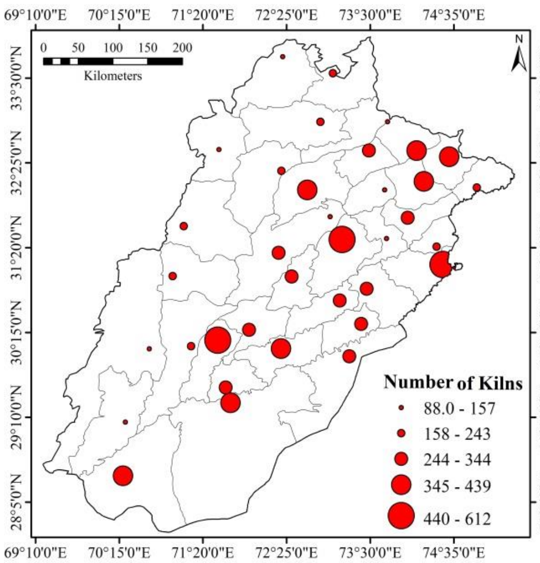

Figure 4. Bick kilns in Punjab

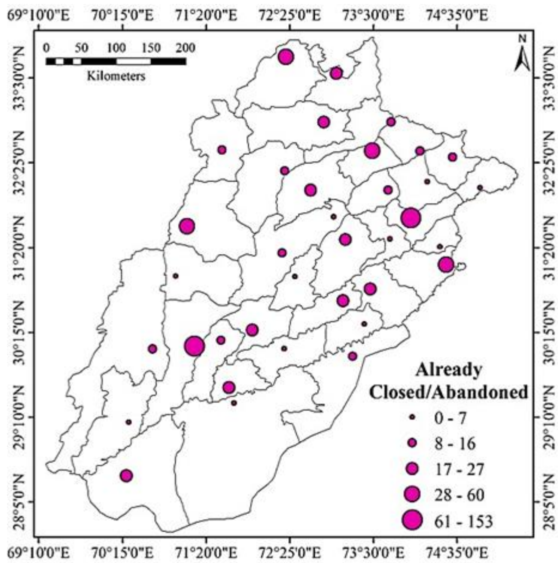

Figure 5. Closed/abandoned kilns in Punjab

3.3 Leased and operational kilns by owners in Punjab

From the granular understanding of Figure 6, it can be clearly seen that the gargantuan size of brick units are operating on lease such as in Gujranwala, Mandi Bahauddin, Okara, Multan, Khanewal, Layyah, and Rahim Yar Khan. In fact, leased land is profitable for manufacturers to run bricks business using local resources (Das, 2015).

Nevertheless, results of Figure 6 indicated that common old technology brick kilns preferred by brick manufacturers because of low investment with high profit (Luby et al., 2015). To date, the unorganized conventional brick kilns are in practice due to financial constraints, erratic power supply and un-trained technicians. Moreover, COVID-19 has been one of the main hurdles (Khan et al., 2020) to switch to resource-efficient Zig-Zag technology, although brick producers are well aware that they are one of the biggest emitters of air pollutants (Khan and Vyas, 2008) and high environmental cost is being paid by the government on the production of construction material resulting in crude emissions which ultimately lead to loss of valuable top fertile soil, biodiversity etc.

Figure 7 results show that least brick units run by the land owners are in Lahore, Narowal, Attock, Rawalpindi, Rahimyar Khan, Bhakar, and Dera Ghazi Khan. Das (2015) study has highlighted one of the major reasons to run the brick furnaces on rented land are economic aspect.

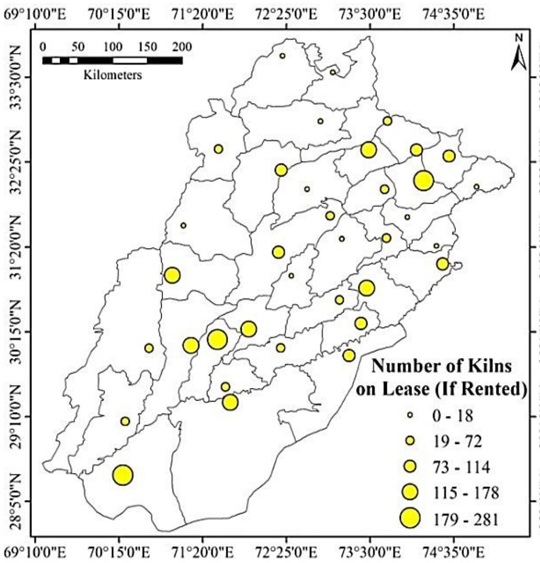

Figure 6. Brick kilns on lease in Punjab

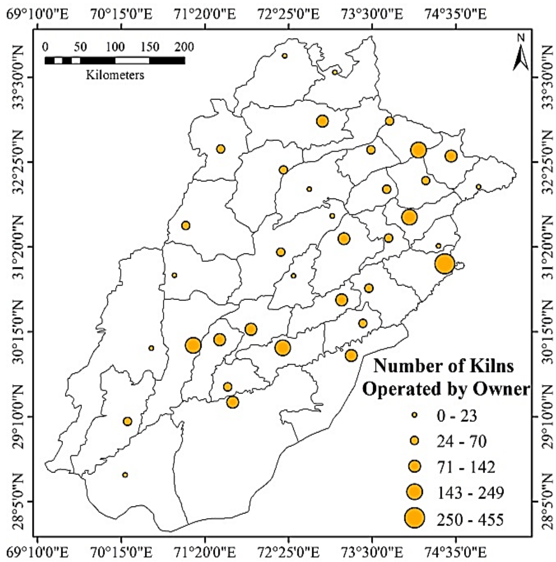

Figure 7. Brick Kilns operated by owner in Punjab

3.4 Aerosol optical depth (AOD) assessment in February and April 2020

Aerosol optical depth (Pathak et al., 2016; Misra et al., 2019) presence in the atmosphere represents the situation of air quality. A low value in terms of palest yellow exhibits a clear sky with high visibility while a reddish colour shows the hazy condition. AOD data highlighted that the particulate matter in Punjab's air is shifting its trends with the passage of time. In the current scenario, in comparison of the results with metrological factor, it is recorded that there is no contribution of rainfall in the AOD level reduction. But the decrease in AOD level is because of COVID-19 lockdown (Kumar et al., 2020). Figure 8 illustrates the highest level of AOD in the northern part of Punjab and lowest level in the southern region of the province. Analyzing the results, it also recorded that the maximum part of the Punjab has the highest level of AOD which is a negative sign for the existing environment. Comparing results of April with February 2020 it is noted that AOD level were reduced during lockdown in the most polluted city of Punjab, i.e., 'Lahore' and supports the findings of the study conducted in Spain (Baldasano, 2020). Kasur which has the highest number of kilns in the province also recorded noticeable results of low AOD. Analyzing Figures 8 and 9, the low concentration is visualized in the northern part and highest level of aerosol is visible in the southern part of Punjab. But overall results of lockdown represent the improved quality of air in April and similar findings have been reported in the study by Gupta et al. (2020).

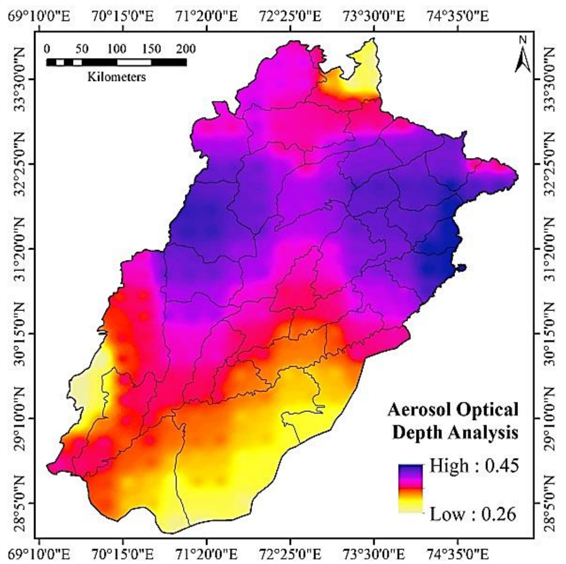

Figure 8. AOD level in February 2020

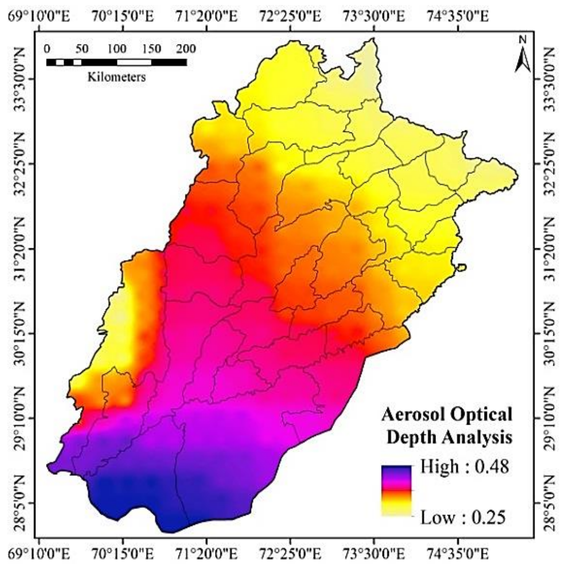

Figure 9. AOD level in April 2020

3.5 Carbon monoxide (CO) assessment in February and April 2020

Carbon monoxide (Guttikunda et al., 2013) is one of the emissions produced by the brick kiln sector (Sanjel et al., 2016). Results of NASA data show the distribution level of CO in the Punjab Province. The satellite-based observations in Punjab exhibit the CO variation before COVID and during the lockdown periods. Analyzing results of the nationwide lockdown has highlighted the prominent reduction in CO level at the study site, similar to results reported in a study conducted by Huang et al. (2020) in China. In addition, Figures 10 and 11 exhibit the CO trend towards the north-eastern zone of Punjab which is the most affected areas of the province in terms of CO emissions, while the south-western region of Punjab is noted with a low level of carbon monoxide during COVID-19 lockdown.

In addition, comparing district wise results, the districts affected by CO are Lahore, Nankana Sahib, Rawalpindi, Sheikhupura, Gujranwala, Sialkot, Narowal, Faisalabad, Kasur, Muzafargarh, and Multan. The prime contributors of carbon monoxide emissions into the atmosphere are thermal power stations and brick industry (Arif et al.,2018) and both of these industries are operating in the highest smog prone districts of Punjab. Further, comparing results with February, it is revealed that intensity of CO is not much reduced in lockdown when all economic and social activities were banned throughout the province.

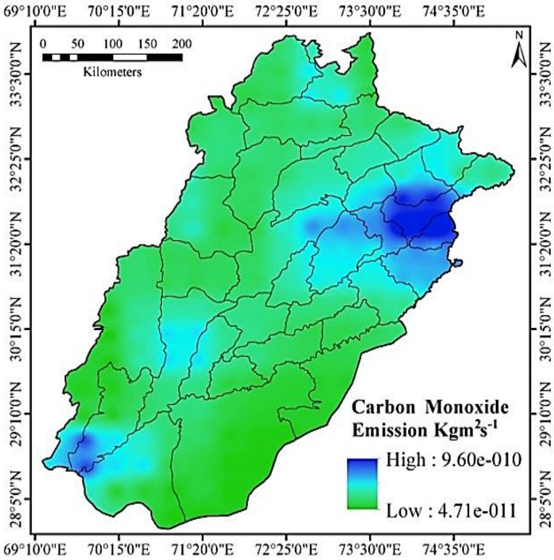

Figure 10. CO level in February 2020

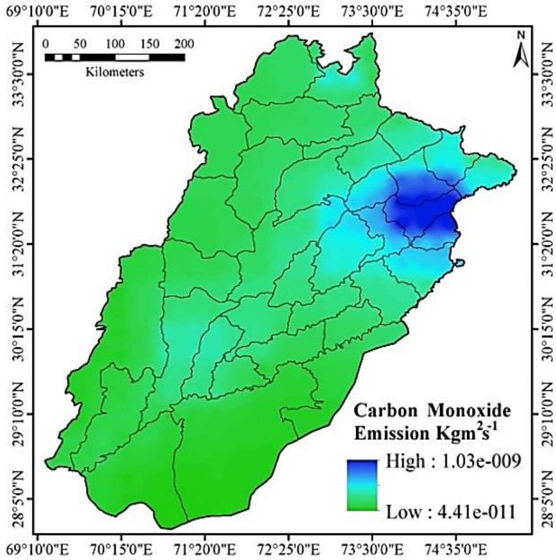

Figure 11. CO level in April 2020

3.6 Ozone assessment in February and April 2020

Spatial trend of ozone in Figures 12 and 13 illustrated that a high proportion of ozone level has been detected in the northern regions of Punjab, similar to results observed in the research conducted in China (Shi and Brasseur, 2020). Analyzing results of the Punjab, it is noted that the intensity of ozone is elevated during lockdown in the central part of the study site. Basic reason for the increase in the level of ozone in Punjab is the reduction of NO level (Quan et al., 2014) during lockdown. Therefore, in lockdown period i.e., April 2020, the ozone level increased when compared to February 2020, which is also supported by the results of recent research conducted by Dantas et al. (2020) and (Collivignarelli et al., 2020).

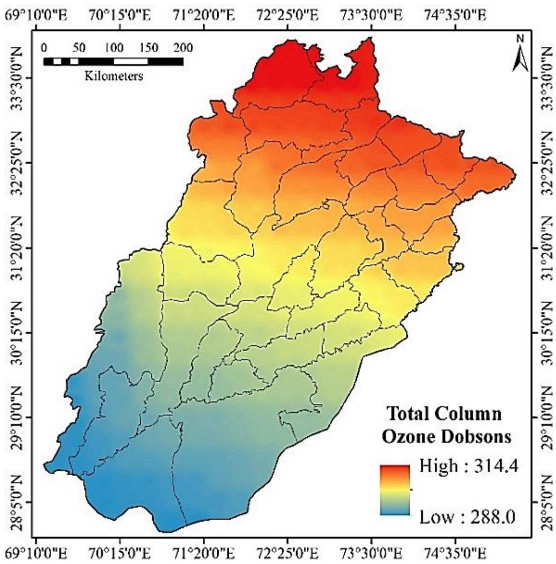

Figure 12. TCO level in February 2020

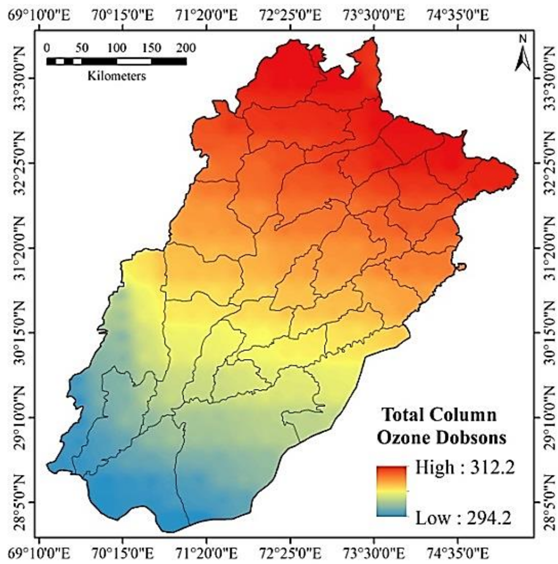

Figure 13. TCO level in April 2020

3.7 Sulfur dioxide assessment in February and April 2020

Brick makers use coal as a primary fuel and significantly rely on it (Alam et al., 2014). Besides coal, the other sources such as old tyres, firewood and waste leather material are also used in kilns as fuel (Sanjel et al., 2016) resulting in sulfur emissions. Considering the spatial pattern of below Figures 14 and 15, a sharp decline is witnessed in sulfur dioxide (SO_2) level all over the Punjab. Although SO_2 (the leading pollutant) associated with brick sector is remarkably decreased, this reduction is not surprising as it is the outcome of policy measures which were taken to control the deadly virus in the wake of the COVID-19 event. Whereas, during the pandemic, the highest influence of sulfur dioxide is visible in Khanewal, Multan, and Muzafargarh by having large brick sector. Further, it is pertinent to mention here, the distribution level of SO_2 shows that the economic activities were in practice during lockdown in both cities. So, comparing results with Figures 14 and 15 of carbon monoxide also show and support the high concentration of SO_2 level in the similar parts of Punjab. While a medium level of sulfur emissions is seen in the Kasur, Lahore, Nankana Sahib, and Faisalabad which are the known districts of brick kilns. Overall, the minimum level of SO_2 is observed in the maximum parts of the Punjab, which was also witnessed in Morocco (Otmani et al., 2020) during lockdown.

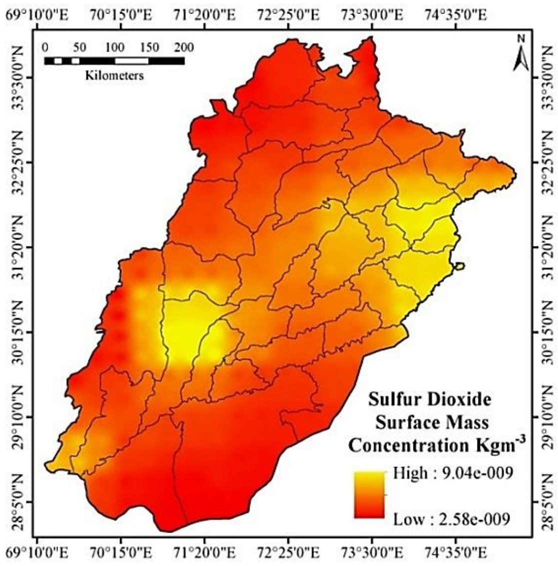

Figure 14. SO_2 level in February 2020

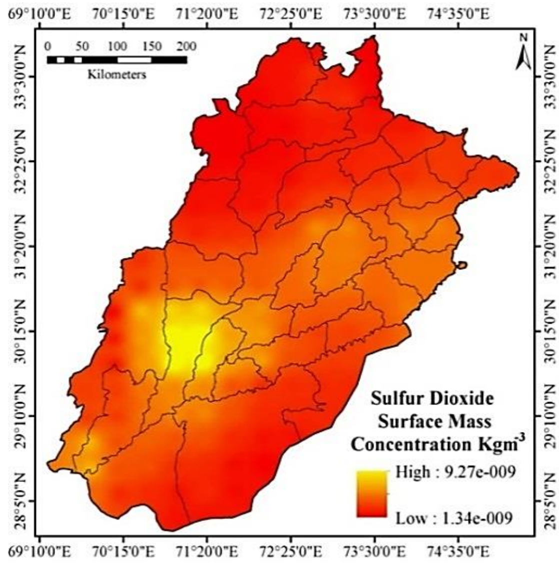

Figure 15. SO_2 level in April 2020

3.8 Carbon dioxide (CO_2) assessment in February and April 2020

The fuel consumed in brick kilns pumps out the harmful noxious gas (carbon dioxide-CO_2) (Alam et al., 2018; Nepal et al., 2019). Figures 16 and 17 have presented the concentration level of CO_2 in February 2020 and April 2020, the lockdown period in Punjab. On comparison, it has been observed that there is noticeable reduction in CO_2 after lock down (March 22nd, 2020). Notably, it is also found that Lahore is one of the most polluted cities of Punjab and, in the present case of suspended human activities, the reduction in carbon emission is visualized in the specific district of eastern side including north-western parts, supporting the findings of the study conducted by Gupta et al. (2020). Thus, the sudden decline in atmospheric CO_2 in most of the Punjab is seen due to the shutdown of industrial units, transport networks and all types of businesses. Similarly, the results of above study support findings of the study conducted in Kolkata during lockdown (Mitra et al., 2020). Further, comparing results with other parts, the high emission level of carbon is visible in the upper and central parts of Punjab such as Rawalpinid (north), Khushab (central), Narowal (north-east), Bahawalnagar (south-east), Rahim Yar Khan (south), and Muzafargarh (south-western).

3.9 Metrological factors in February and April 2020

Meteorological factors determine the quality of air (Kayes et al., 2019). Results of Pre-COVID (Figure 18) depict that highest level of rainfall is received in the northern region of Punjab and very low level is recorded in the rest of the province. So, during COVID-19, the provincial meteorological factors have slight impact on the environmental parameters. In the lockdown period, April 2020, the clear sky provided an opportunity to air pollutants to uplift the concentration of ozone in the northern and central part of Punjab (Figures 18 and 19). The raise in ozone level is due to the reduction of nitrogen oxides which is the outcome of suspended human activities and reported in the study conducted by Spinrad (2020).

Therefore, absence of rains during April did not help in lowering the level of air pollutants in the north and north-eastern part of the Punjab. On comparison of metrological factors in the Figures 18 and 19, the reduction in environmental parameters (carbon monoxide, carbon dioxide, sulfur dioxide, and aerosol optical depth) is visualized in COVID-19 lockdown.

Conclusively, in the present study, the meteorological elements played no significant role in the reduction of toxic air pollutants. Therefore, this credit only goes to stringent control measures which were imposed to tackle COVID-19 pandemic.

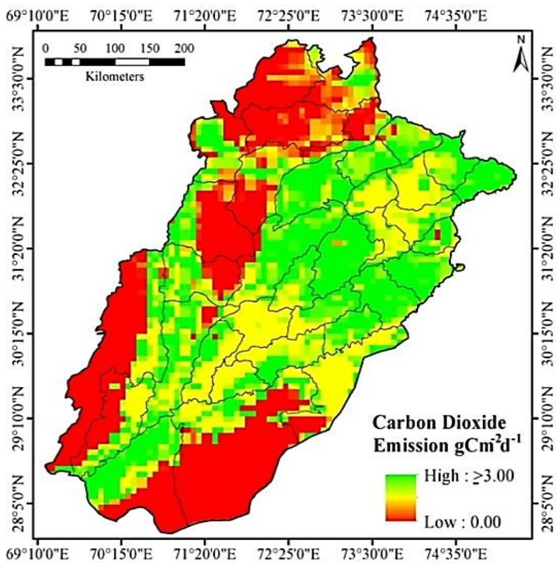

Figure 16. CO_2 level in February 2020

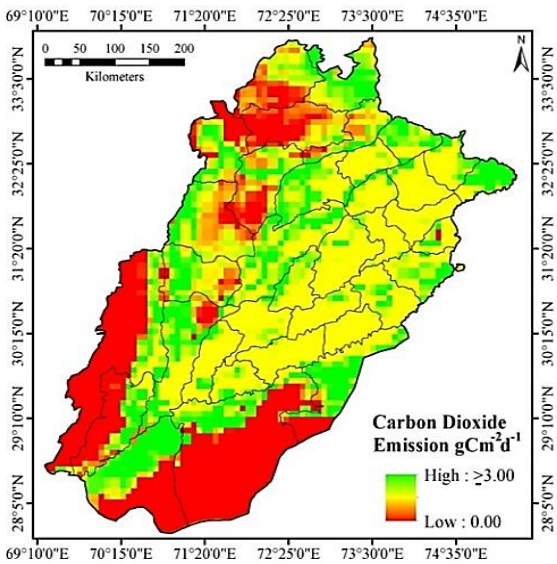

Figure 17. CO_2 level in April 2020

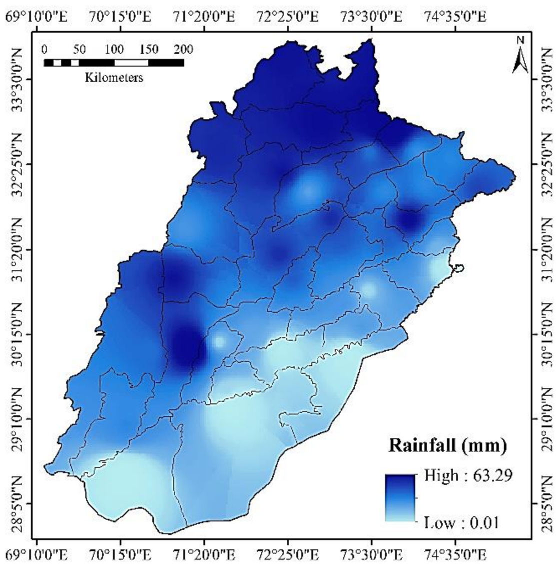

Figure 18. Metrological factors in February 2020

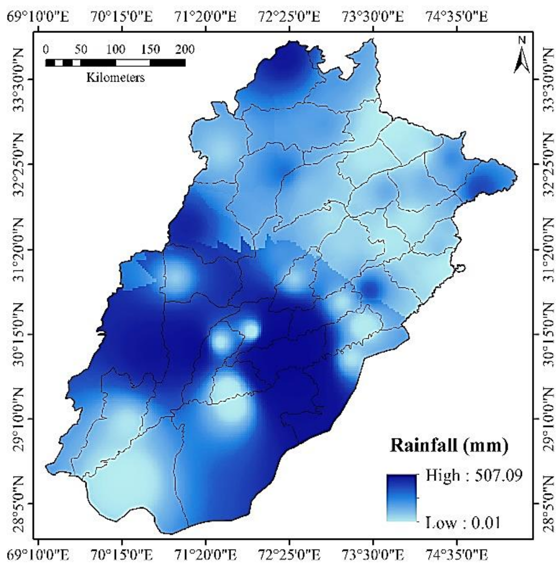

Figure 19. Metrological factors in April 2020

4. CONCLUSION

Results of the present study inferred that Punjab is the hub of brick making units and the fuel used in kilns contributes to degrade the quality of air. Therefore, analysis of spatial results exhibited the fluctuation of aerosol particles and carbon dioxide during COVID-19 lockdown which highlighted the improvement in the air, while the concentration level of CO, SO_2, and TOC depicted the variation throughout the Punjab during the pandemic lockdown. Similarly, like other countries, air pollution is the greatest challenge reported as deadly as Coronavirus. So to overcome air borne sludge and smog menace, the Government of Punjab has banned the operations of old technology brick kilns which are one of the challenges of environmental development in 2020 with Coronavirus. Thus, for the time being the short-term plan can be adopted to hold the level of air emission by adopting stringent actions using credible monitoring and rigorous enforcement. Using good quality coal, improve feeding and firing practices by retrofitting kilns are another short-term solution to handle the situation. Although, the initiative of Government of the Punjab is commendable to restrain old technology brick kilns emitting hazardous pollutants into air during winter season. In the future, measures like shutting down old brick kilns would be insufficient to control smog like the previous year of 2019. Thus, the way forward for the Government of the Punjab is not only to restrict and stop the old technology brick kilns but at the same time install green belts around the kilns which would be an effective approach to clean foul air. In addition, technical capacity building programs should be initiated to achieve desirable goals by guiding and providing the benefits of clean technology to brick manufacturers.

ACKNOWLEDGEMENTS

This research received no external funding. Authors would like to thank Punjab Metrological Department to provide weather data. Moreover, the use of official data of Punjab Brick Kilns available at http://dashboards.urbanunit.gov.pk/brick_kiln_dashboard/ is highly acknowledged.

REFERENCES

Achakzai K, Khalid S, Adrees M, Bibi A, Ali S, Nawaz R, et al. Air pollution tolerance index of plants around brick kilns in Rawalpindi, Pakistan. Journal of Environmental Management 2017;190:252-8.

Alam K, Mukhtar A, Shahid I, Blaschke T, Majid H, Rahman S, et al. Source apportionment and characterization of particulate matter (PM10) in urban environment of Lahore. Aerosol and Air Quality Research 2014;14(7):1851-61.

Alam MZ, Armin E, Haque M, Kayesh JHE, Qayum A. Air pollutants and their possible health effects at different locations in Dhaka City. Journal of Current Chemical Pharmaceutical Sciences 2018;8(1):111.

Arif M, Kumar R, Kumar R, Eric Z, Gourav P. Ambient black carbon, $PM_{2.5}$ and PM_{10} at Patna: Influence of anthropogenic emissions and brick kilns. Science of the Total Environment 2018;624:1387-400.

Aslam M, Srivastava RS, Minocha AK, Gupta RG. Air pollution hazards from brick kilns. Journal of the Institutions of Engineers (India), Environmental Engineering Division 1994;74:83-7.

Badshah SL, Ullah A, Badshah SH, Ahmad I. Spread of novel coronavirus by returning pilgrims from Iran to Pakistan. Journal of Travel Medicine 2020;27(3):1-3.

Baldasano JM. COVID-19 lockdown effects on air quality by NO_2 in the cities of Barcelona and Madrid (Spain). Science of the Total Environment 2020;741:140353.

Bandyopadhyay A, Basak AK, Bandyopadhyay P, Tripathy S. Peak expiratory flow rate in female brick-field workers of West Bengal, India. Ergonomics SA: Journal of the Ergonomics Society of South Africa 2006;18(1):22-7.

Bhanarkar AD, Gajghate DG, Hasan MZ. Assessment of air pollution from small scale industry. Environmental Monitoring and Assessment 2002;80(2):125-33.

Blackman A. Informal sector pollution control: What policy options do we have? World Development 2000;28(12):2067-82.

Chen Y, Du W, Zhuo S, Liu W, Liu Y, Shen G, et al. Stack and fugitive emissions of major air pollutants from typical brick kilns in China. Environmental Pollution 2017;224:421-9.

Collivignarelli MC, Abbà A, Bertanza G, Pedrazzani R, Ricciardi P, Miino MC. Lockdown for COVID-2019 in Milan: What are the effects on air quality? Science of the Total Environment 2020;732:139280.

Comunian S, Dongo D, Milani C, Palestini P. Air pollution and COVID-19: The role of particulate matter in the spread and increase of Covid-19's morbidity and mortality. International Journal of Environmental Research and Public Health 2020;17(12):4487.

Das B, Gangopadhyay S. An ergonomics evaluation of posture related discomfort and occupational health problems among rice farmers. Occupational Ergonomics 2011;10(1,2):25-38.

Das R. Causes and consequences of land degradation in and around the brick kilns of khejuri CD blocks over Coastal Medinipur in West Bengal. International Journal of Innovative Research and Development 2015;4(2):185-94.

Dantas G, Siciliano B, França BB, da Silva CM, Arbilla G. The impact of COVID-19 partial lockdown on the air quality of the city of Rio de Janeiro, Brazil. Science of the Total Environment 2020;729:139085.

Darain KMU, Jumaat MZ, Islam AS, Obaydullah M, Iqbal A, Adham MI, et al. Energy efficient brick kilns for sustainable environment. Desalination and Water Treatment 2016;57(1): 105-14.

Figà-Talamanca I. Occupational risk factors and reproductive health of women. Occupational Medicine 2006;56(8):521-31.

Gomes E, Hossain I. Transition from traditional brick manufacturing to more sustainable practices. Energy for Sustainable Development 2003;7(2):66-76.

Gupta S, Narayan, R. Brick kiln industry in long-term impacts biomass and diversity structure of plant communities. Current Science 2010;201072-9.

Gupta N, Tomar A, Kumar V. The effect of COVID-19 lockdown on the air environment in India. Global Journal of Environmental Science and Management 2020;6:31-40.

Guttikunda SK, Begum BA, Wadud, Z. Particulate pollution from brick kiln clusters in the Greater Dhaka Region, Bangladesh. Air Quality, Atmosphere and Health 2013;6(2):357-65.

Hameed A, Abbas S, Qazi AU, Haider U. Effect of waste glass on properties of burnt clay bricks. Pakistan Journal of Engineering and Applied Sciences 2018;22(1):56-63.

Haque MI, Nahar K, Kabir MH, Salam, A. Particulate black carbon and gaseous emission from brick kilns in Greater Dhaka Region, Bangladesh. Air Quality, Atmosphere and Health 2018;11(8):925-35.

Hilten RN, Lawrence TM, Tollner EW. Modeling storm water runoff from green roofs with HYDRUS-1D. Journal of Hydrology 2008;358(3-4):288-93.

Hossain MA, Zahid AM, Arifunnahar M, Siddique MNA. Effect of brick kiln on arable land degradation, environmental pollution and consequences on livelihood of Bangladesh. Journal of Science, Technology and Environment Informatics 2019;6(2):474-88.

Huang X, Ding A, Gao J, Zheng B, Zhou D, Qi X, et al. Enhanced secondary pollution offset reduction of primary emissions during COVID-19 lockdown in China. National Science Review 2020;1-9.

Ismail M, Muhammad D, Khan FU, Munsif F, Ahmad T, Ali S, et al. Effect of brick kilns emissions on heavy metal (Cd and Cr) content of contiguous soil and plants. Sarhad Journal of Agriculture 2012;28(3):403-9.

Iqbal MJ. Bonded labor in the brick kiln industry of Pakistan. The Lahore Journal of Economics 2006;11(1):99-119.

Javid K, Akram MAN, Ranjha MM, Pervaiz S. GIS-based assessment of aridity over Punjab Province, Pakistan, by using climatic indices. Arabian Journal of Geosciences 2020;13(7):1-12.

Joshi SK, Dudani I. Environmental health effects of brick kilns in Kathmandu valley. Kathmandu University Medical Journal 2008;6(1):3-11.

Kamal A, Malik RN, Martellini T, Cincinelli A. Cancer risk evaluation of brick kiln workers exposed to dust bound PAHs in Punjab Province (Pakistan). Science of the Total Environment 2014;493:562-70.

Kataria JR, Usman A, Hussain S, Usman M, Amjad A. Breaking the bonds of poverty: Effectiveness of microcredit in improving the wellbeing of Brick Kilns' Laborers in Pakistan. Research Journal of South Asian Studies 2018;33:253-74.

Kayes I, Shahriar SA, Hasan K, Akhter M, Kabir MM, Salam MA. The relationships between meteorological parameters and air pollutants in an urban environment. Global Journal of Environmental Science and Management 2019;5(3);265-78.

Kazmi SMS, Abbas S, Munir MJ, Khitab A. Exploratory study on the effect of waste rice husk and sugarcane bagasse ashes in burnt clay bricks. Journal of Building Engineering 2016;7:372-8.

Khaliquzzaman M, Harinath AS, Ferdousi SA, Khan SMMH. Thirty years' quest for emission reduction and energy efficiency improvement of brick kilns in Bangladesh. International Journal of Environmental Monitoring and Analysis 2020;8(1):11-22.

Khan R, Vyas H. A study of impact of brick industries on environment and human health in Ujjain City (India). Journal of Environmental Research and Development 2008;2(3):421-5.

Khan AR, Iqbal J, Parveen N, Ahmad F. Brick kiln and sugar mill: Severe environmental health hazards cause respiratory diseases in Tehsil Darya Khan, District Bhakkar, Punjab. Pakistan Journal of Applied Environment Biology Science 2015;5:31-8.

Khan MNA, Liaqat N, Ahmed I, Basit A, Umar M, Khan MA. Effect of brick dust on strength and workability of concrete. In IOP Conference Series: Materials Science and Engineering 2018;414(1):012005.

Khan MW, Ali Y, De Felice F, Salman A, Petrillo A. Impact of brick kilns industry on environment and human health in Pakistan. Science of the Total Environment 2019;678:383-9.

Khan KA, Mubbin M, ul Haq MI, Hussain N, Maqbool MM, Ahmad M, et al. Air quality index with particulate matter ($PM_{2.5}$) improved after national lockdown during COVID-19 outbreak across Pakistan. Open Access Journal of Biogeneric Science and Research 2020;3(2):1-6.

Kumbhar S, Kulkarni N, Rao AB, Rao B. Environmental life cycle assessment of traditional bricks in western Maharashtra, India. Energy Procedia 2014;54(0):260-9.

Kumar CS, Parvathi S, Rudramoorthy R. Impact categories through life cycle assessment of coal-fired brick. Procedia Technology 2016;24:531-7.

Kumar P, Hama S, Omidvarborna H, Sharma A, Sahani J, Abhijith KV, et al. Temporary reduction in fine particulate matter due to 'anthropogenic emissions switch-off'during COVID-19 lockdown in Indian Cities. Sustainable Cities and Society 2020;102382.

Luby SP, Biswas D, Gurley ES, Hossain I. Why highly polluting methods are used to manufacture bricks in Bangladesh. Energy for Sustainable Development 2015;28:68-74.

Maithel S, Uma R. Environmental regulations and the Indian brick industry. Environmental Practice 2000;2(3):230-1.

Mehmood K, Ahmad HR, Abid AA, Guo P. A preliminary assessment and control strategy of size segregated pollutants in urban and peri-urban areas of Metropolitan Faisalabad, Pakistan. Journal of Analytical and Environmental Chemistry 2018;19(2):146-52.

Misra P, Imasu R, Takeuchi W. Impact of urban growth on air quality in Indian cities using hierarchical bayesian approach. Atmosphere 2019;10(9):517.

Mitra A, Ray Chadhuri T, Mitra A, Pramanick P, Zaman S. Impact of COVID-19 related shutdown on atmospheric carbon dioxide level in the city of Kolkata. Parana Journal of Science and Education 2020;6(3):84-92.

Momčilović-Petronijević A, Topličić-Ćurčić G, Ćurčić A. Architecture and ceramic materials, development through time: Adobe and brick. Facta Universitatis-series: Architecture and Civil Engineering 2018;16(3):387-400.

Mondal A, Das S, Sah RK, Bhattacharyya P, Bhattacharya SS. Environmental footprints of brick kiln bottom ashes: Geostatistical approach for assessment of metal toxicity. Science of the Total Environment 2017;609:215-24.

Naveen S. Production and marketing network chain of brick kiln product: A case study of Hyderabad City. International Journal of Managing Value and Supply Chains 2016;7(1):27-37.

Nazir S, Tufail M, NisaW, Ghauri M. Modelling for capture of carbon dioxide using aqueous ammonia from flue gases of a brick kiln. International Journal of Chemical Environment and Engineering 2011;2(3):2013-20.

Nepal S, Mahapatra PS, Adhikari S, Shrestha S, Sharma P, Shrestha KL, et al. Comparative study of stack emissions from straight-line and zigzag brick kilns in Nepal. Atmosphere 2019;10(3):107.

Otmani A, Benchrif A, Tahri M, Bounakhla M, El Bouch M, Krombi MH. Impact of Covid-19 lockdown on PM_{10}, SO_2, and NO_2 concentrations in Salé City (Morocco). Science of the Total Environment 2020;139541.

Pathak B, Subba T, Dahutia P, Bhuyan PK, Moorthy KK, Gogoi MM, et al. Aerosol characteristics in North-east India using ARFINET spectral optical depth measurements. Atmospheric Environment 2016;125:461-73.

Punjab Brick Kilns Census (PBC). Brick kiln census. Labor and Human Resource Department, Government of Punjab, Lahore [Internet]. 2016 [cited 2020 Jun 10]. Available from: http://dashboards.urbanunit.gov.pk/brick_kiln_dashboard/.

Pervaiz S, Khan FZ, Akram MAN. Impact of COVID-19 lockdown policy on air and automotive industry. Pen Acclaims 2020a;10:1-8.

Pervaiz S, Javid K, Khan FZ, Zahid Y, Akram MA. Preliminary assessment of air during COVID-19 lockdown: An unintended benefit to environment. Environment and Natural Resources Journal 2020b;18(4):363-75.

Peter C, Mohan K, Greens S, George S. Energy efficient production of clay bricks using industrial waste. Heliyon 2018;4(10):1-12.

Pokhrel R, Lee H. Integrated environment impact assessment of brick kiln using environmental performance scores. Asian Journal of Atmospheric Environment 2014;8(1):15-24.

Quan J, Tie X, Zhang Q, Liu Q, Li X, Gao Y, et al. Characteristics of heavy aerosol pollution during the 2012-2013 winter in Beijing, China. Atmospheric Environment 2014;88:83-9.

Rajarathnam U, Athalye V, Ragavan S, Maithel S, Lalchandani D, Kumar S, et al. Assessment of air pollutant emissions from brick kilns. Atmospheric Environment 2014;98:549-53.

Ramasamy D. Enchanted improvements in air quality across India: A study from COVID-19 lockdown perspective. Adalya Journal 2020;9(5):101-25.

Raza A, Qamer MF, Afsheen S, Adnan M, Naeem S, Atiq M. Particulate matter associated lung function decline in brick kiln workers of Jalalpur Jattan, Pakistan. Pakistan Journal of Zoology 2014;46(1):237-43.

Rupan S. Air Quality Impacts of Brick Kilns in India: A Report Analyzing the Production Limitations, its Impacts on Local Air Quality and Subsequent Adaptable Measures for Improvement [dissertation]. Sustainable Environmental Systems Pratt Institute; 2017.

Sanjel S, Thygerson SM, Khanal SN, Joshi SK. Environmental and occupational pollutants and their effects on health among brick kiln workers. Open Journal of Safety Science and Technology 2016;6:81-98.

Sanjel S, Khanal SN, Thygerson SM, Carter WS, Johnston JD, Joshi SK. Respiratory symptoms and illnesses related to the concentration of airborne particulate matter among brick kiln workers in Kathmandu Valley, Nepal. Annals of Occupational and Environmental Medicine 2017;29(1):9.

Salve PR, Satapathy DR, Katpatal YB, Wate SR. Assessing spatial occurrence of ground level ozone around coal mining areas of Chandrapur District, Maharashtra, India. Environmental Monitoring and Assessment 2007;133(1-3):87-98.

Saikia J, Narzary B, Roy S, Bordoloi M, Saikia P, Saikia BK. Nanominerals, fullerene aggregates, and hazardous elements in coal and coal combustion-generated aerosols: An environmental and toxicological assessment. Chemosphere 2016;164:84-91.

Schmidt CW. Modernizing artisanal brick kilns: A global need. Environmental Health Perspectives 2013;121(8):a242-9.

Shahzad M, Ali Z. Cleaning of Dalwal-Punjab coal by using shaking table. Pakistan Journal of Scientific and Industrial Research Series A: Physical Sciences 2018;61(1):56-8.

Shaikh S, Nafees AA, Khetpal V, Jamali AA, Arain AM, Yousuf A. Respiratory symptoms and illnesses among brick kiln workers: A cross sectional study from rural districts of Pakistan. BMC Public Health 2012;12(1):1-6.

Shi X, Brasseur GP. The response in air quality to the reduction of Chinese economic activities during the COVID-19 outbreak. Geophysical Research Letters 2020;e2020GL088070.

Skinder BM, Sheikh AQ, Pandit AK, Ganai BA. Brick kiln emissions and its environmental impact: A Review. Journal of Ecology and the Natural Environment 2014;6(1):1-11.

Sikder AHF, Begum K, Parveen Z, Hossain MF. Assessment of macro and micro nutrients around brick kilns agricultural environment. Information Processing in Agriculture 2016;3(1):61-8.

Spinrad P. The Ozone weekend effect [Internet]. 2020 [cited 2020 Mar 25]. Available from: https://engineering.berkeley.edu/news/2009/03/the-ozone-weekend-effect/.

Suresh R, Kumar S, Mahtta R, Sharma S. Emission factors for continuous fixed chimney bull trench brick kiln (FCBTK) in India. International Journal of Advanced Engineering, Management and Science 2016;2(6):239494.

Tahir SNA, Rafique M. Emission of greenhouse gases (GHGs) from burning of biomass in brick kilns. Environmental Forensics 2009;10(4):265-7.

Tusher TR, Ashraf Z, Akter S. Health effects of brick kiln operations: A study on largest brick kiln cluster in Bangladesh. South East Asia Journal of Public Health 2018;8(1):32-6.

Wahid A, Ahmad SS, Ahmad MN, Khaliq B, Nawaz M, Shah SQ, et al. Assessing the effects of hydrogen fluoride on mango (*Mangifera indica* L.) in the vicinity of a brick kiln field in southern Pakistan. Fluoride 2014;47(4):307-14.

Weyant C, Athalye V, Ragavan S, Rajarathnam U, Lalchandani D, Maithel S, Bond TC. Emissions from South Asian brick production. Environmental Science and Technology 2014;48(11):6477-83.

Unni JC. Social effects of Covid-19 pandemic on children in India. Indian Journal of Practical Pediatrics 2020;22:102-4.

Zhang MK, Fang LP. Effect of tillage, fertilizer and green manure cropping on soil quality at an abandoned brick making site. Soil and Tillage Research 2007;93(1):87-93.

Zhong M, Saikawa E, Avramov A, Chen C, Sun B, Ye W, et al. Nepal ambient monitoring and source testing experiment (NAMaSTE): Emissions of particulate matter and sulfur dioxide from vehicles and brick kilns and their impacts on air quality in the Kathmandu Valley, Nepal. Atmospheric Chemistry and Physics 2019;19(12):8209-28.

Environment and Natural Resources Journal 2021; 19(2): 165-175

Mapping Above-Ground Carbon Stock of Secondary Peat Swamp Forest Using Forest Canopy Density Model Landsat 8 OLI-TIRS: A Case Study in Central Kalimantan Indonesia

Raden Mas Sukarna*, Cakra Birawa, and Ajun Junaedi

Forestry Department, Faculty of Agriculture, University of Palangka Raya, Kampus UPR Tunjung Nyaho, Yos Sudarso Sreet, Kotak Pos 2/PLKUP 73111, Palangka Raya, Central Kalimantan, Indonesia

ARTICLE INFO

Received: 16 Sep 2020
Received in revised: 18 Nov 2020
Accepted: 5 Jan 2021
Published online: 8 Feb 2021
DOI: 10.32526/ennrj/19/2020209

Keywords:
Peat swamp forest/ Landsat/ Forest Canopy Density/ Above-ground biomass/ Carbon stock

*** Corresponding author:**
E-mail: sukarna@for.upr.ac.id

ABSTRACT

Mapping the above-ground carbon potential by using a non-destructive method has been a serious challenge for researchers in the effort to improve the performance of natural forest management in Indonesia, particularly in the ex-Mega Rice Project (MRP) area in Central Kalimantan Province. Nevertheless, the rapid and dynamic changes in secondary peat swamp forests are currently mapped effectively with the remote sensing technology using the Forest Canopy Density (FCD) model. FCD analysis as done by integrating vegetation index, soil index, temperature index and shadow index of Landsat 8 OLI images. The result was an FCD class map. In each class, parameter measurements were established for seedling, sapling, poles and tree stages. Above-ground carbon stock was calculated using three allometric equations. The results revealed that the values of carbon stock in ±16,147.26 ha dense secondary peat swamp forest, ±1,509.66 ha moderately dense scrub swamp forest, and ±632.07 ha sparse scrub swamp forest were, respectively, 79.28-122.96; 74.06-113.06; and 40.48-63.60 ton/ha. These results show that FCD application could be used to classify forest density effectively and in line with the variety of their attributes such us aboveground biomass and carbon stock potential.

1. INTRODUCTION

With a total area of 15,798,359 ha, Central Kalimantan Province has a large proportion of peatland that can be classified into primary peat swamp forest (228,773 ha), secondary peat swamp forest (45,927 ha), shrub swamp (1,979,807 ha), and peat swamp area (549,007 ha) (Wardoyo, 2002). The average degradation rate of peat swamp forests in 1991-2001 is approximately 3.3% (Boehm et al., 2002). The relatively rapid development and changes of swamp forest status have not been accompanied by specific and comprehensive monitoring system activities. Page et al. (2009) reported that peat land clearing for agricultural use has caused a decrease in the level of groundwater 176 cm in the dry season and flooding up to 100 cm above ground level in the rainy season. Rehman et al. (2015) reported that logging activities cause the humid tropical forests to be highly prone to forest fires and desiccation. Therefore, there is an urgency to devise an inventory system that is able to provide information on carbon potential of forest. Since the beginning of 1990, the Japan Overseas Forestry Consultants Association (JOFCA) and the International Timber Trade Organization (ITTO) have succeeded in creating a Forest Canopy Density (FCD) model with an accuracy level above 90% (Rikimaru, 1996). The classification of forest canopy density using the FCD model is in line with the variety of structural and floristic composition of peat swamp forest (Sukarna, 2009; Sukarna and Syahid, 2015). Previous studies using the FCD model have been carried out by Deka et al. (2012) and Banerjee et al. (2014).

The territorial inventory of vast forest areas with dynamic development and limited access requires significant funds, time and energy (Mon et al., 2012; Wannasiri et al., 2013). The research problem entails how to develop an indirect and non-destructive

Citation: Sukarna RM, Birawa C, Junaedi A. Mapping above-ground carbon stock of secondary peat swamp forest using forest canopy density model Landsat 8 OLI-TIRS: A case study in Central Kalimantan Indonesia. Environ. Nat. Resour. J. 2021;19(2):165-175. (https://doi.org/10.32526/ennrj/19/2020209)

method for estimating above-ground carbon stock. It is necessary to standardize the objectives and models that will be developed in mapping the carbon stock. Previous studies of above ground biomass and carbon stock have been carried out by Laurance et al. (1999), Rahayu et al. (2007), Ballhorn et al. (2007), Moder et al. (2008), and Rosalina et al. (2013).

Studies on the estimation of above-ground carbon stock of peat swamp forests by employing Alos Palsar imagery has been conducted by Yuwono et al. (2015). The study claimed the positive coefficient of correlation between backscatter and carbon stock. Furthermore, MOD17 imagery from the Terra/Aqua MODIS satellite has also been the subject in a study carried out by Vetrita and Hirano (2012). Based on the problem and priorities, the objectives of the present study are described as follows: (1) to develop a forest canopy classification model based on Landsat 8 OLI-TIRS images; and (2) to estimate the above-ground carbon stock of the secondary peat swamp forest using allometric equations.

2. METHODOLOGY

2.1 Study area

The study area was conducted in the Block C area of ex-Mega Rice Project (MRP) in Central Kalimantan Province, Indonesia (Figure 1). The ex-MRP is the most important peat swamp ecosystem and also well known for their extreme fragility (Boehm and Siegert, 2004; Fahmi and Radjagukguk, 2013). It has since burned during the annual dry season spewing out a choking haze and large volumes of carbon emissions. It is urgent to study above-ground carbon stock related to the ecosystem condition.

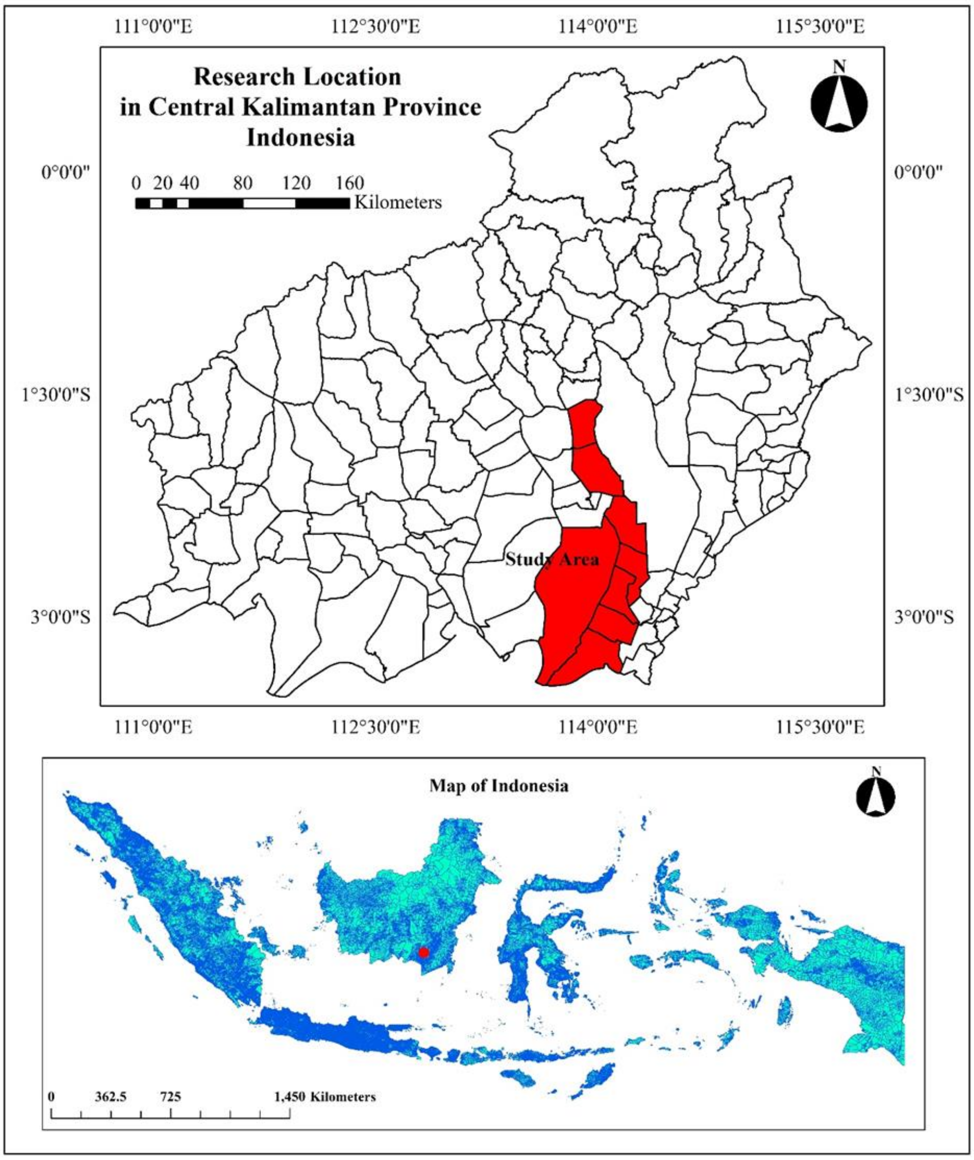

Figure 1. Map of study area

2.2 Data acquisition

The Landsat 8 OLI/TIRS path/row 118/062 on 21 August 2016 were used to cover the study area, then map of Central Kalimantan Province.

2.3 Correction and normalization

The correction of the spectral value of imagery is required due to the cloud and atmospheric disturbances. The histogram matching method and data normalization through contrast stretching technique were carried out by FCD Mapper Version 2.0 to correct the data, resulting in new images with a value between 0 to 255 for all bands. Geometric correction was done using the Indonesia Topographic Map through affine transformation with geographic coordinates and the World Geodetic System datum (WGS 84) in Quantum GIS version 3.14.

2.4 Image processing of FCD

Classification was carried out through a spectral data of Landsat images using the FCD models (Rikimaru, 1996; Rikimaru, 1997; Roy et al., 1997), with formulations as follows:

- Advanced vegetation index: $(\mathrm{AVI}) = \{(\mathrm{NIR}+1)\times(256-\mathrm{Red})\times(\mathrm{NIR}-\mathrm{Red})\}^{\frac{1}{3}}$
- Bare soil index: $(\mathrm{BI}) = \left\{(\mathrm{SWIR}+\mathrm{Red}) - \frac{(\mathrm{NIR}+\mathrm{Blue})}{(\mathrm{SWIR}+\mathrm{Red})} + (\mathrm{NIR}+\mathrm{Blue})\right\}\times 100 + 100$
- Shadow index: $(\mathrm{SI}) = \{(256-\mathrm{Blue})\times(256-\mathrm{Green})\times(256-\mathrm{Red})\}^{1/3}$
- Temperature index: $(\mathrm{TI}) \rightarrow \mathrm{L} = \frac{[\mathrm{L.min}+(\mathrm{L.max}-\mathrm{L.min})]}{255}\times \mathrm{Q}$

With the spectral bands Landsat 8 OLI/TIRS consisting of: Blue Band, Green Band, Red Band, Near Infra Red (NIR) Band, Short Wave Infra Red (SWIR) Band, L (Thermal infrared radiance), and Q is the digital number of the image.

The Advanced Vegetation Index (AVI) is used to measure and analyze green vegetation density changes, the Bare soil Index (BI) is used to analyze open areas, the Shadow Index (SI) is used to analyze forest canopy cover conditions, and the Thermal Index (TI) is used to determine the differences of micro temperature in each land cover unit (Roy et al., 1997).

Based on these 4 (four) indices, the forest canopy density value is estimated using the following equation (Rikimaru, 1996).

- Forest Canopy Densisty $(\mathrm{FCD}) = (\mathrm{VD}\times \mathrm{SSI}+1)^{1/2}-1$

Where; VD is the Vegetation Density and SSI is the Scaled Shadow Index.

2.5 Field survey

Field survey was carried out to investigate and measure the conditions at each canopy density of the peat swamp forest. For each unit of forest canopy density, a sample plot was established in a stratified sampling with a size of 10 × 10 m for the tree/pole level, 2 × 2 m for the sapling level, and 1 × 1 m for the seedling level. Totally, there were 60 sample plots, consisting of 20 plots in the secondary peat swamp forest with dense canopies, 20 plots in the secondary peat swamp forest with moderately dense canopies (shrubs), and 20 plots in the forests with sparse canopy (scrub swamp).

2.6 Estimation of above-ground carbon stock potential

In the present study, the calculation of the above-ground carbon stock potential of vegetation was estimated using the allometric equations of biomass/dry weight and subsequently used to calculate the carbon stored in vegetation.

- Allometric equation model proposed by Kettering et al. (2001): $\mathrm{DW} = 0.11\ \rho\ \mathrm{D}^{2.62}$
- Allometric equation model proposed by Murdiyarso et al. (2004): $\mathrm{DW} = 0.19\ \rho\ \mathrm{D}^{2.37}$
- Allometric equation model proposed by Jaya et al. (2007): $\mathrm{DW} = 0.107\ \mathrm{D}^{2.486}$

Where; DW=dry weight/tree biomass (kg/tree); ρ=wood density (gr/cm^3); D=tree diameter at breast height (dbh) (cm); The amount of carbon stored in vegetation using the Brown (1997) equation:

$$\mathrm{C}\left(\frac{\mathrm{kg}}{\mathrm{tree}}\right) = \mathrm{DW}\times 0.50$$

3. RESULTS AND DISCUSSION

3.1 Image analysis of FCC, AVI, BI, SI, and TI

The results of the vegetation density analysis derived from the integration of AVI and BI images obtained highly detailed land cover classes compared to the false color composite image (FCC 654; Figure 2), particularly in distinguishing open area and dense above-ground vegetation. Nevertheless, the Vegetation Density image still had a few shortcomings, including dense grasslands and shrubs revealed a higher percentage value of vegetation density (>80%) than young scrub swamp forests (40-60%), which is an error in interpreting the peat swamp forest vegetation structure.

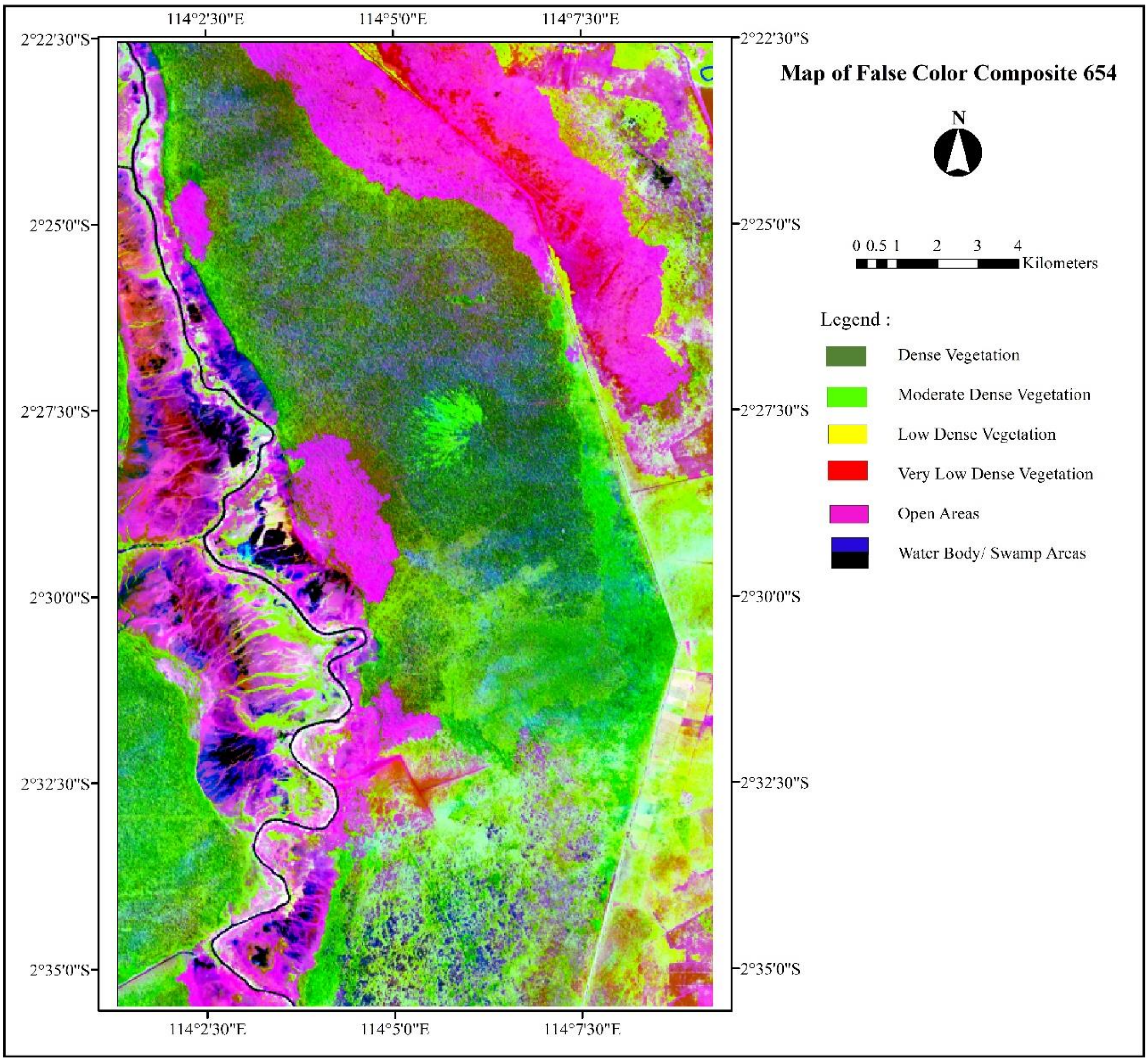

Figure 2. Map of false color composite 654

To evade misidentification and classification of the vegetation structure, a method has been developed by inputting the values of shadow index (SI) and thermal index (TI). Rikimaru (1997) suggested that the maximum value of the vegetation index does not primarily depend on tree or forest density since it is saturated earlier than the shadow index (SI). On the contrary, the SI value is highly dependent on the amount of tall vegetation such as trees with a significant canopy shadow. The higher the tree vegetation density level, the higher the shadow level. Therefore, the higher the SI value, the lower the thermal index (TI) value (Figure 3).

The results of the analysis revealed the negative correlation between SI and TI with a correlation value of -0.684. It explains the phenomenon of the higher the vegetation canopy shadow in the peat swamp forests, the lower the temperature (TI). On the contrary, it also revealed the positive correlation between BI and TI with a correlation value of 0.783. It explains the phenomenon of the higher the open area index value at the study area, the higher the temperature (TI). The combination of AVI, BI, SI and TI as presented in Table 1.

Table 1. Correlation value of AVI, BI, SI, and TI combination

No.	Combination	Landsat 8 OLI-TIRS		
		Correlation	Mean	Deviation
1	AVI-BI	-0.601	101.048	30.833
2	SI-TI	-0.684	133.124	51.171
3	AVI-SI	0.123	101.048	30.833
4	BI-SI	-0.661	123.901	20.660
5	BI-TI	0.783	123.901	20.660

Remark: AVI=Advanced Vegetation Index; BI=Bare Soil Index; SI=Shadow Index; TI=Thermal Index

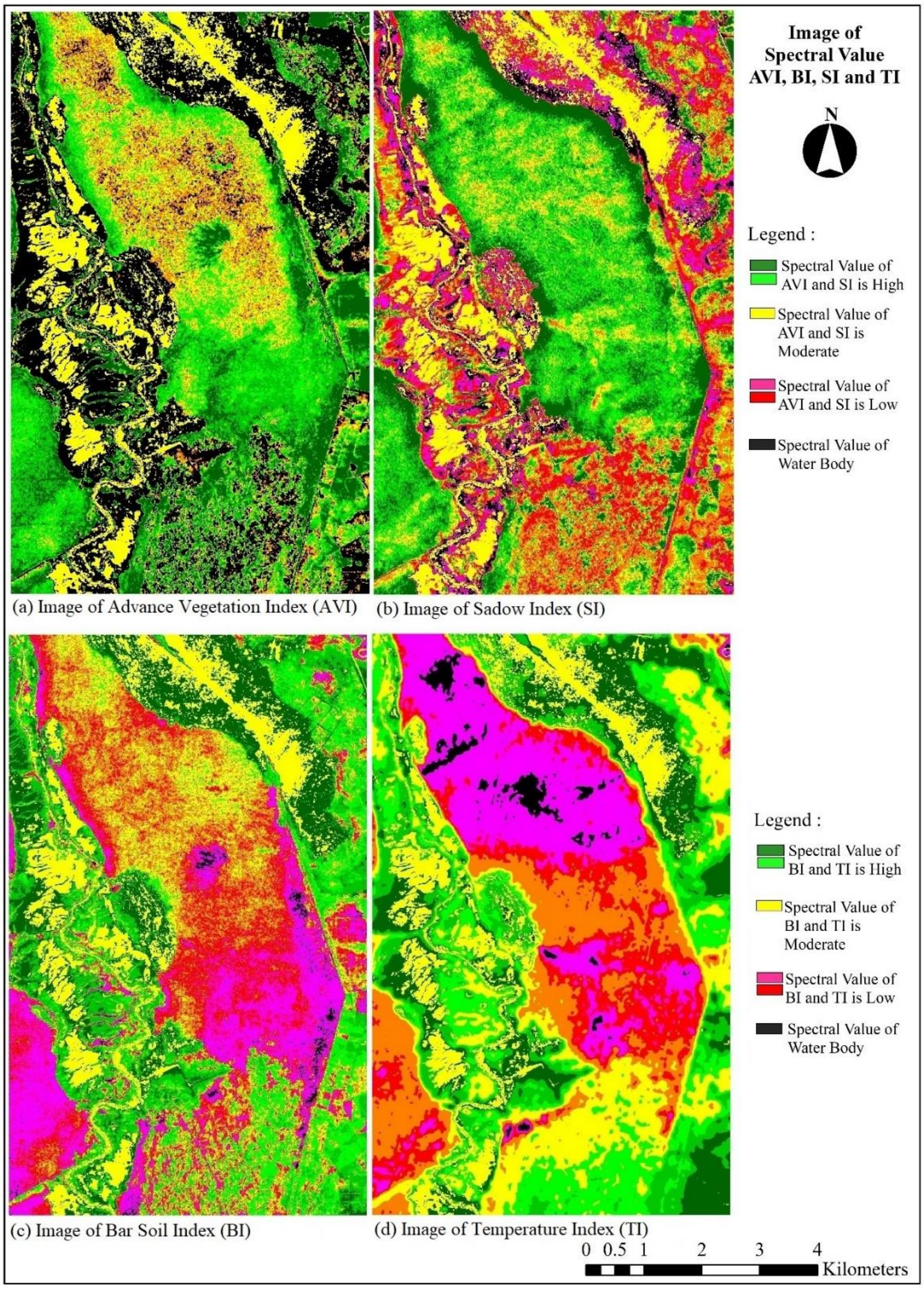

Figure 3. Image of Spectral Value (a) AVI image; (b) SI image; (c) BI image; and (d) TI image

3.2 Image analysis of forest cluster

The integration between the thermal index (TI) and the canopy shadow index (SI) resulted in the Advanced Shadow Index (ASI). The application of ASI is used as a reference for creating a Scaled Shadow Index (SSI) model which serves to determine the detailed structural clusters of peat swamp forests. The results of the analysis revealed that forest areas that were classified in dense canopy structure (SI>60%) had a lower value of TI (<60%). Meanwhile, forest areas with sparse canopy structures (SI<60%) had a higher value of TI (>60%). As a consequence, the SI value of almost all areas with dense canopy shadow is more than 80%, and it certainly became a problem in determining and analyzing forest structure in a factual basis. The analysis of the spectral data clusterization of Landsat 8 OLI-TIRS images generated 8 forest clusters based on the characteristics of the spectral value as presented in Table 2. The results of the analysis of forest clusters generated a new image, namely a scaled shadow index (SSI) image.

Forest clustering derived from the spectral analysis of SSI Image relatively provides information based on the differences in the vertical structure of the forest canopy density (Figure 4). The results of the forest clustering analysis are useful to identify the differences and variations in forest canopy structure based on the conditions of the canopy classes. Moreover, the provisional identification of the forest clustering revealed that forest with dense vegetation canopy had a higher SSI value, while forest with low or sparse vegetation canopy had a lower SSI value. Rikimaru (1996) explained that in areas where the SSI value is zero, this corresponds with forests that have the lowest shadow value (i.e., 0%). In areas were the SSI value is 100, this corresponds with forests that have the highest possible shadow value (i.e., 100%). The SSI can clearly differentiate between vegetation in the canopy and vegetation on the ground. It significantly improves the capability to provide more accurate results from data analysis than was possible in the past

Table 2. The spectral value of forest clusters in SSI landsat 8 OLI-TIRS image

No.	AVI	BI	SI	TI
1	56.8	140.3	12.4	140.1
2	28.9	157.6	59.5	203.5
3	144.9	126.6	131.0	158.0
4	136.6	123.2	163.0	123.2
5	136.6	113.9	175.7	63.0
6	179.3	103.5	179.1	73.5
7	188.6	108.1	172.2	108.3
8	200.3	112.2	162.1	143.8

Remark: AVI=Advanced Vegetation Index; BI=Bare Soil Index; SI=Shadow Index; TI=Thermal Index

3.3 Image analysis of vegetation density

In order to reduce and neutralize possible spectral misinterpretations in analyzing forest clustering through the SSI image model, the present study attempted to develop a vegetation density image model (VD model). The analysis of vegetation density image was intended to enhance the validity of the vegetation density model in accordance with the factual green vegetation density (green biomass) in the field (Figure 5). The results of the visualization of the SSI Image and the VD Image demonstrated opposite results in describing the condition of the vegetation canopy density. It revealed that the dense vegetation with the structure of vegetation on the ground had a higher density index in VD image, and on the contrary, had a lower canopy shadow index in SSI image.

3.4 Image analysis of forest canopy density

Based on the results of the analysis of Vegetation Density (VD) and Scaled Shadow Index (SSI) image, an integration process was carried out to obtain a new image model, namely the Forest Canopy Density (FCD) image which is expected to produce variations in the spectral value of the vertical structure of forest canopy and horizontal density of forest vegetation (Figure 6). Ultimately, the new image would provide a more representative and accurate classification in determining the condition of the canopy structure of peat swamp forest. The results of spatial analysis of the FCD image showed that the total area of the study area was ±28,968.48 ha, which could be classified into 6 categories according to the level of vegetation canopy density (Table 3).

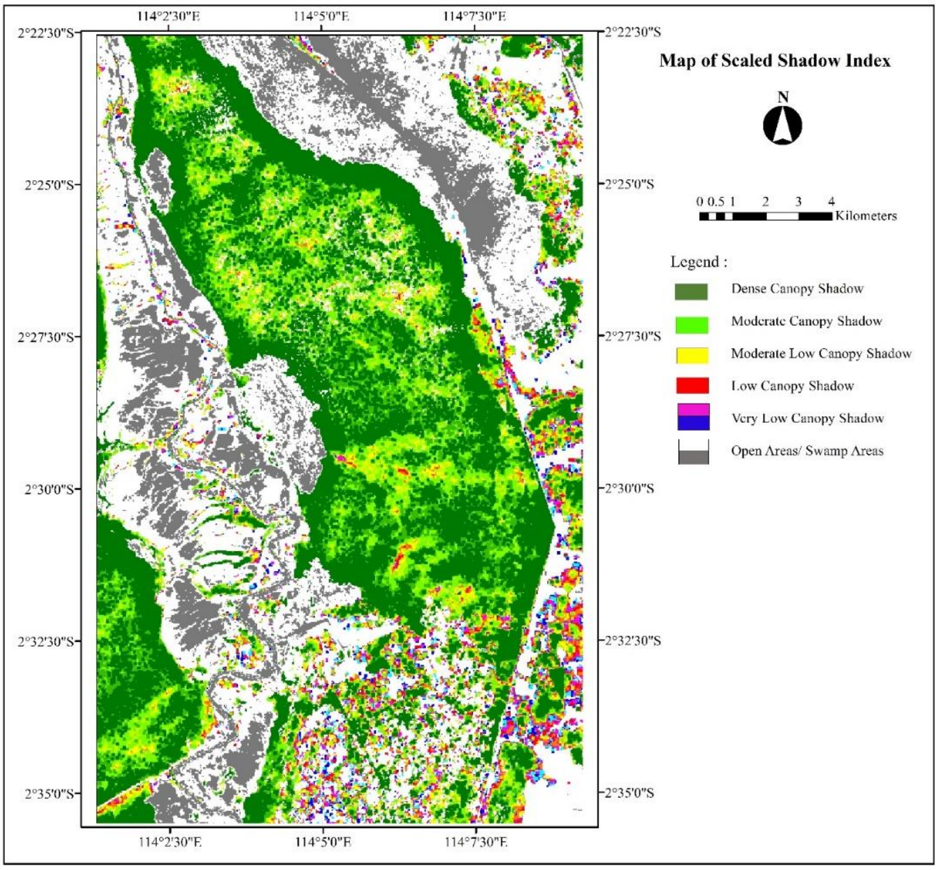

Figure 4. Map of forest cluster based on SSI.

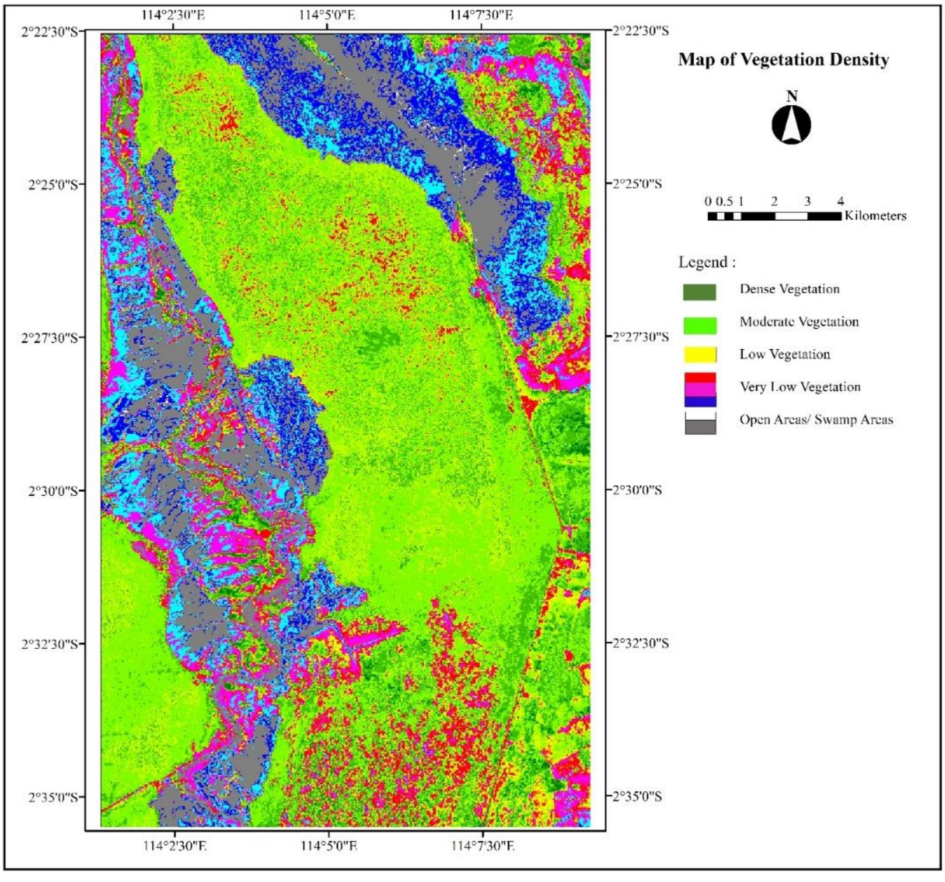

Figure 5. Map of vegetation density

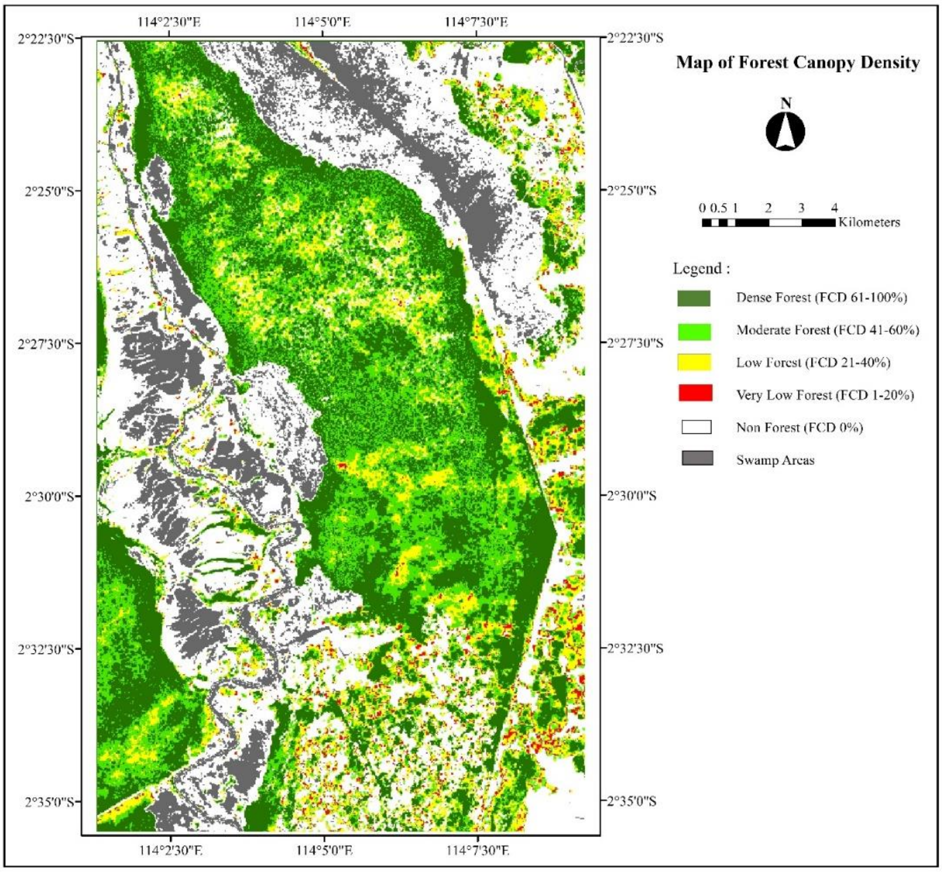

Figure 6. Map of forest canopy density

Table 3. Result of FCD image analysis, identification and interpretation of object in secondary swamp forest, Central Kalimantan

No.	Interval of FCD (%)	Area (ha)	Identification and interpretation
1	0	10,508.13	Open area, grasslands, ferns, and shrubs
2	1-20	130.77	Grasslands, ferns, and small trees with very low dense trees/ forest
4	21-40	632.07	Scrub swamp, sparse trees with shrubs with low dense trees/ forest
5	41-60	1,509.66	Scrub swamp with moderately dense trees
6	61-100	16,147.26	Secondary peat swamp forest with dense trees
Total area (ha)		28,968.48	

3.5 Above-ground carbon stock potential

In the present study, the calculation of the estimated above-ground carbon stock potential included trees and tree regeneration. The carbon stock potential is calculated using allometric equations according to Kettering et al. (2001); Murdiyarso et al. (2004); and Jaya et al. (2007). The classification of forest cover classes was obtained from FCD image analysis, namely: dense secondary peat swamp forest, moderately dense forest, and low dense forest. The data gained from the calculation of the above-ground carbon stock potential using 3 (three) allometric equations in each forest cover class are presented in Table 4.

The calculation using three allometric equations models for each class of peat swamp forest cover demonstrated a variety of value distribution. The dense secondary peat swamp forest had the highest distribution value of total above-ground carbon stock potential (92.59 to 122.96 ton/ha), followed by moderately dense forest (74.06 to 113.06 ton/ha), while the lowest was dense forest (40.48 to 63.60 ton/ha). The high distribution of the carbon stock potential in the dense secondary peat swamp forest is possibly influenced by its vegetation density level. In fact, it has a higher vegetation density (93,075 tree individual/ha) than moderate dense swamp forest (45,173 tree individual/ha) or low dense swamp forest

(6,840 tree individual/ha). Vegetation density is one of the parameters that affect the value of vegetation biomass and carbon stock potential in an ecosystem (Kusmana et al., 1992; Dharmawan and Siregar, 2008; Rachmawati et al., 2014; Chairul et al., 2016). We found that a dense forest is not a forest with larger trees than a sparse forest. The difference between dense forest and sparse forest is the number of trees per hectare. In addition, the study area is a secondary peat swamp forest for a long-time disturbance such us hydrological cycle, logging and forest fire (Boehm et al., 2002; Boehm and Siegert, 2004).

Table 4. Above-ground carbon stock potential (trees and regeneration) of different allometric equation models and forest cover classes in secoundary swamp forest

Stage of tree	Allometric equation	Carbon stock potential (ton/ha) of peat swamp forest based on cover classes					
		Dense forest	%	Moderately dense forest	%	Low dense forest	%
Seedling	Kettering et al. (2001)	1.16	1.25	0.47	0.57	0.94	1.95
	Murdiyarso et al. (2004)	1.97	2.48	0.79	1.07	1.31	3.24
	Jaya et al. (2007)	2.24	1.82	0.91	0.80	1.63	2.56
Sapling	Kettering et al. (2001)	23.99	25.91	52.94	63.65	7.56	15.65
	Murdiyarso et al. (2004)	25.89	32.66	49.45	66.77	7.76	19.17
	Jaya et al. (2007)	36.22	29.46	73.86	65.33	11.12	17.48
Pole and tree	Kettering et al. (2001)	67.44	72.84	29.76	35.78	39.80	82.40
	Murdiyarso et al. (2004)	51.42	64.86	23.82	32.16	31.41	77.59
	Jaya et. al. (2007)	84.50	68.72	38.29	33.87	50.85	79.96
Total	Kettering et al. (2001)	92.59	100	83.17	100	48.30	100
	Murdiyarso et al. (2004)	79.28	100	74.06	100	40.48	100
	Jaya et al. (2007)	122.96	100	113.06	100	63.60	100

In general, the distribution of the above-ground carbon stock potential in each class of peat swamp forest cover as revealed in the present study was relatively higher than those of the peat swamp forests of South Sumatra (Heriyanto et al., 2020) and Riau (Suwarna et al., 2012). Nevertheless, compared to the results reported by Ludang and Jaya (2007) on the distribution of carbon stock potential in Central Kalimantan, the value was lower. The distributions value of above-ground (trees and regeneration) carbon stock potential in several classes of peat swamp forest cover in Indonesia are presented in Table 5.

Based on Table 5, the distribution value of above-ground carbon stock in the dense secondary peat swamp forest as generated in this study was higher than that in the secondary peat swamp forests in Riau (Suwarna et al., 2012) and South Sumatra (Heriyanto et al., 2020). It indicates that the secondary succession process of vegetation in this study area was faster than the process in the secondary peat swamp forest in Riau and Sumatra. Similarly, in the dense and sparse scrub peat swamp forest, the results of the present study were higher than those in the old scrub peat swamp in South Sumatra (Heriyanto et al., 2020) and in open area or barren peatland with the estimated carbon stock between 4 to 7 ton/ha (Moore et al., 2002).

The contribution of carbon stock at each stage of tree growth to the total carbon stock in each class of peat swamp forest cover was diverse. The stage of tree and poles had the highest contribution to the total above-ground carbon stock potential in the dense secondary peat swamp forest and sparse scrub peat swamp. Meanwhile, the highest contribution of carbon stock to total above-ground carbon stock in the moderately dense scrub peat swamp was found in the sapling stage. The lowest contribution was in the seedling phase. The contribution percentage of carbon stock in the seedling stage as generated in the present study was higher than that in dry-land primary forests as reported by Junaedi (2007). The other reseach using a destructive method reported that the carbon stock potential of burned peat swamp forest in South Sumatra Indonesia was 11.82 ton/ha (Widyasari et al., 2010). In the same way, Perdhana (2009) reported that carbon stock potential of virgin peat swamp forest in Riau Indonesia was 172.16 ton/ha.

Table 5. Distribution value of above-ground carbon stock potential in several peat swamp forest cover classes in Indonesia

Class of forest cover	Estimated carbon (ton/ha)	Study area	Source of data
Old secondary peat swamp forest	90.79	South Sumatera	Heriyanto et al. (2020)
Young secondary peat swamp forest	58.51		
Old scrub swamp	0.66		
Logged-over peat swamp forest	97.19	Riau	Suwarna et al. (2012)
Burnt peat swamp forest	2.96		
Secondary peat swamp forest	86.43		
Primary peat swamp forest	351.33	Central Kalimantan	Ludang and Jaya (2007)
Logged-over peat swamp forest	173.33		
Burned peat swamp forest	143.33		
Dense secondary peat swamp forest	92.59*	Central Kalimantan	Present study
	79.28**		
	122.96***		
Moderately dense scrub swamp	83.17*		
	74.06**		
	113.06***		
Sparse scrub swamp	48.30*		
	40.48**		
	63.40***		

*Calculation using allometric model in Kettering et al. (2001); **Calculation using allometric model in Murdiyarso et al. (2004); *** Calculation using allometric model in Ludang and Jaya (2007).

4. CONCLUSION

Usage FCD model Landsat 8 OLI/TIRS in this study is accurate and capable to identify forest structure and its attributes effectively and with less information of ground validation. The results show that FCD model are able to provide an accurate classification of above ground carbon stock of peat swamp forest. It means that assessment of FCD is a prerequisite for various forest planning activities especially at large areas. Results based on FCD found that on average the above-ground carbon stock in ex-MRP is relatively lower compared to previous studies carried out in different sites. This shows that the low of above ground carbon stock is related to ecosystem stability. These facts illustrate that peat swamp forest in this area is decreasing in terms of its environment. We can consider to manage peat swamp forest ecosystem using forest canopy density model that is in line with the variety of their attributes such us aboveground biomass and carbon stock potential.

REFERENCES

Ballhorn U, Mott C, Siegert F. Peat Dome Mapping and Analysis. Palembang, Indonesia: South Sumatera Forest Fire Management Project; 2007.

Banerjee K, Panda S, Bandyopadhyay J, Jain MK. Forest canopy density mapping using advance geospatial technique. International Journal of Innovative Science, Engineering and Technology 2014;1(7):58-63.

Boehm HDV, Siegert F, Liews SC. Remote sensing and aerial survey of vegetation cover change in lowland peat swamp of Central Kalimantan during the 1997 and 2002 fires. Proceeding of the International Symposium on Land Management and Biodiversity in Southeast Asia; 2002 Sep 17-20; The Indonesia Institute of Sciences, Bogor: Indonesia; 2002.

Boehm HDV, Siegert F. The impact of logging on land use change in Central Kalimantan, Indonesia. International Peat Journal 2004;1(12):3-10.

Brown S. Estimating biomass and biomass change of tropical forest: A primer. Rome, Italy: FAO Forestry Paper; 1997. p. 134.

Chairul C, Muchktar E, Mansyurdin, Tesri M, Indra G. Structure of vegetation density and estimation of carbon sequestration in several forest conditions on Siberut Island, West Sumatra. Journal of Metamorfosa 2016;3(1):15-22.

Deka J, Tripathi OK, Khan ML. Implementation of forest canopy density model to monitor tropical deforestation. Journal of the Indian Society of Remote Sensing 2012;41(2):469-75.

Dharmawan IWS, Siregar CA. Soil carbon and stands carbon estimation of *Avicennia marina* (Forsk.) Vierh in Ciasem, Purwakarta. Journal of Forest Research and Nature Conservation 2008;5(4):317-28.

Fahmi A, Radjagukguk B. The role of peat on total of soil nitrogen in swamp land, biology news, Indonesian Institute of Sciences. Journal of Life Sciences 2013;12(2):223-30.

Heriyanto MN, Priatna D, Samsoedin I. Stands structure and carbon sequestration in the secondary forest of Muara Merang forest group, South Sumatra. Journal of Sylva Lestari 2020;8(2):30-40.

Jaya A, Siregar UJ, Daryono H, Suhartana S. Tropical peat swamp forest biomass under various land cover conditions. Journal of Forest Research and Nature Conservation 2007;4(4):41-52.

Junaedi A. Impact of Timber Harvesting and Silvicultural Treatment of Selective Cutting and Line Planting (TPTJ) on Carbon Sequestraton Potential in Tropical Natural Forest Vegetation (Case study in the IUPHHK Area of PT. Sari Bumi Kusuma, Central Kalimantan) [dissertation]. Bogor, Bogor Agricultural Institute; 2007.

Ludang Y, Jaya HP. Biomass and carbon content in tropical forest of Central Kalimatan. Journal of Applied Science in Environmental Sanitation 2007;2(1):7-12.

Ketterings QM, Coe R, Van Noordjwik M, Ambagau Y, Palm CA. Reducing uncertainty in the use of allometric biomass equations for predicting above-ground tree biomass in mixed secondary forests. Forest Ecology and Management 2001;146(1-3):199-209.

Kusmana C, Sabiham S, Abe K, Watanabe H. An estimation of above ground tree biomass of a mangrove forest in East Sumatera. Tropics 1992;1(4):243-57.

Laurance WF, Fearnside PM, Laurance SGW, Delamonica P, Lovejoy TE, Rankin-de Merona JM, et al. Relationship between soils and Amazon forest biomass: A landscape-scale study. Forest Ecology and Management 1999;118(1-3):127-38.

Moder F, Siegert F, Schlessinger P. Carbon stock estimation in peat swamp forest area of Merang-Kepayang. Palembang, Indonesia: South Sumatera Forest Fire Management Project; 2008.

Mon MS, Mizoue N, Htun NZ, Kajisa T, Yoshida S. Estimating forest canopy density of tropical mixed deciduous vegetation using landsat data: A comparison of three classification approaches. International Journal of Remote Sensing 2012;33(4):1042-57.

Moore TR, Bubier JL, Frolking SE, Lafleur PM, Roulet NT. Plant biomass and CO_2 exchange in an ombrotrophic bog. Journal of Ecology 2002;90(1):25-36.

Murdiyarso D, Rosalina U, Hairiah K, Muslihat L, Suryadiputra INN, Jaya A. Measuring carbon stock in peat soils: Practical guidelines. Bogor, Indonesia: Proyek Climate Change, Forest and Peatlands in Indonesia, Wetlands International-Indonesia Program and Wildlife Habitat; 2004.

Page SE, Hosciło A, Wosten H, Jauhiainen J, Silvius M, Rieley JO, et al. Restoration ecology of lowland tropical peatlands in Southeast Asia: Current knowledge and future research directions. Ecosystems 2009;12:888-905.

Perdhana RF. The Effect of Timber Harvesting with the Indonesian Selective Cutting on the Carbon Potential in Peat Forest Vegetation (Case study in Rokan Hilir Regency Riau Indonesia) [dissertation]. Bogor, Indonesia: Bogor Agricultural Institute; 2009.

Rachmawati D, Setyobudiandi I, Hilmi E. The estimated carbon stock potential in mangrove vegetation in the coastal area of Muara Gembong, Bekasi Regency. Journal Omni-Akuatika 2014;10(2):85-91.

Rahayu S, Lusiana B, van Noordwijk M. Estimating Above-ground Carbon Stocks in Various Land Use Systems in Nunukan Regency, East Kalimantan. Bogor, Indonesia: World Agroforestry Centre; 2007.

Rehman SAR, Sabiham S, Sudadi U, Anwar S. Impacts of oil palm plantations on climate change: A review of peat swamp forests' conversion in Indonesia. International Journal of Plant and Soil Science 2015;4(1):1-17.

Rikimaru A. Landsat TM data processing guide for forest canopy density mapping and monitoring model. Proceedings of the ITTO Workshop on Utilization of Remote Sensing in Site Assessment and Planting of Logged-over Forest; 1996 Jul 30-Aug 1; Bangkok: Thailand; 1996.

Rikimaru A. Development of forest canopy density mapping and monitoring model using indices of vegetation, bare soil and shadow. Proceeding of the 18th Asian Conference on Remote Sensing; 1997 Oct 20; Kuala Lumpur: Malaysia; 1997.

Rosalina Y, Kartawinata K, Nisyawati N, Nurdin E, Supriatna J. The carbon sequestration in the peat swamp forest in the conservation area of PT. National Sago Prima, Meranti Islands, Riau. Buletin Kebun Raya 2013;16(2):115-30.

Roy PS, Rikimaru A, Miyatake S. Biophysical spectral response modeling approach for forest density stratification. Proceeding of the 18th Asian Conference on Remote Sensing; 1997 Oct 20; Kuala Lumpur: Malaysia; 1997.

Sukarna RM. Spectral Study of Landsat 7 ETM+ for a Floristic Model of Peat Swamp Forest in Central Kalimantan [dissertation]. Yogyakarta, Indonesia: Gadjah Mada University; 2009.

Sukarna RM, Syahid Y. FCD application of landsat for monitoring mangrove in Central Kalimantan. Indonesian Journal of Geography 2015;47(2):160-70.

Suwarna U, Elias, Darusman D, Istomo. Estimating total carbon stock in soil and tropical peat forest vegetation in Indonesia. Journal of Tropical Management 2012;18(2):118-28.

Vetrita Y, Hirano T. Evaluation of fashionable gross primary production products in Indonesia's peat swamp forests. Journal of Remote Sensing 2012;9(2):114-25.

Wannasiri W, Nagai M, Honda K, Santitamnont P, Miphokasap P. Extraction of mangrove biophysical parameters using airborne LiDAR. Remote Sensing 2013;5(4):1787-808.

Wardoyo. The Forest Condition, The Role of Remote Sensing and GIS in the Forestry Sector. Indonesia: Forest Area Consolidation of Regional V Banjarbaru, Central and South Kalimantan; 2002.

Widyasari NAK, Saharjo BH, Solichin S, Istomo. Estimation of aboveground biomass and bonded carbon potential in burned peat swamp forests in South Sumatra; Indonesian. Journal of Agricultural Sciences 2010;15(1):41-9.

Yuwono T, Jaya SNI, Elias. Peat swamp forest carbon mass estimation model ALOS PALSAR image. Journal of Forest Research and Nature Conservation 2015;12(1):45-58

INSTRUCTION FOR AUTHORS

Publication and Peer-reviewing processes of Environment and Natural Resources Journal

Environment and Natural Resources Journal is a peer reviewed and open access journal that is published twice a year (January-June and July-December). Manuscripts should be submitted online at https://ph02.tci-thaijo.org/index.php/ennrj/about/submissions by registering and logging into this website. Submitted manuscripts should not have been published previously, nor be under consideration for publication elsewhere (except conference proceedings papers). A guide for authors and relevant information for the submission of manuscripts are provided in this section and also online at: https://ph02.tci-thaijo.org/index.php/ennrj/author. All manuscripts are refereed through a **double-blind peer-review** process.

Submitted manuscripts are reviewed by outside experts or editorial board members of **Environment and Natural Resources Journal**. This journal uses double-blind review, which means that both the reviewer and author identities are concealed from the reviewers, and vice versa, throughout the review process. Steps in the process are as follows:

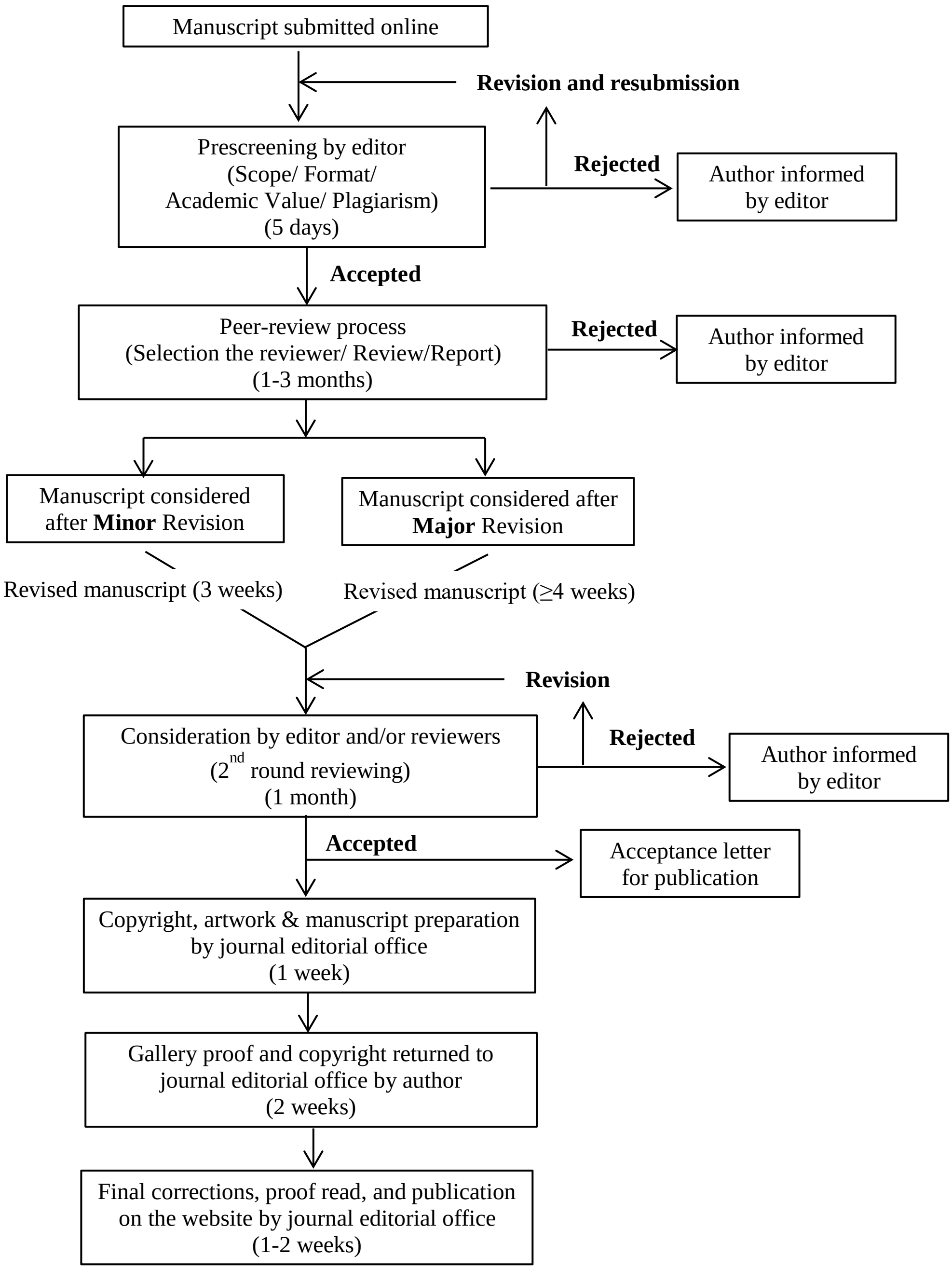

The Environment and Natural Resources Journal (EnNRJ) accepts 2 types of articles for consideration of publication as follows:

- *Original Research Article:* Manuscripts should not exceed 3,500 words (excluding references).
- *Review Article (by invitation):* This type of article focuses on the in-depth critical review of a special aspect in the environment and also provides a synthesis and critical evaluation of the state of the knowledge of the subject. Manuscripts should not exceed 6,000 words (excluding references).

Submission of Manuscript

Cover letter: Key points to include:

- Statement that your paper has not been previously published and is not currently under consideration by another journal
- Brief description of the research you are reporting in your paper, why it is important, and why you think the readers of the journal would be interested in it
- Contact information for you and any co-authors
- Confirmation that you have no competing interests to disclose

Manuscript-full: Manuscript (A4) must be submitted in Microsoft Word Files (.doc or .docx). Please make any identifying information of name(s) of the author(s), affiliation(s) of the author(s). Each affiliation should be indicated with superscripted Arabic numerals immediately after an author's name and before the appropriate address. Specify the Department/School/Faculty, University, Province/State, and Country of each affiliation.

Manuscript-anonymized: Manuscript (A4) must be submitted in Microsoft Word Files (.doc or .docx). Please remove any identifying information, such as authors' names or affiliations, from your manuscript before submission and give all information about authors at title page section.

Reviewers suggestion *(mandatory)*: Please provide the names of 3 potential reviewers with the information about their affiliations and email addresses. *The recommended reviewers should not have any conflict of interest with the authors. Each of the reviewers must come from a different affiliation and must not have the same nationality as the authors.* Please note that the editorial board retains the sole right to decide whether or not the recommended potential reviewers will be selected.

Preparation of Manuscript

Manuscript should be prepared strictly as per guidelines given below. The manuscript (A4 size page) must be submitted in Microsoft Word (.doc or .docx) with Times New Roman 12 point font and a line spacing of 1.5. *The manuscript that is not in the correct format will be returned and the corresponding author may have to resubmit*. The submitted manuscript must have the following parts:

Title should be concise and no longer than necessary. Capitalize first letters of all important words, in Times New Roman 12 point bold.

Author(s) name and affiliation must be given, especially the first and last names of all authors, in Times New Roman 11 point bold.

Affiliation of all author(s) must be given in Times New Roman 11 point italic.

Abstract should indicate the significant findings with data. A good abstract should have only one paragraph and be limited to 250 words. Do not include a table, figure or reference.

Keywords should adequately index the subject matter and up to six keywords are allowed.

Text body normally includes the following sections: 1. Introduction 2. Methodology 3. Results and Discussion 4. Conclusions 5. Acknowledgements 6. References

Reference style must be given in Vancouver style. Please follow the format of the sample references and citations as shown in this Guide below.

Unit: The use of abbreviation must be in accordance with the SI Unit.

Format and Style

Paper Margins must be 2.54 cm on the left and the right. The bottom and the top margin of each page must be 1.9 cm.

Introduction is critically important. It should include precisely the aims of the study. It should be as concise as possible with no sub headings. The significance of problem and the essential background should be given.

Methodology should be sufficiently detailed to enable the experiments to be reproduced. The techniques and methodology adopted should be supported with standard references.

Headings in Methodology section and Results and Discussion section, no more than three levels of headings should be used. Main headings should be typed (in bold letters) and secondary headings (in bold and italic letters). Third level headings should be typed in normal and no bold, for example;

2. Methodology
2.1 Sub-heading
2.1.1 Sub-sub-heading

Results and Discussion can be either combined or separated. This section is simply to present the key points of your findings in figures and tables, and explain additional findings in the text; no interpretation of findings is required. The results section is purely descriptive.
Tables Tables look best if all the cells are not bordered; place horizontal borders only under the legend, the column headings and the bottom.
Figures should be submitted in color; make sure that they are clear and understandable. Please adjust the font size to 9-10, no bold letters needed, and the border width of the graphs must be 0.75 pt. *(Do not directly cut and paste them from MS Excel.)* Regardless of the application used, when your electronic artwork is finalized, please 'save as' or convert the images to TIFF (or JPG) and separately send them to EnNRJ. The images require a resolution of at least 300 dpi (dots per inch). If a label needed in a figure, its font must be “Times New Roman” and its size needs to be adjusted to fit the figure without borderlines.

All Figure(s) and Table(s) should be embedded in the text file.

Conclusions should include the summary of the key findings, and key take-home message. This should not be too long or repetitive, but is worth having so that your argument is not left unfinished. Importantly, don’t start any new thoughts in your conclusion.

Acknowledgements should include the names of those who contributed substantially to the work described in the manuscript but do not fulfill the requirements for authorship. It should also include any sponsor or funding agency that supported the work.

References should be cited in the text by the surname of the author(s), and the year. This journal uses the author-date method of citation: the last name of the author and date of publication are inserted in the text in the appropriate place. If there are more than two authors, “et al.” after the first author’ name must be added. Examples: (Frits, 1976; Pandey and Shukla, 2003; Kungsuwas et al., 1996). If the author’s name is part of the sentence, only the date is placed in parentheses: “Frits (1976) argued that . . .”

Please be ensured that every reference cited in the text is also present in the reference list (and vice versa).

In the list of references at the end of the manuscript, full and complete references must be given in the following style and punctuation, arranged alphabetically by first author’s surname. Examples of references as listed in the References section are given below.

Book
Tyree MT, Zimmermann MH. Xylem Structure and the Ascent of Sap. Heidelberg, Germany: Springer; 2002.

Chapter in a book
Kungsuwan A, Ittipong B, Chandrkrachang S. Preservative effect of chitosan on fish products. In: Steven WF, Rao MS, Chandrkachang S, editors. Chitin and Chitosan: Environmental and Friendly and Versatile Biomaterials. Bangkok: Asian Institute of Technology; 1996. p. 193-9.

Journal article
Muenmee S, Chiemchaisri W, Chiemchaisri C. Microbial consortium involving biological methane oxidation in relation to the biodegradation of waste plastics in a solid waste disposal open dump site. International Biodeterioration and Biodegradation 2015;102:172-81.

Published in conference proceedings
Wiwattanakantang P, To-im J. Tourist satisfaction on sustainable tourism development, amphawa floating marketSamut songkhram, Thailand. Proceedings of the 1st Environment and Natural Resources International Conference; 2014 Nov 6-7; The Sukosol hotel, Bangkok: Thailand; 2014.

Ph.D./Master thesis

Shrestha MK. Relative Ungulate Abundance in a Fragmented Landscape: Implications for Tiger Conservation [dissertation]. Saint Paul, University of Minnesota; 2004.

Website

Orzel C. Wind and temperature: why doesn't windy equal hot? [Internet]. 2010 [cited 2016 Jun 20]. Available from: http://scienceblogs.com/principles/2010/08/17/wind-and-temperature-why-doesn/.

Report organization:

Intergovernmental Panel on Climate Change (IPCC). IPCC Guidelines for National Greenhouse Gas Inventories: Volume 1-5. Hayama, Japan: Institute for Global Environmental Strategies; 2006.

Remark

** Please be note that manuscripts should usually contain at least 15 references and some of them must be up-to-date research articles.*

** Please strictly check all references cited in text, they should be added in the list of references. Our Journal does not publish papers with incomplete citations.*

Copyright transfer

The copyright to the published article is transferred to Environment and Natural Resources Journal (EnNRJ) which is organized by Faculty of Environment and Resource Studies, Mahidol University. The accepted article cannot be published until the Journal Editorial Officer has received the appropriate signed copyright transfer.

Online First Articles

The article will be published online after receipt of the corrected proofs. This is the official first publication citable with the Digital Object Identifier (DOI). After release of the printed version, the paper can also be cited by issue and page numbers. DOI may be used to cite and link to electronic documents. The DOI consists of a unique alpha-numeric character string which is assigned to a document by the publisher upon the initial electronic publication. The assigned DOI never changes.

Mahidol University

Wisdom of the Land

Research and Academic Service Section, Faculty of Environment and Resource Studies, Mahidol University
999 Phutthamonthon 4 Rd, Salaya, Nakhon Pathom 73170, Phone +662 441-5000 ext. 2108 Fax. +662 441 9509-10
E-mail: ennrjournal@gmail.com Website: https://www.tci-thaijo.org/index.php/ennrj